Relaminarization of Fluid Flows

R. NARASIMHA and K. R. SREENIVASAN*

Indian Institute of Science
Bangalore, India

* Present address: Department of Engineering and Applied Science, Yale University, New Haven, Connecticut 06520.

I. Introduction

A. General Remarks

It is so often said that turbulence is the natural state of fluid motion that reports purporting to have observed relaminarization of a turbulent flow were until not long ago greeted with varying degrees of disbelief. Indeed, a common reaction when the subject was mentioned used to be that the implied transition from disorder to order was thermodynamically impossible! But these reverting flows that we shall discuss below are not closed

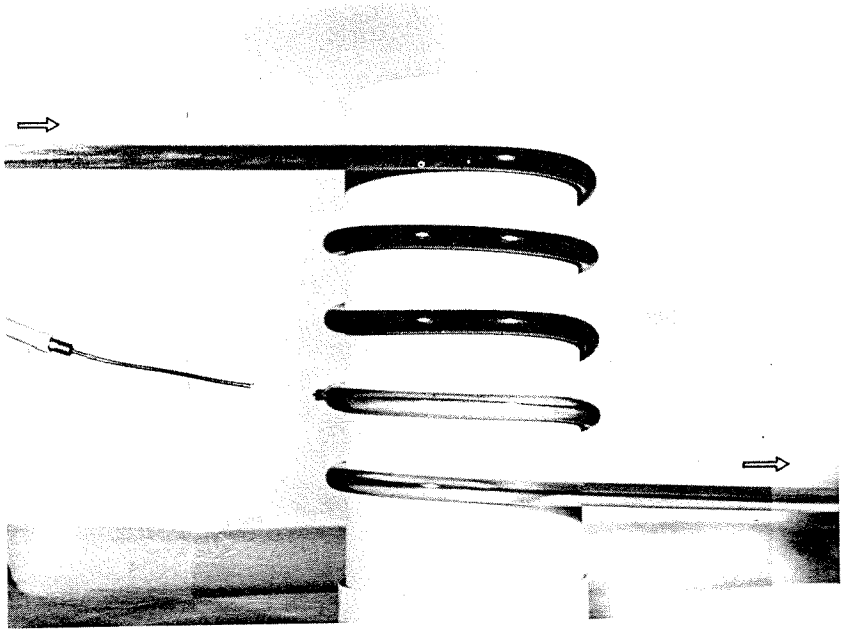

FIG. 1. Reversion in a coiled tube. Flow enters at top left, leaves at bottom right. Dye injected continuously at the fourth coil does not diffuse, indicating laminar flow. Dye injected at entry diffuses rapidly, indicating turbulence (photograph is taken just before this dye reaches the fourth coil). Inner diameter of tube about 8 mm; radius of curvature about 55 mm. (From Viswanath *et al.*, 1978.)

systems; if crystallization is possible out of liquids, so too is relaminarization from a turbulent state.

Indeed, should there still be any doubters, it is easy to set up simple experiments showing relaminarization (variously also called reversion, and inverse or reverse transition). We may begin with two examples of a few such experiments described by Viswanath *et al.* (1978). The first is similar to one made by G. I. Taylor in 1929. Turbulent flow is established in a tube of about 8 mm diameter, made of some flexible transparent material like tygon. The tube is then wrapped around a cylinder (say about 100 mm diameter) in a few coils, and comes out straight again. As is easily confirmed by injecting dye, the flow can be made to come in and go out turbulent in the straight sections, while remaining apparently laminar within the coil! Thus, in Fig. 1, the dye continuously injected at the fourth coil does not diffuse at all, indicating laminar flow there; but the dye injected into the straight section just upstream of where the tube bends into a coil always diffuses very rapidly, indicating turbulence. The flow similarly becomes turbulent again in the straight section downstream, although this is not shown in the photograph.

In the second experiment (Fig. 2), we inject a jet of dye vertically upward from the bottom into a tank of water. If the jet velocity is sufficiently high

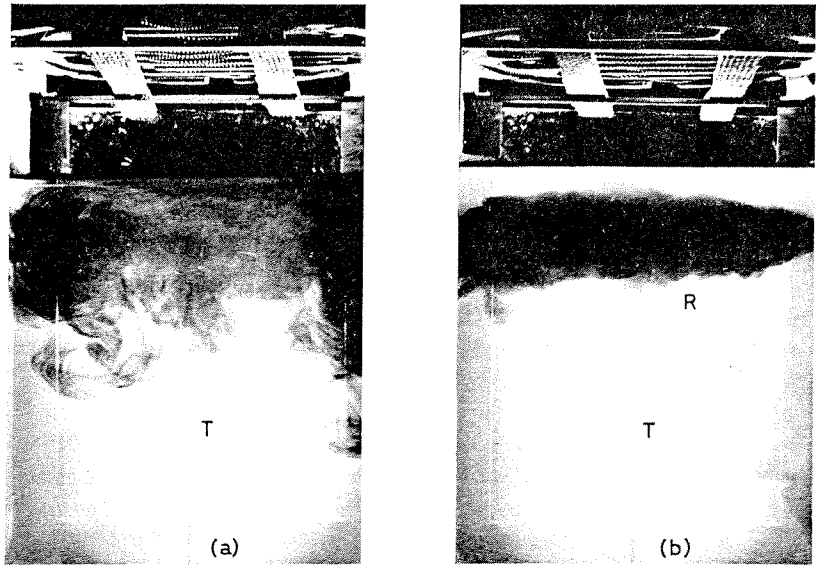

FIG. 2. Reversion in stably stratified flow. (a) Cold flow. (b) Flow with top fluid layers heated. Note the point of transition to turbulence in the jet (marked T), followed by reversion (marked R) in (b). (From Viswanath *et al.*, 1978.)

it breaks into turbulence as usual. If the upper layers of water are heated now, say with an ordinary heating coil placed on top of the tank, the turbulence in the jet dies out and a smooth layer of dye cloud collects near the top; we can observe here both transition and reversion in the jet.

In fact, once the idea of possible reversion is accepted, its presence is seen everywhere. When a laminar jet is seen issuing from a water faucet, such reversion must have occurred between the mains and the faucet, as the flow in the mains will invariably be turbulent. When we are breathing hard, say after exertion, the flow in the wind pipe is turbulent (especially because the flow detaches from the vocal cords in the glottic aperture), but deep inside the bronchioles in the lungs the flow must be laminar—relaminarization has therefore been occurring under our very noses all along! Inversions in the atmosphere (involving an *increase* in the temperature with height) can lead to fairly sudden suppression of turbulence as in the second experiment mentioned above, and were studied more than 50 years ago by Richardson (1920); Prandtl and Reichardt (1934) investigated the effect of stable stratification on turbulent shear flows by heating the top floor of a wind tunnel. Evidence of reversion of some kind has also been found when the flow is subjected to acceleration (Sternberg, 1954; Sergienko and Gretsov, 1959), magnetic fields (e.g., Murgatroyd, 1953), rotation (e.g., Halleen and Johnston, 1967), curvature (e.g., So and Mellor, 1973), heating (e.g., Perkins and Worsoe-Schmidt, 1965), suction (Dutton, 1960), blowing (e.g., Eckert and Rodi, 1968), and so on. Indeed, if turbulence *is* the natural state of fluid motion, the chances are that any flow that is observed to be laminar must have been the consequence of a reversion somewhere (often having passed through the trivial intermediate state of rest!).

Nevertheless, there is also evidence that the pendulum of opinion has perhaps swung too far in the other direction now; there is a strong temptation to attribute any observed departure from some presumed turbulent law to relaminarization. But there are few universally valid turbulent laws; those that pass as such (e.g., the log-law in wall flows) are at best asymptotic limits, and may not be valid in flows that, while being unusual or abnormal, are nonetheless turbulent. Choosing criteria for relaminarization based on such presumed laws is therefore a risky venture.

B. Scope of the Article

At the present time it seems opportune to examine the mechanisms that cause such reversion, and to see if there are any similarities or general principles that govern them. In carrying out this examination, we adopt a rather pragmatic definition of reversion, according to which a flow (or a part of it) has relaminarized if its development can be understood without

recourse to any model for turbulent shear flow. This implies, in particular, that the turbulent fluctuations need not necessarily have completely vanished in the relaminarized state; but that, if present, their contribution to mean flow dynamics (e.g., to momentum transport) is negligible. Under these circumstances the flow may be called quasi-laminar; it usually carries a residual turbulence that is inherited from the previous history of the flow, but has been rendered passive.

We begin by considering (in Sections III, IV, and V) three reverting flows in some detail, as we believe them to be basic archetypes (Narasimha, 1977). In the first, turbulent energy is dissipated through the action of a molecular transport property like the viscosity or conductivity, and the governing parameter is typified by the Reynolds number. In the second class, turbulence energy is destroyed or absorbed by work done against an external agency like buoyancy forces or flow curvature; the typical parameter is a Richardson number. In both cases experimental evidence indicates that the suppression of turbulence may go beyond the mere decay of energy to an actual decorrelation of the velocity components contributing to the crucial Reynolds shear stress that governs the mean flow.

The third class of reverting flows is exemplified by a turbulent boundary layer subjected to severe acceleration. Here a two-layer model is suggested. In the outer layer turbulence is fairly rapidly distorted and the Reynolds shear stress is nearly frozen; the inner viscous layer exhibits random oscillations in response to the forcing provided by the residue of the original turbulence. Reversion here is not so much the result of dissipation or destruction of energy (although these mechanisms are also operating), but rather of the domination of pressure forces over slowly responding Reynolds stresses in the outer region, accompanied by the generation of a new laminar subboundary-layer stabilized by the acceleration.

A number of other different reverting flows are then considered in the light of the analysis of these archetypes (Sections VI to XI). We believe that this examination sheds considerable light on certain instances of turbulence suppression which have hitherto been regarded in isolation, and shows how a combination of different mechanisms is often operating. Nevertheless, it will not be possible to come to definite conclusions about the primary mechanism (if there is one) in all cases, either because they have not yet been studied thoroughly or because they are too complex. It is hoped, however, that the attempt to take an overall view will reveal where further work needs to be done. In particular, in some instances of turbulence suppression (e.g., curvature), the observed effect is much larger than what might be expected from naive estimates of energy balance. The explanation lies presumably in the stabilization of the flow; perhaps here one is interfering with the organization of motion in the coherent structures now believed to be present in turbulent shear flows—the destruction of phase differences may

be as important as that of amplitudes. A fuller understanding of the nature of such organized motion is likely to provide more insight into relaminarization as well.

In addition to being an attempt at a fairly comprehensive survey of relaminarizing flows, the present article includes the results of some previously unpublished analyses.

We begin with a brief summary of the flow equations to which we will need to make constant reference in the rest of the paper.

II. The Governing Equations

It is convenient from the outset to split the flow into mean and fluctuating components (the latter denoted by a prime, with a mean that is necessarily zero). For an incompressible fluid of constant density, all stresses and forces may be expressed in kinematic units by dividing through by the density. Vector or tensor notation will be used as convenient; in the latter case the convention is adopted that all terms with a repeated Greek suffix are to be summed over the values 1, 2, 3 for the suffix.

The equations governing the mean flow of an incompressible fluid may be written (see, e.g., Monin and Yaglom, 1971, Chapter 6) as

$$\frac{\partial u_\alpha}{\partial x_\alpha} = 0, \tag{2.1}$$

$$\frac{\partial u_i}{dt} \equiv \frac{\partial u_i}{\partial t} + u_\alpha \frac{\partial u_i}{\partial x_\alpha} = -\frac{\partial p}{\partial x_i} + \nu \nabla^2 u_i - \frac{\partial}{\partial x_\alpha} \langle u'_\alpha u'_i \rangle + X_i. \tag{2.2}$$

These equations respectively express the laws of conservation of mass and momentum, with $\mathbf{u} = (u_\alpha)$ being the mean velocity, p the mean pressure, $\mathbf{X} = (X_i)$ the mean body force (per unit mass), and ν the kinematic viscosity; $\nabla^2 \equiv \partial^2/\partial x_\alpha \partial x_\alpha$. The quantity $-\langle u'_i u'_\alpha \rangle$, where the angular brackets denote the mean value, represents the (kinematic) Reynolds stress tensor. An equation for the components of this tensor may be easily derived from the momentum equation for the total velocity $\mathbf{u} + \mathbf{u}'$ (see, e.g., Monin and Yaglom, 1971, Chapter 6):

$$\begin{aligned} \frac{d}{dt}\langle u'_i u'_j \rangle = & -\langle u'_i u'_\alpha \rangle \frac{\partial u_j}{\partial x_\alpha} + \langle u'_i X'_j \rangle \\ & + \nu \langle u'_i \nabla^2 u'_j \rangle - \left\langle u'_i \frac{\partial p'}{\partial x_j} \right\rangle \\ & - \frac{1}{2} \frac{\partial}{\partial x_\alpha} \langle u'_i u'_j u'_\alpha \rangle + [i \leftrightarrow j]. \end{aligned} \tag{2.3}$$

Here $[i\langle\!\!-\!\!-\!\!-\!\!\rangle j]$ indicates additional terms obtained by switching i and j in all the other terms on the right.

Considerable insight is often gained by examining the turbulent energy

$$q \equiv \tfrac{1}{2}\langle u'_\alpha u'_\alpha \rangle = \tfrac{1}{2}\hat{u}_\alpha \hat{u}_\alpha, \hat{u}_\alpha = \langle u'^2_\alpha \rangle^{1/2}; \tag{2.4}$$

the governing equation is obtained by putting $i = j$ in (2.3) and summing:

$$\begin{aligned} \frac{dq}{dt} = & \underbrace{-\langle u'_\alpha u'_\beta \rangle \frac{\partial u_\beta}{\partial x_\alpha}}_{\text{(i)}} + \underbrace{\langle u'_\alpha X'_\alpha \rangle}_{\text{(ii)}} - \underbrace{\varepsilon}_{\text{(iii)}} \\ & + \nu \nabla^2 q + \underbrace{\nu \frac{\partial^2}{\partial x_\alpha \partial x_\beta} \langle u'_\alpha u'_\beta \rangle}_{\text{(iva)} \quad \text{(ivb)}} \\ & - \frac{\partial}{\partial x_\alpha} \underbrace{[\langle p' u'_\alpha \rangle}_{\text{(va)}} + \underbrace{\langle q' u'_\alpha \rangle]}_{\text{(vb)}}, \end{aligned} \tag{2.5}$$

where

$$q' = u'_\alpha u'_\alpha - \langle u'_\alpha u'_\alpha \rangle, \tag{2.6}$$

and

$$\varepsilon = \frac{1}{2} \nu \left\langle \left(\frac{\partial u'_\alpha}{\partial x_\beta} + \frac{\partial u'_\beta}{\partial x_\alpha} \right) \left(\frac{\partial u'_\alpha}{\partial x_\beta} + \frac{\partial u'_\beta}{\partial x_\alpha} \right) \right\rangle \tag{2.7}$$

represents viscous dissipation, i.e., loss of kinetic energy into heat through the action of viscosity. Terms (iva) and (ivb) in (2.5) are diffusion-like viscous terms; the gradient terms (va) and (vb) may be called diffusion by pressure and turbulent transport, respectively. Terms (i) and (ii) may together be said to represent "generation": term (i) is the energy production by the action of the Reynolds stresses on the mean shear, and term (ii), which we shall call "absorption" to distinguish it from the mean flow term (i), represents the work done against the fluctuating body forces. The nomenclature must not be interpreted to mean that (i) invariably tends to enhance the energy, or (ii) to diminish it—under appropriate conditions the contrary is indeed possible. If $\mathbf{X}'$ is a conservative body force (like gravity), the absorption term represents conversion of turbulent kinetic energy to (e.g., gravitational) potential energy. However, it is possible for the absorption term to represent irreversible dissipation also; one instance is when $\mathbf{X}'$ is the magnetic force on an electrically conducting fluid in a magnetic field. In this case $\mathbf{X}'$ depends on the current and therefore the conductivity of the fluid; the absorption, in the limit of low magnetic Reynolds numbers that will be discussed in Section X, represents ohmic dissipation. We will use the same nomenclature for the corresponding terms in (2.3).

As is well known, equations like (2.3) for the second-order quantities $\langle u_i' u_j' \rangle$ are incomplete, as they contain third-order quantities like $\langle u_\alpha' u_\beta' u_\beta' \rangle$; equations for these can also be written down, but they would contain terms of the fourth order, and so on. Equations for the evolution of moments up to any given order are not closed, because the basic nonlinearity in the equations of motion always introduces higher order moments. No complete theory of turbulent or reverting flows can therefore be constructed solely from equations of the above type, but much insight can nevertheless be obtained by their examination.

It is clear from (2.5) that turbulent energy could be altered by the action of (i) dissipation, (ii) production against mean shear, (iii) absorption by fluctuating external forces, or (iv) diffusion (in a generalized sense). It appears that observations in reverting flows can usually be traced to the action of one or more of the first three, but there is some evidence (in curved flows, for example, see Section VI) that changes in the diffusion terms can be important.

It is of course possible that the turbulent energy transport described by Eq. (2.5) is affected by a basic change in the mean flow, governed by (2.1) and (2.2); e.g., the imposition of a pressure gradient or a new body force may alter the mean flow sufficiently to cause (as a *consequence*) significant changes in the turbulence structure. In principle, the mean flow equations (2.1), (2.2), and the turbulent transport equations (2.3) and (2.5) are closely coupled to each other, so either set cannot be considered in isolation. However, there are situations where changes are faster in some variables than in others, so it becomes possible to identify rate-controlling mechanisms. We shall illustrate this in the following sections.

III. Reversion by Dissipation

A. Introduction

A mechanism that is comparatively easy to understand is the relative increase in dissipation that occurs when the Reynolds number goes down in a flow. Consider a two-dimensional parallel or nearly parallel flow with a mean velocity along the x-axis given by $u = u(y)$ and fluctuating velocity components u', v' along the x- and y-axes, respectively. Comparing terms (ii) and (iv) in (2.5), we find

$$\frac{\text{production of turbulent energy}}{\text{dissipation}} = \frac{-\langle u'v' \rangle \, \partial u/\partial y}{\varepsilon}; \qquad (3.1)$$

we may in general expect this ratio to decrease when the mean flow Reynolds number Re becomes sufficiently low. If therefore Re decreases downstream in a flow, we may expect reversion for the same reason that a flow whose Reynolds number decreases in time will revert.

B. Enlargement in Ducts

Experimental investigations of such reverting flows have been reported by Laufer (1962), Sibulkin (1962), and Badri Narayanan (1968). The general situation in these experiments involves the gradual enlargement of a pipe or channel from one diameter or width to another, as illustrated in Fig. 3 (for a channel): the angle of divergence is kept sufficiently small to ensure that no flow separation occurs. In this case the Reynolds number (based on the section-average flow velocity $\bar{U}$ and channel half-height or pipe radius a) goes down from say Re_1 upstream of the divergence to Re_2 downstream. If, therefore, $\mathrm{Re}_1 > \mathrm{Re}_{cr}$ and $\mathrm{Re}_2 < \mathrm{Re}_{cr}$, where Re_{cr} is an appropriate critical Reynolds number, it may be expected that an approaching turbulent flow will revert to the laminar state.

This is indeed found to be the case: the turbulence decays, and the mean flow asymptotically approaches the classical laminar (Poiseuille) solution. However, there are several interesting features in the flow that merit attention. Experiments show, for example, that the skin friction reaches the laminar value well before the velocity distribution in the middle reaches the value

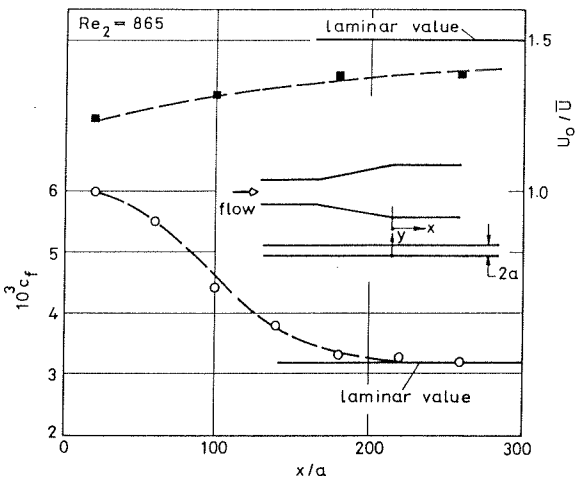

Fig. 3. Variation of center-line velocity U_0 and skin friction coefficient c_f in reverting channel flow. Experimental data from Badri Narayanan (1968).

characteristic of the well-known parabolic profile (see Fig. 3). An inner layer thickness, defined by the location of the maximum of the rms value of the fluctuating longitudinal velocity component, grows downstream like $x^{1/2}$, in a manner typical of *laminar* boundary layers (Fig. 4): there is here an assumption that the distribution of $\hat{u}$ is related to that of the mean velocity, and we shall return to this point in Section V.

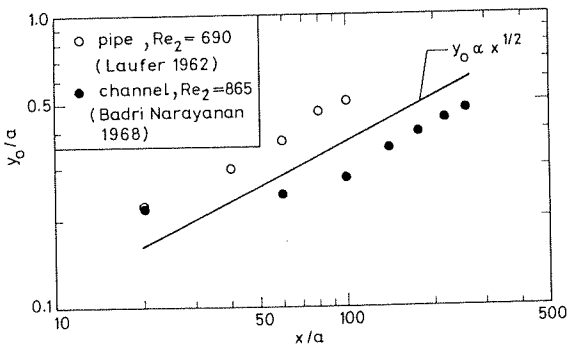

FIG. 4. Growth of the inner layer thickness during relaminarization due to duct enlargement: y_0 is the distance from the surface at which the rms value of the fluctuating longitudinal velocity component u' is a maximum. The $y_0 \propto x^{1/2}$ line shows the growth rate characteristic of a laminar boundary layer.

The picture that emerges, of relatively rapid adjustment near the wall and a much slower process in the outer layer, is consistent with the general findings in turbulent flow. There is also the suggestion that the process of reversion is associated with the conversion of the viscous sublayer into an effectively new laminar boundary layer near the wall, rather like the entry region in a pipe, except that the core in the reverting flow is sheared and carries the residue of an originally turbulent flow.

We shall now discuss some of these features of the flow in greater detail.

1. *Approach to the Laminar Mean Velocity Profile*

The state of the flow in an advanced stage of reversion must be capable of being described by a perturbation expansion on the final asymptotic state. Downstream of the enlargement in the duct, the effectively new laminar layer referred to above grows until it eventually fills the duct and establishes an entirely laminar profile all across. In an advanced stage of reversion where this has not quite happened, the Reynolds number $\bar{U}\delta/\nu$ based on the thickness δ of this laminar layer is fairly large, and its inverse $\gamma = \nu/\bar{U}\delta$ serves as a convenient small parameter. Outside the layer is a core where departures

from the laminar profile can be represented by a power series in γ, say

$$u(x, y) = u_0(y) + \gamma u_1(x, y) + O(\gamma^2), \tag{3.2a}$$

$$v(x, y) = -\gamma v_0(x, y) + O(\gamma^2), \tag{3.2b}$$

$$u'(x, y) = \gamma u_1'(x, y) + O(\gamma^2), \tag{3.2c}$$

$$v'(x, y) = \gamma v_1'(x, y) + O(\gamma^2), \tag{3.2d}$$

where $u_0(y)$ represents the asymptotic laminar state. (This is of course the reason why the expansions for the fluctuations u', v' begin with terms of order γ.) As we shall see later, the correlation coefficient

$$C_\tau \equiv \tau/\hat{u}\hat{v}, \tag{3.3}$$

where $\tau = -\langle u'v' \rangle$, decreases rapidly with increasing x, so that it is possible to assume it to be small for sufficiently large x. Thus,

$$\tau = o(\gamma^2). \tag{3.4}$$

Finally, assuming dp/dx as given, substituting the expansions (3.2) and (3.4) in the momentum equation (2.2) for $i = 1$, we have, to order unity,

$$dp/dx = \nu(d^2u_0/dy^2),$$

with the well-known Poiseuille solution

$$u_0 = \frac{1}{2\nu}\frac{dp}{dx}(\xi^2 - a^2), \qquad \xi = y - a. \tag{3.5}$$

To order γ we have

$$\left(u_0 - \xi\frac{du_0}{d\xi}\right)\frac{\partial u_1}{\partial x} = \nu\frac{\partial^2 u_1}{\partial \xi^2},$$

or, from (3.5),

$$-\frac{1}{2}\frac{dp}{dx}(\xi^2 + a^2)\frac{\partial u_1}{\partial x} = \nu\frac{\partial^2 u_1}{\partial \xi^2}. \tag{3.6}$$

Writing

$$u_1(x, \xi) = u_{1x}(x)u_{1y}(\xi),$$

we get, from (3.6),

$$\frac{du_{1x}}{u_{1x}} = C\frac{dx}{(dp/dx)},$$

where C is a positive constant. If dp/dx is a constant, as it indeed appears to be the case (as shown by the constancy of c_f, see Fig. 3) in the later stages

of reversion, we have

$$u_{1x} \sim \exp(-\alpha x/2a), \tag{3.7}$$

where $\alpha = -2aC/(dp/dx)$ is another positive constant. According to (3.7), the deviation of the velocity profile from the Poiseuille value, at any given y in the core of the flow, decreases exponentially with x. Along the centerline, for both pipe and channel flows undergoing reversion, the data of Fig. 5 show this to be indeed the case—perhaps surprisingly from as small a downstream distance as $20a$!

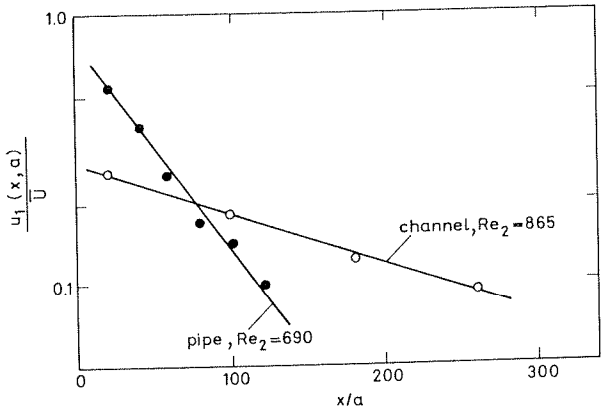

FIG. 5. Departure of measured mean velocity at the center-line from the Poiseuille value in relaminarizing duct flow.

The equation for u_{1y} can be written as

$$\frac{d^2u_{1y}}{d\zeta^2} + u_{1y}\left(\frac{1}{4}\zeta^2 - \beta\right) = 0, \tag{3.8}$$

where

$$\zeta \equiv \xi\left(\frac{2C}{\nu^2}\right)^{1/4}, \qquad \beta \equiv -\frac{a^2}{2\nu}\left(\frac{C}{2}\right)^{1/2}. \tag{3.9}$$

Equation (3.8) should therefore be solved with the boundary conditions

$$u_{1y} = 0 \qquad \text{at} \quad \xi = \pm a. \tag{3.10}$$

Because the equation as well as the boundary conditions are homogeneous, it is clear that nontrivial solutions can exist only for certain values β_n of the separation constant β. In the later stages of reversion, the laminar boundary layers growing on the two walls will fill a substantial part of the channel

width. As a consequence, u_{1y} is exponentially small in magnitude in the two laminar boundary layers. It is then clear that to represent u_{1y} reasonably accurately inside the laminar layers, we require a large number of eigenfunctions which oscillate rather rapidly. To avoid the need for evaluating these eigenfunctions, we may assume *a priori* that u_{1y} is identically zero in these regions and, instead of (3.10), apply the modified boundary condition

$$u_{1y} = 0 \qquad \text{at} \quad \xi = \pm(a - \delta). \tag{3.11}$$

This cannot be strictly correct because it demands an implicit dependence of u_{1y} on x (since δ is a function of x), but should be satisfactory if $d\delta/dx \ll 1$. In spite of a slight inconsistency, the advantage of using (3.11) instead of (3.10) is that there is hope that the first eigenfunction represents u_{1y} reasonably accurately. In any case, it will be sufficient for the purpose of illustrating the principle of the method of calculation.

An approximate solution to (3.8) can be written (see, e.g., Abramowitz and Stegun, 1965, p. 688) as

$$u_{1y}(\zeta) = 1 + \beta\frac{\zeta^2}{2!} + \left(\beta^2 - \frac{1}{2}\right)\frac{\zeta^4}{4!} + \left(\beta^3 - \frac{7}{2}\beta\right)\frac{\zeta^6}{6!} + \left(\beta^4 - 11\beta^2 + \frac{15}{4}\right)\frac{\zeta^8}{8!} + \cdots, \tag{3.12}$$

where β is to be determined by imposing the boundary condition (3.11). Then (3.12) gives the theoretical velocity distribution $u_1(x, y)/u_1(x, a)$.

Figure 6 shows a comparison of the experimental data with the above calculations for the reverting channel flow at $x/a = 260$. For this station, choosing (from measurement) $\delta \simeq 0.4a$, we require $\beta \simeq -1.18$; the corresponding solution agrees well with the measurement.

As an aside we note that the value of α in (3.7), obtained from Fig. 5 implies that the separation constant β is about -1.15 for the reverting channel flow.

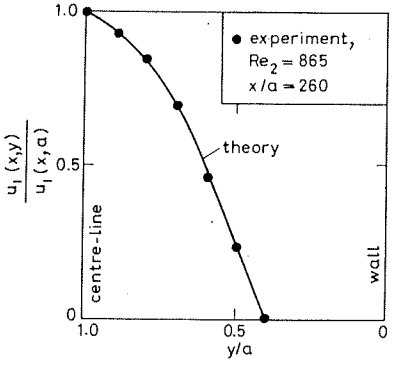

FIG. 6. Distribution of mean velocity in the core in reverting channel flow: departure from Poiseuille solution compared with present theory, Eq. (3.12). Experimental data from Badri Narayanan (1968).

We recall that this value of β is obtained from a consideration of $u_1(x,0)$ at several x/a. That this agrees well with the β evaluated from a consideration of the velocity profile $u_1(x, y)$ at a single x/a in a good indication of the consistency of the calculations.

2. *The Decay of Turbulence*

The precise manner in which turbulence decays in such a reverting flow raises many interesting questions. Again, in the parallel (or nearly parallel) two-dimensional shear flow we are considering, with $x_1 = x$, $x_2 = y$, $x_3 = z$ and $u_1 = u$ (y only), $u_2 = v = 0, u_3 = w = 0$, Eq. (2.3) shows that the Reynolds stress components have the following production terms:

$$\frac{1}{2}\hat{u}^2 : -\langle u'v'\rangle \frac{\partial u}{\partial y},$$

$$\hat{v}^2, \hat{w}^2 : 0,$$

$$-\langle u'v'\rangle : \hat{v}^2 \frac{\partial u}{\partial y}. \tag{3.13}$$

We shall examine experimental observations in the light of these equations.

Figure 7 shows some representative measurements of turbulence quantities in a reverting flow in a channel, from the experiments of Badri Narayanan (1968). It is seen that both $\hat{u}$ and $\hat{v}$ decay exponentially with distance, and that $\hat{v}$ decays more rapidly than $\hat{u}$. At $\mathrm{Re}_2 = 865$, it takes a streamwise distance of $115a$ for a halving in $\hat{u}^2$ at the centerline, but only $75a$ for $\hat{v}^2$. The ratio $\hat{u}/\hat{v}$ is around 4 at $x = 20a$, and increases to 6 at $x = 220a$; over the same distance, the ratio has been found to increase to nearly 15 at $\mathrm{Re}_2 = 625$! Thus, the decaying turbulent flow is strongly anisotropic. From (3.13) the production of turbulence occurs only in the $\hat{u}^2$ component; clearly, inter-component energy transfer is too slow and ineffective to correct the anisotropy.

It is further seen from Fig. 7 that the correlation coefficient C_τ [defined by Eq. (3.3)] goes down, from a maximum value of 0.36 at $x = 20a$ to 0.13 at $x = 180a$. This shows that a decorrelation mechanism must be at work, thus implying a weakening of the nonlinear effects. It is then clear from Eq. (3.13) that $\hat{u}^2$ must decay because of dissipation overtaking the production. Note that the Reynolds shear stress decreases nearly linearly in x unlike the turbulent energy components $\hat{u}^2$ and $\hat{v}^2$, which decay nearly exponentially in x.

Finally, we may surmise that the decorrelation of u' and v' fluctuations is connected with the destruction of the coherent motion in the wall-layer,

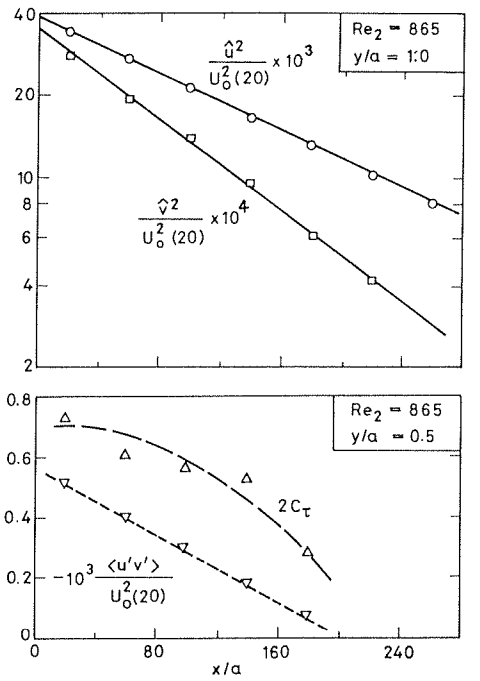

FIG. 7. Decay of turbulence intensity and the shear correlation coefficient in reverting channel flow. U_0 (20) = center-line velocity at $x/a = 20$. (Experimental data from Badri Narayanan, 1968.)

which recent work suggests is a key to the production of turbulent energy (e.g., Laufer, 1975).

3. *The Decay Rate*

Owen (1969) has presented an interesting argument to estimate the rate of decay of the turbulence intensity for given downstream Reynolds number Re_2. He assumes that in the turbulent energy balance equation (2.5) only the production and dissipation terms are significant. This is however not in general valid; Laufer's (1962) measurements, analyzed by Coles (1962), show in fact that on the axis of the pipe diffusion is comparable to or greater than dissipation, at both the first and the last measurement station ($x/a = 20, 100$).

A better procedure is to consider the integral of the energy balance equation (2.5) over (say) the half-height of the channel; the diffusion terms then drop out and we get

$$\int_0^a u \frac{\partial q}{\partial x}\, dy = -\int_0^a \langle u'v'\rangle \frac{\partial u}{\partial y}\, dy - \int_0^a \varepsilon\, dy. \tag{3.14}$$

Following Owen, one may put

$$\frac{\partial u}{\partial y} \sim \frac{U_*}{a}, \quad -\langle u'v' \rangle = b_0 q, \tag{3.15}$$

where $U_* = \tau_0^{1/2}$ is the friction velocity, τ_0 is the wall stress and b_0 is taken as a constant of order 10^{-1}. (Note that this ignores the decorrelation effect mentioned above.) The dissipation ε is often estimated as

$$\varepsilon = 15\nu \left\langle \left(\frac{\partial u'}{\partial x} \right)^2 \right\rangle = 15\nu \frac{\hat{u}^2}{\lambda^2}, \tag{3.16}$$

where λ is the Taylor microscale; the expression assumes that the small eddies responsible for dissipation are isotropic, following Kolmogorov's famous postulate. Owen replaces (3.16) by

$$\varepsilon \simeq b_2 \nu q / a^2, \tag{3.17}$$

where b_2 is taken to be a constant of order 10; the crucial assumption is made that λ is proportional to a. If q^* is a characteristic value of q, the energy equation (3.14) then takes the form

$$\frac{dq^*}{dx} = q^* \left(A_1 - \frac{A_2}{\mathrm{Re}} \right) = A_3 q^* \left(\frac{1}{\mathrm{Re}_{cr}} - \frac{1}{\mathrm{Re}} \right),$$

whose solution is

$$q^* \sim \exp\left[-\frac{A(x - x_0)}{a} \left(\frac{1}{\mathrm{Re}} - \frac{1}{\mathrm{Re}_{cr}} \right) \right], \tag{3.18}$$

where A, A_1, A_2, A_3, and x_0 are all some constants. Owen finds that the experimental evidence is not inconsistent with the above expression.

This analysis is however not entirely satisfactory. The decorrelation mentioned earlier shows that $\langle u'v' \rangle$ does not decay in proportion to q but much faster. Because of the large anisotropy the usual estimate (3.16) for dissipation is likely to be in error; furthermore, experiments show that λ does not remain constant during decay (at any rate as estimated from the u' data), but rather tends to increase like $\hat{u}^{-2}$ (Laufer, 1962), so that ε is proportional to $\hat{u}^6$ rather than $\hat{u}^2$. (It is however possible that the dissipation will be governed by the microscale in the normal direction, which could well be limited by the dimension of the duct.)

Figure 8 shows the channel data of Badri Narayanan (1968) plotted against 1/Re. The data do not lie too convincingly on a straight line, as they should if (3.18) were valid.

On the other hand, a good fit to the data is a law of the type

$$\hat{u}^2 \sim \exp[-B(\mathrm{Re}_{cr} - \mathrm{Re})^3 (x - x_0)/a], \qquad \mathrm{Re} < \mathrm{Re}_{cr}, \tag{3.19}$$

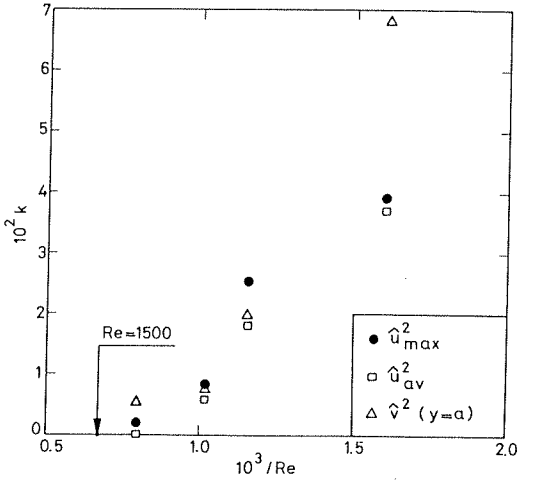

FIG. 8. Turbulence decay rates in relaminarizing channel flows. k is defined by $\hat{u}^2 \propto \exp(-kx/2a)$.

where B is some positive constant (Fig. 9). Indeed the diagram suggests, by extrapolation, $\mathrm{Re}_{cr} \simeq 1500$. Note that measurements in reverting pipe flow are also included with the channel data in Fig. 9. Based on the (only) two available data points, it does not seem necessary to infer a different critical Reynolds number for reversion in pipe flow. It may be of interest to note, however, that the value $\mathrm{Re}_{cr} = 1500$ (equivalent to 3000, if based on the pipe diameter), corresponds to the *end* of the transitional regime and the maximum skin friction coefficient, rather than to the beginning of transition and the minimum skin friction (both of which occur at a diameter-Reynolds number of about 2300).

A remarkable feature of this kind of dissipative reversion is its slowness. In a channel, even at $\mathrm{Re}_2 = 865$, which is about 60% of the critical Reynolds number, it takes a distance of $200a$ for $\hat{u}$ to fall to a third of its initial value.

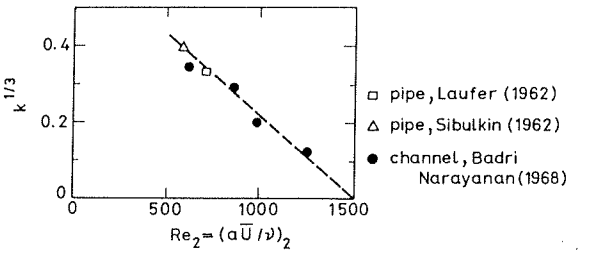

FIG. 9. Turbulence decay rates at different downstream Reynolds numbers in reverting duct flows.

The reason for this is that there is apparently only a slight difference between production and dissipation in the flow even at Reynolds numbers well below the critical. Consequently, the flow is nearly in a state of equilibrium; and both spectra and intensity distributions show a universal similarity during decay (Laufer, 1962). We next discuss this briefly.

4. *The Turbulent Spectrum*

In all the experiments reported (Laufer, 1962; Sibulkin, 1962; Badri Narayanan, 1968), the measured spectral density of u' at the centerline exhibits an approximate similarity over the entire wave-number range, when normalized by the centerline velocity and the turbulence integral scale l. This is an unusual simplicity, considering that even in homogeneous turbulence no such similarity over the entire wave-number region is found (see, e.g., Batchelor, 1953) during the major part of the decay process. Furthermore, the observed spectral similarity* in reverting flows is of the type $e^{-k_1 l/2}$, where k_1 is the component of the wave-number vector in the direction of the man flow. This suggests considerable nonlinear interaction among wave numbers, and in this sense the decay process is not entirely viscous-dominated: if it were, the situation would be diffusion-controlled as in the "final period" of decay in homogeneous turbulence, where the spectral density exhibits a similarity of the type $e^{-\beta k_1^2}$ (Batchelor and Townsend, 1948). We have however already seen in earlier sections that intercomponent correlations become increasingly less important with increasing downstream distance.

Another pointer to the importance of the nonlinear mechanism in spectral energy transfer is that, during a major part of the process of decay, the Reynolds number $\mathrm{Re}_\lambda (\equiv \hat{u}\lambda/\nu)$ *increases* downstream. For example, in Laufer's (1962) reverting pipe flow, Re_λ increases by a factor of nearly 2.5 from $x/a \simeq 25$ to $x/a \simeq 100$. However, the quantitative significance of this observation is doubtful because of the increasing anisotropy of the turbulence field.

C. Other Instances of Reversion by Dissipation

There are a large number of situations where the variation of flow parameters increases dissipation and so suppresses turbulence. The decrease in Reynolds number can occur either due to an increase in the cross-sectional area of a single duct carrying the fluid, as in the flows studied above, or by branching. An interesting example of the latter is in the human lungs, where Reynolds numbers (based on diameter) vary from about 3100 in the trachea to 1230 in the segmental bronchi (Owen, 1969). Although the bronchial tubes in the upper airways are too short for developed flow to be obtained, the decrease in Reynolds numbers is such that well before the very fine bronchial tubes are reached, the flow will have reverted to the laminar state.

Another example of dissipative reversion occurs in a pipe of uniform diameter containing an orifice, say for metering fluid flow. There is a certain Reynolds number range in which turbulence arises just downstream of the orifice even when the approach flow is laminar, as the free shear layers springing from the orifice lip are highly unstable. Further downstream of the orifice, however, this turbulence must be suppressed as the flow reverts to its original laminar state. Measurements by Alvi and Sridharan (see Alvi, 1975) show how the orifice characteristics are affected by the sequence of events going through transition in the shear layer followed by reversion downstream to fully turbulent flow everywhere (Fig. 10). In particular, the so-called settling length, defined as a measure of the distance downstream of the orifice required for the reestablishment of the pressure gradient characteristic of fully developed flow, increases rapidly to more than 20 diameters as the pipe critical Reynolds number of about 2300 (based on diameter) is reached; this is a simple consequence of the slowness of the dissipative reversion process that we have already noted above. Once the critical Reynolds number is exceeded the settling length drops steeply to six to seven diameters, characteristic of fully developed turbulent flow.

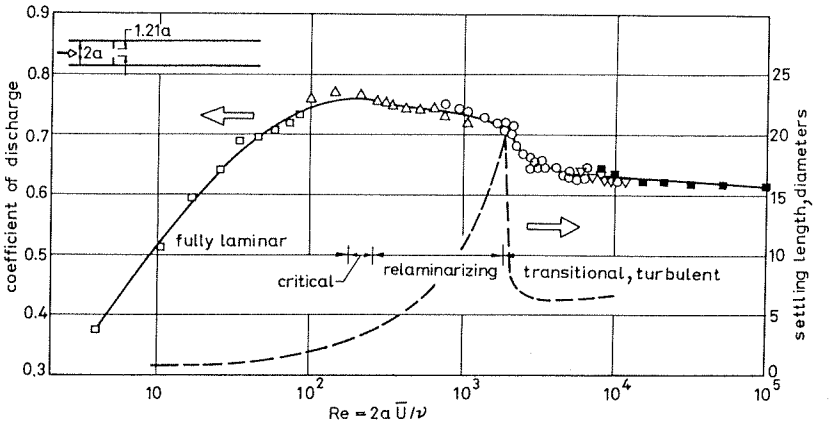

FIG. 10. Variation of selected flow characteristics for a sharp-edged orifice with approach flow pipe Reynolds number. (Data from Alvi, 1975.)

* There are two consequences of this similarity. First the two-point double-velocity correlation $\langle u'(x_0)\, u'(x_0 + x)\rangle$ decreases rather slowly with distance (like x^{-2} at large x). No measurements of this correlation have been made, however, in this class of reverting flows. Second, the spectral similarity implies that the ratio λ/l is a constant during decay. This constant is about $\frac{1}{3}$ in Laufer's experiment and about $\frac{1}{2}$ in Sibulkin's and Badri Narayanan's experiments.

Other characteristics of the orifice, like the discharge coefficient, also show the effects of reversion at the appropriate Reynolds numbers, but these are much less pronounced.

Other forms of dissipation arising from different molecular transport properties (e.g., thermal or electrical conductivity) may also bring about reversion. Magnetohydrodynamic flows provide some interesting examples, but they are sufficiently complex to demand separate attention, and so are discussed in Section X.

IV. Reversion in Stably Stratified Flows

A. Introduction

As noted in Section I, the possibility of the suppression of turbulence in the presence of a stabilizing density gradient has been known for a long time. However, although it is almost 60 years since Richardson proposed a criterion for the phenomenon in 1920, no full-fledged theory exists yet. Physically, the presence of a lighter fluid on top (i.e., lighter than when the fluid is in hydrostatic equilibrium) means that rising fluid has to work against gravity, and so turbulent energy could be converted into gravitational potential energy. It is such energy absorption that leads to the reversion shown in Fig. 2.

Such stable stratification can be observed frequently in the atmosphere. For example, following sunset on a day during which sunshine has produced much convection, there can be sudden cooling of the ground by radiation (see, e.g., Scorer, 1958, p. 209), producing stable density gradients and a suppression of turbulence; this phenomenon can be recognized by the appearance of clouds with flat, smooth tops, similar to that in Fig. 2. Similar effects may take place following a sharp cooling shower of rain (Fig. 11), and may also occur during a solar eclipse, which we shall discuss in Section IV,C below.

B. Analysis

The effects of stratification can be approximately analyzed by making what is known as the Boussinesq assumption, according to which the only effect of density changes is to provide an additional body force, the fluid being otherwise incompressible—effectively therefore its mass remains constant but weight changes. (See a discussion of this assumption in Monin and Yaglom, 1971, Chapter 6.) There is now therefore a body force in Eq. (2.3), represented by

$$\mathbf{X}' = -\mathbf{k}\rho g b', \tag{4.1}$$

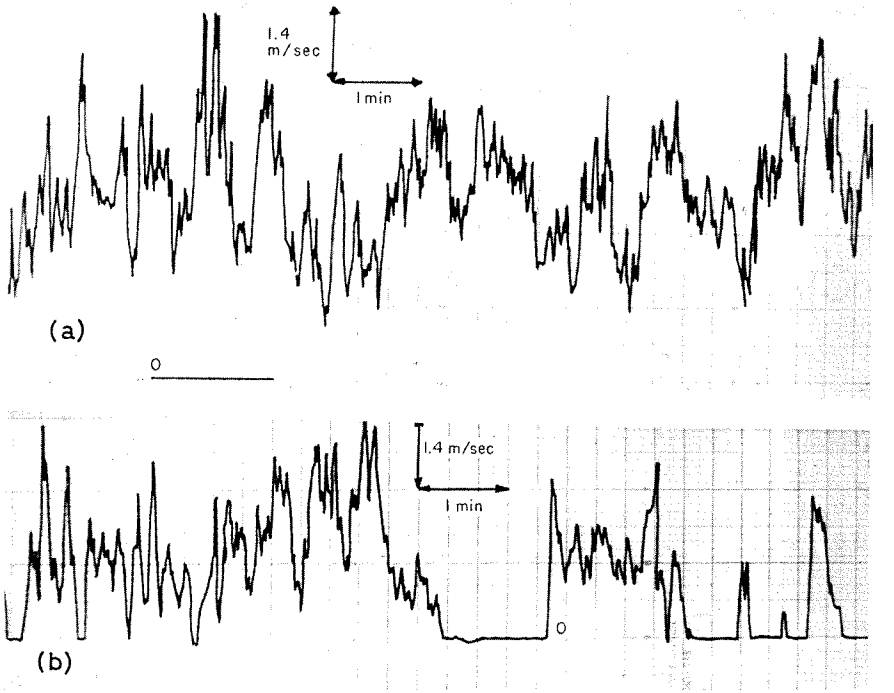

Fig. 11. Traces of horizontal wind speed from a low inertia cup anemometer, just before (a) and after (b) a cooling rain shower: note the patches of laminar flow in (b). (From A. Prabhu, unpublished, 1977.)

where $\mathbf{k}$ is a unit vector along the vertical, g is the acceleration due to gravity, and b' is the fluctuating part of the specific volume ρ^{-1}.

Consider now a steady mean flow $u(z)$ along the x-axis, with the z-axis being vertical and the flow assumed homogeneous in all horizontal planes. The relevant generation terms in (2.3) are then respectively as follows (see also Stewart, 1959):

$$\tfrac{1}{2}\hat{u}^2 : -\langle u'w'\rangle \frac{\partial u}{\partial z}, \tag{4.2a}$$

$$\tfrac{1}{2}\hat{v}^2 : 0, \tag{4.2b}$$

$$\tfrac{1}{2}\hat{w}^2 : -g\rho\langle b'w'\rangle, \tag{4.2c}$$

$$-\langle u'w'\rangle : g\rho\langle b'u'\rangle + \hat{w}^2 \frac{\partial u}{\partial z}. \tag{4.2d}$$

In addition, we may derive from the energy equation the generation terms for the specific volume fluctuation $\hat{b}$ and the flux $\langle b'w' \rangle$:

$$\hat{b}^2 : -\langle b'w' \rangle \frac{d}{dz}\left(\frac{1}{\rho}\right), \tag{4.3a}$$

$$-\langle b'w' \rangle : \rho g \hat{b}^2 + \hat{w}^2 \frac{d}{dz}\left(\frac{1}{\rho}\right). \tag{4.3b}$$

It is interesting to note that there is a production from interaction with the mean flow only for the component $\hat{u}$, but this production depends also on $\langle u'w' \rangle$. In turn, $\langle u'w' \rangle$ can be produced through the interaction of $\hat{w}$ and du/dz; however $\hat{w}$, not being directly produced by mean flow interaction, must be sustained by transfer of energy from the other components through the action of pressure (see discussion in Batchelor, 1953, p. 84, about the mechanism). If, however, $\hat{w}$ is suppressed through the buoyancy term $\langle b'w' \rangle$, then the production of $\hat{u}$ and $\langle u'w' \rangle$ will also diminish.

A measure of the ratio of the energy so absorbed by buoyancy forces to the production through the mean shear is the so-called flux Richardson number,

$$Rf \equiv \frac{\rho g \langle b'w' \rangle}{\langle u'w' \rangle \, du/dz} = \frac{g}{T} \frac{\langle T'w' \rangle}{\langle u'w' \rangle \, du/dz}, \tag{4.4}$$

where $T' = T\rho'/\rho$ is the temperature fluctuation in a perfect gas, making the reasonable assumption that in low-speed flows the relative pressure fluctuation p'/p is negligible.

If mean flow production and viscous dissipation are approximately equal, as they are in many shear flows (see, e.g., the energy balance in a turbulent boundary layer, presented below in Section V,B,1), then a relatively small loss to buoyancy can affect turbulence intensities appreciably; suppression of $\hat{w}^2$ quickly diminishes the other components as well. Townsend (1958) has made a detailed analysis of the energy balance in such stratified flows, and shows that the critical flux Richardson number $\mathrm{Rf}_{\mathrm{cr}}$ must be less than $\frac{1}{2}$, as otherwise it is impossible to find a real turbulence intensity that will satisfy the equation for turbulent energy as well as that for temperature fluctuations. Experimental observations, to be discussed in the next section, show that $\mathrm{Rf}_{\mathrm{cr}}$ is in fact much less than Townsend's upper bound, being only 0.1 or less. Ellison (1957) has presented an analysis that suggests $\mathrm{Rf}_{\mathrm{cr}} \simeq 0.15$, and further that density and velocity fluctuations are decoupled rather than destroyed under stable conditions.

Before examining the experimental evidence, it is worth noting that, if the energy and momentum fluxes in (4.4) are respectively proportional to the gradients of $1/\rho$ and u (through appropriate eddy diffusivities of heat and momentum, say K_h and K_m), we can write

$$Rf = \frac{K_h}{K_m} \frac{g \, d(1/\rho)/dz}{(du/dz)^2} = \frac{K_h}{K_m} Ri, \tag{4.5}$$

where Ri is known as the gradient Richardson number. In an atmosphere at rest, hydrostatic equilibrium requires $dp/dz = -\rho g$, and if entropy were constant the temperature would decrease with altitude at the so-called dry adiabatic lapse rate $dT/dz = -g/c_{\mathrm{p}}$, where c_{p} is the specific heat at constant pressure. (The temperature of a parcel of dry air would change at this rate if it were to move vertically at constant entropy.) The temperature gradient that is relevant for stability is therefore the excess over the adiabatic lapse rate, i.e., $(dT/dz) + (g/c_{\mathrm{p}})$, or the gradient of the potential temperature $T + gz/c_{\mathrm{p}}$. The appropriate definition of Ri in this case is thus

$$\mathrm{Ri} = -\frac{g}{T} \frac{(dT/dz + g/c_{\mathrm{p}})}{(du/dz)^2}. \tag{4.6}$$

Note that if the gradients in these definitions are estimated in terms of characteristic velocity and length scales U and L, Ri is proportional to $gL\Delta\rho/\rho U^2$, which is often called a bulk Richardson number and resembles an inverse Froude number.

A large number of experimental observations quote a critical Ri rather than a critical Rf, presumably because the former is easier to measure. The significance of $\mathrm{Ri}_{\mathrm{cr}}$ is, however, less certain because of the variability of the ratio K_m/K_h [see (4.4)] with stability conditions. Even so, the observed values of $\mathrm{Ri}_{\mathrm{cr}}$ also seem to be fairly low.

We may note in passing that Miles (1961) showed that the sufficient condition for an inviscid stratified flow to be stable is that $\mathrm{Ri} > \frac{1}{4}$ everywhere in the flow.

C. Experimental Observations

Apart from the early work of Prandtl and Reichardt (1934) and the interesting measurements recently reported by Nicholl (1970), there have not been many detailed turbulence measurements in stably stratified turbulent shear flows. By using a hot wire at two widely different temperatures, Nicholl was able to measure both the turbulent intensities and the fluctuating

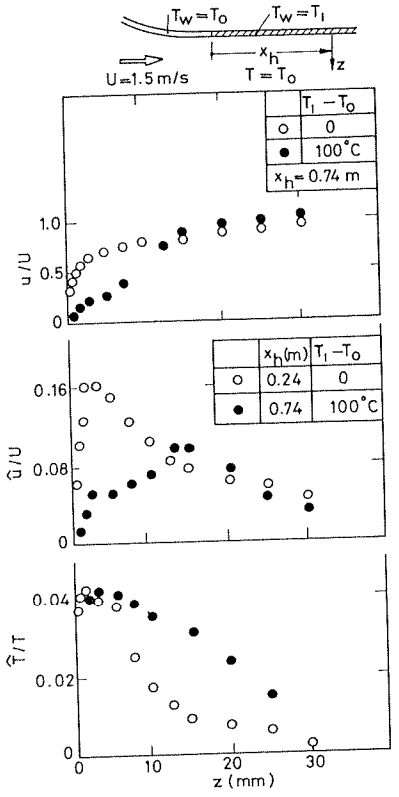

FIG. 12. Suppression of turbulence in the boundary layer on the heated roof of a wind tunnel; experimental data from Nicholl (1970). Note that while velocity fluctuations are much lower on the heated surface, temperature fluctuations are not.

temperature T'. The measurements were made in the boundary layer on the roof of a wind tunnel, a step change in the surface temperature, making it about 100°C hotter than the free stream, subjected an approaching "cold" turbulent boundary (at a momentum thickness Reynolds number of about 600) to a stable stratification beyond a certain streamwise station. Measurements 74 cm (about 25δ) downstream of this station show a large deceleration of the mean flow near the wall, an appreciable drop in $\hat{u}$, and an *increase* in $\hat{T}$ in the outer layer (Fig. 12). The increase in $\hat{T}$ is presumably due to strong vertical motions induced by the deceleration near the surface and the resulting increase in the displacement of the outer streamlines. Interestingly, Nicholl found no significant changes in either the shear stress or the heat flux correlation coefficients,*

$$-\frac{\langle u'w' \rangle}{\hat{u}\hat{w}}, \qquad \frac{\langle w'T' \rangle}{\hat{w}\hat{T}}.$$

* Measurements by Webster (1964), in a flow with uniform velocity and density gradients at a Reynolds number that was perhaps not high enough, show on the other hand an appreciable drop in these correlation coefficients (in particular the heat flux one) with increasing Ri.

Townsend (1958), making an analysis of these (then still unpublished) measurements, plotted distributions of the local gradient Richardson number (4.6) across the boundary layer. The scatter in estimates of Ri was so large that Townsend felt "only the most docile reader would agree . . . that the mean values [of Ri] in the outer parts of the layers are all less than 0.1 in." But using mean gradients, Townsend concluded that the Richardson number just before collapse of turbulence was less than 0.1; indeed, in one of the experiments, at $\mathrm{Ri} \simeq 0.022$ the collapse of turbulence was nearly complete.

In an interesting study of the wake of a circular cylinder towed in stably stratified salt water ($\mathrm{Ri} \simeq 0.15$), Pao (1969) observed that the turbulence created in the near-wake region died away sufficiently far from the cylinder. At a distance of 110 diameters, for example, both large- and small-scale turbulence had collapsed, and the residual motion (as observed by shadowgraph pictures) consisted exclusively of periodic internal waves.

Ellison and Turner (1960) examined the behavior of a layer of dense salt solution introduced through a slot in the floor of a sloping rectangular channel in which there was a main turbulent flow. When the main flow was uphill, the stabilizing effect of the density gradient caused a suppression of the spread of the salt solution. Ellison and Turner showed that their observations on the transfer coefficients of salt and momentum were consistent with a critical value of about 0.15 for the flux Richardson number.

Similar interesting observations have also been made in the atmosphere. Measurements of velocity and temperature distributions across inversions, explicitly showing the disappearance of turbulence, have been reported by Businger and Arya (1974). They estimated Ri_{cr} to be about 0.21. Lyons *et al.* (1964) have reported atmospheric measurements in which turbulence always existed for $\mathrm{Ri} \simeq 0.15$, but was completely absent when $\mathrm{Ri} > 0.5$; presumably the critical value is somewhere in-between.

Another illustrative case is that of a total (or nearly total) solar eclipse. As a result of the sudden cessation of the incoming solar radiation, the ground cools off faster than the air above it, and a stable temperature gradient gets established relatively quickly near the ground. If this cooling of the surface continues, the depth of the stably stratified layer grows, and reaches a height where, presumably, a critical value of Ri is reached. This then results in a sudden decay of turbulence. Measurements made recently during a total (R. Luxton, private communication, 1976) or near-total solar eclipse (Antonia *et al.*, 1979) essentially confirm these expectations (Fig. 13).* An interesting feature of these measurements is the nearly constant time lag between the decay of temperature and velocity fluctuations. The reason probably is that

* Unfortunately, the final stages of the eclipse (which lasted roughly from 1500 to 1700 hr) gradually merged into the normal sunset period, so the return to normal sunny conditions were not obtained.

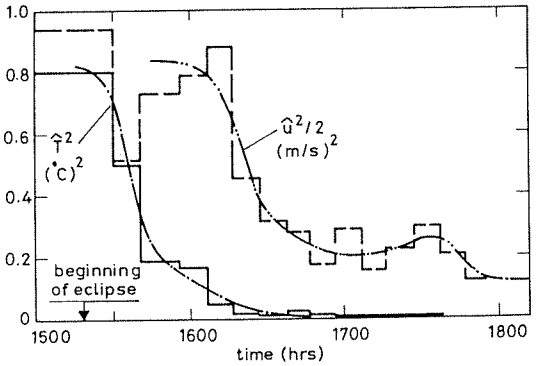

FIG. 13. Decay of velocity and temperature fluctuations during a nearly total solar eclipse (data from Antonia *et al.* 1979). Note how the velocity fluctuations lag behind the temperature fluctuations by a nearly constant time interval (about 50 min).

the temperature fluctuation starts decaying almost instantaneously in response to the cessation of solar radiation, while velocity fluctuations start decaying only after the stably stratified layer has been established and has grown to the height above the ground of the measurement station ($\simeq 4$ m in this case).

V. Reversion in Highly Accelerated Flows

A. Introduction

We now examine a class of reverting flows that do not seem to belong entirely to either of the other two types we have described until now, namely, a turbulent boundary layer subjected to a large favorable pressure gradient or acceleration. In their well-known work on transition from laminar to turbulent flow, Schubauer and Skramstad (1947) and Liepmann (1943, 1945) had already observed how a favorable pressure gradient could suppress incipient turbulence. But the first evidence that a fully turbulent flow subjected to large accelerations may revert to a laminar state appears to have come from experiments at high speeds, such as those of Sternberg (1954) at the shoulder of a cone-cylinder junction and of Sergienko and Gretsov (1959) in an axisymmetric supersonic nozzle. Indeed, Sternberg's remarkable report must have inspired many of the studies that followed in later years. Although we shall defer discussion of high speed flows until Section V,C, it is worthwhile to take a quick look at Figs. 14(a) and (b) which show

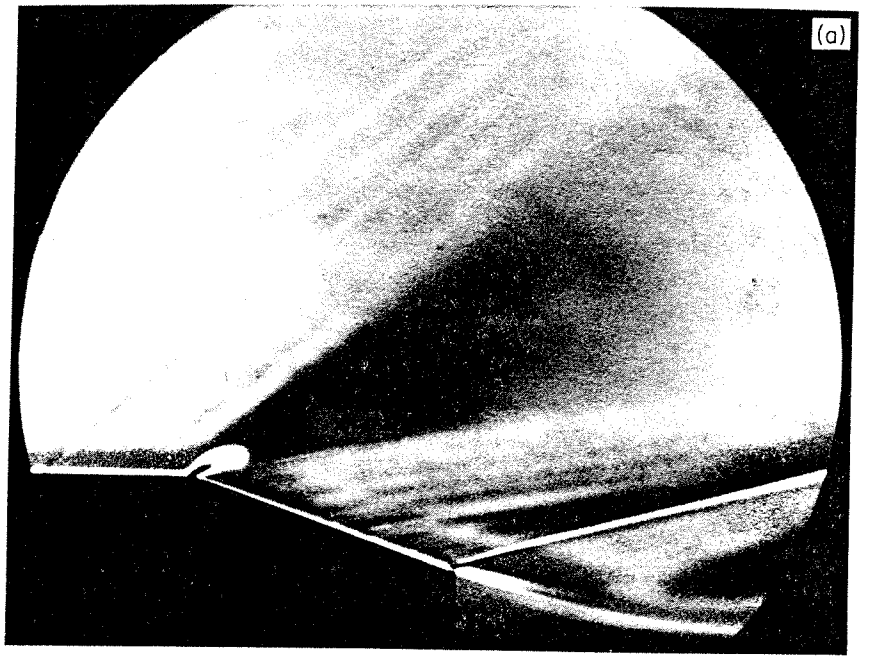

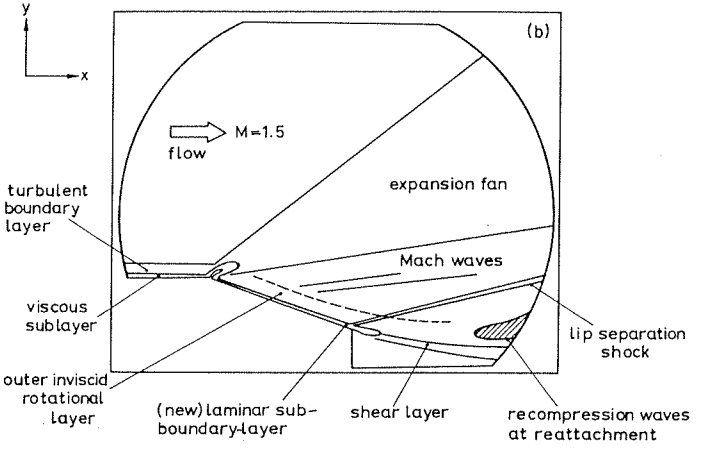

FIG. 14. (a) Schlieren photograph of flow past a boat-tailed step. Note how, downstream of the Prandtl–Meyer corner, a thin streak representing a laminar subboundary-layer grows underneath the thick remnant of the original turbulent boundary layer. (From Viswanath and Narasimha, 1975.) (b) Key to Fig. 14(a).

(among other things) the behavior of an initially turbulent boundary layer as it negotiates a Prandtl–Meyer corner in supersonic flow. The photograph, which is a *schlieren* from Viswanath and Narasimha (1975), shows clearly the generation of a thin new boundary layer downstream of the corner—a layer that measurements of quantities such as wall temperature and surface heat flux show to be essentially laminar. This new laminar layer is embedded underneath the remnant of the original turbulent boundary layer.

It is, however, the flow at low speeds that has been extensively studied in recent years and we examine these first. (For a critical review of the experimental data, see Sreenivasan, 1972.)

B. Low Speed Flows

1. *General Remarks*

To fix our thoughts, consider the situation in which a fully turbulent boundary layer develops at constant pressure up to the point x_0, beyond which a steep favorable pressure gradient is imposed. Observation shows that downstream of x_0 the boundary layer thins down; eventually the velocity profile departs from the well-known law of the wall, the shape factor (H) increases, the skin friction coefficient (c_f) drops, the relative turbulence intensity goes down, and the flow becomes effectively laminar. Figure 15 demonstrates how complete such reversion can be, in terms of the velocity profile.

Many detailed studies of such flows have been made in the last 15 years, but different workers have used different methods for recognizing the onset of relaminarization, and proposed different parameters as criteria for the

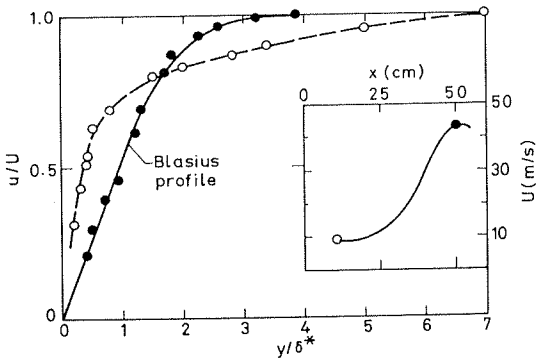

FIG. 15. Relaminarization in accelerated boundary layer flow: velocity profiles just before and after acceleration, shown in inset. (Data from Ramjee, 1968.)

occurrence of reversion (see Table I: some of the symbols used here will be defined as we proceed). The large majority of these proposals involve the viscosity of the fluid, and so can be interpreted as some kind of Reynolds number: the differences therefore lie in the choice of length and velocity scales. The original flow being turbulent, it offers both the free stream velocity U and the friction velocity U_* as velocity scales, and because the perturbation is a *function* describing the pressure distribution $p(x)$, many choices are possible for the scales that may form the Reynolds number. One of the most widely used parameters, namely

$$K = \nu U'/U^2, \qquad U' \equiv dU/dx, \tag{5.1}$$

where $U(x)$ is the free stream velocity, carries no information at all about the boundary layer whose reversion is the object of study: it is purely a free stream parameter (and, for that reason, a very convenient one to use). Various combinations of K and the skin friction coefficient c_f, of the form Kc_f^{-n} with n varying between $\frac{1}{2}$ and $\frac{3}{2}$, have also been suggested (Back *et al.*, 1964; Launder and Stinchcombe, 1967), but it is clear that the general approach has been, "Seek the Reynolds number."

The difficulties with some of these proposals have been discussed by Narasimha and Sreenivasan (1973). It is eminently reasonable that departure from the standard log-law in the wall layer depends on the pressure gradient non-dimensionalized with respect to the wall variables,

$$\Delta p = \nu p_x/U_*^3, \qquad p_x \equiv dp/dx, \tag{5.2}$$

as suggested by Patel (1965). However, as pointed out by Narasimha and Sreenivasan (1973), this parameter reaches a minimum *upstream* of where Patel and Head (1968) infer reversion to have occurred—so that the suggested critical value for $-\Delta_p$ has already been encountered once, and exceeded, before reversion apparently occurs. (Note that in favorable pressure gradients $p_x < 0$.) The same objection applies also to the later proposal of Patel and Head (1968), which replaces dp/dx in (5.2) by $\partial\tau/\partial y$:

$$\Delta_\tau = \frac{\nu}{U_*^3}\frac{\partial \tau}{\partial y}. \tag{5.3}$$

There is in this case the further difficulty of measuring or estimating $\partial\tau/\partial y$ in relaminarizing flows.

While these parameters are certainly useful in indicating when the flow begins to depart from the standard constant-pressure laws, we must recognize that such departures may not necessarily imply reversion, although they must certainly precede it. Such "standard" laws are often based on assumptions (e.g., matching similarity solutions) that are only asymptotically valid at large Reynolds numbers, if not on fairly specific models (e.g., mixing length)

TABLE I

STUDIES OF HIGHLY ACCELERATED LOW-SPEED BOUNDARY LAYERS

Reference	Flow studied	Method of identification of reversion	Proposed criterion for reversion
Wilson and Pope (1954)	Turbine nozzle cascade	Reduction in heat transfer coefficient	—
Senoo (1957)	Turbine nozzle cascade	Reduction of high frequency part of turbulent signal in throat region of nozzle	—
Launder (1963, 1964)	Two-dimensional nozzle flow	—	$K = \nu U'/U^2 \gtrsim 2 \times 10^{-6}$ for about 20δ
Schraub and Kline (1965)	Two-dimensional boundary layer flow in a water-channel	Cessation of bursting in wall region	$K/c_f^{1/2}$; $K \gtrsim 3.5 \times 10^{-6}$
Moretti and Kays (1965)	Two-dimensional nozzle flow	Failure of a Stanton number prediction procedure	$K \gtrsim 3.5 \times 10^{-6}$
Patel (1965)	Accelerated wall layer in pipe flow	Breakdown of log-law in wall layer	$-\Delta_p = -\nu p_x/U_*^3 = K(2/c_f)^{3/2} \gtrsim 0.025$
Patel and Head (1968)	Accelerated wall layer in pipe flow	Departure of wall-layer flow from a modified wall law	$-\Delta_\tau = -\frac{\nu}{U_*^3}\frac{\partial \tau}{\partial y} \gtrsim 0.009$
Fielder and Head (1966)	Accelerated turbulent boundary layer	Spreading of intermittency to wall region	
Launder and Stinchcombe (1967)	Sink-flow boundary layer	Departure from normal turbulent boundary layer characteristics	$Kc_f^{-3/2}$
Back and Seban (1967)	Highly accelerated boundary layer	Reduction of heat transfer and skin-friction below that given by a standard prediction procedure	$K \gtrsim 3 \times 10^{-6}$
Bradshaw (1969a)	Highly accelerated boundary layer	Overlapping of energy containing and dissipating eddy scales	$\tau^2/\nu\varepsilon \lesssim 12$
Badri Narayanan and Ramjee (1969)	Highly accelerated boundary layer	Decrease in $(\bar{u}/U)$ sub	$\mathrm{Re}_\theta \lesssim 300$
Narasimha and Sreenivasan (1973)	Highly accelerated boundary layer	Flow described by quasi-laminar limit	$\Lambda = -p_x\delta/\tau_0 \gtrsim 50$
Okamoto and Misu (1977)	Boundary layer in contraction	Departure from log-law	—
Simpson and Shackleton (1977)	Nozzle flow	Cessation of entrainment	—

whose limitations are well known. It is possible that such departures merely indicate that these assumptions are not valid or that the flow is abnormal in some sense, rather than that there is reversion.

If the criterion for reversion is a Reynolds number, it is implied from our discussion in Section III that viscous dissipation exceeds production. Measurements of the turbulent energy balance in an accelerated boundary layer, reported by Badri Narayanan, *et al.* (1974), show however that the dissipation always remains smaller. Figure 16 compares the energy budget at a station where $K \simeq 2.8 \times 10^{-6}$ with that at zero pressure gradient, $K = 0$. All contributions to the budget are nondimensionalized here by the outer scales U and δ, it is seen that while both production and dissipation are reduced in these units, their distributions across the boundary layer remain similar, and dissipation remains smaller. Certain changes in advection and diffusion may be noticed, but, except possibly in the region $y/\delta < 0.1$ which is not covered by the measurements, the observed phenomena cannot be attributed to dissipation.

We need to consider also whether energy production decreases because of a favorable pressure gradient. From (2.5), it can be shown that the relevant terms in two-dimensional flow are

$$q: -\langle u'v' \rangle \frac{\partial u}{\partial y} - (\hat{u}^2 - \hat{v}^2) \frac{\partial u}{\partial x}; \tag{5.4}$$

the last term is negative if $\hat{u} > \hat{v}$, $\partial u/\partial x > 0$. In the energy balance measurements cited above, this term was found to be negligible. More generally,

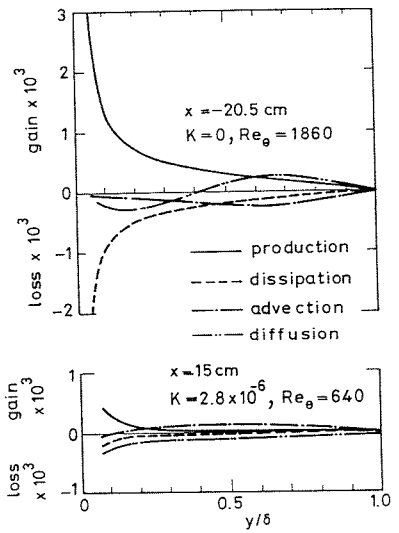

FIG. 16. Turbulent energy balance in constant pressure and accelerated boundary layers; all terms scaled on outer variables U, δ. (Data from Badri Narayanan *et al.*, 1974) $K = 0$ at $x = -20.5$ cm, $K = 2.8 \times 10^{-6}$ at $x = 15$ cm.)

one may define, in analogy with the flux Richardson number (4.4), a parameter that measures the ratio of the "absorption" to the production:

$$\chi = \frac{(\hat{u}^2 - \hat{v}^2)\,\partial u/\partial x}{-\langle u'v' \rangle\,\partial u/\partial y}. \tag{5.5a}$$

At $y_+ \simeq 15$, where the production in a constant-pressure boundary layer is largest, the value of this parameter is estimated by Back *et al.* (1964) to be

$$\chi \simeq \frac{22\nu}{U_*^2}\frac{\partial U}{dx} = 44\frac{K}{c_f}. \tag{5.5b}$$

This shows that for χ to be of order unity, K would have to be about 10^{-4}; in the many flows where reversion has been observed at $K \simeq 3 \times 10^{-6}$, the absorption could clearly have been no more than a few percent where the production is largest. (This conclusion may not be valid in the outer layer; see Section V,B,3.)

Finally, we may note that in accelerated flows there is no evidence of any significant decorrelation among the components contributing to the Reynolds shear stress; Fig. 17 shows that over much of the boundary layer C_τ remains constant at about 0.5 in zero as well as favorable pressure gradients.

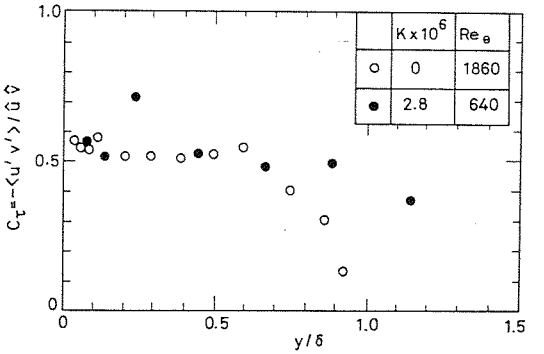

FIG. 17. Shear stress correlation coefficient at two stations (same as in Fig. 16) in a reverting accelerated boundary layer. (Data from Badri Narayanan *et al.*, 1974.)

From considerations such as these, Narasimha and Sreenivasan (1973) were led to propose that reversion in such flows is primarily the result of the domination of pressure forces over nearly frozen Reynolds stresses, rather than of absorption or dissipation, although these could contribute (especially the latter near the wall). They noted first that the completion of the process of reversion has a fairly definite meaning, for it certainly occurs, for the mean flow, when the net effect of the Reynolds stresses is negligible. Random fluctuations inherited from previous history will remain, but they

are no longer relevant to the dynamics of the flow, which under these circumstances may be said to have reached a quasi-laminar state.

2. The Mean Flow

In this approach, we first formulate such a quasi-laminar limit for sufficiently large values of a pressure gradient parameter

$$\Lambda = -\frac{\delta}{\tau_0}\frac{dp}{dx}, \tag{5.6}$$

where δ is the boundary layer thickness and τ_0 the wall stress in the boundary layer just before the pressure gradient is applied. The two-dimensional turbulent boundary layer equations

$$\frac{\partial u}{\partial x} + \frac{\partial v}{\partial y} = 0,$$

$$u\frac{\partial u}{\partial x} + v\frac{\partial u}{\partial y} = -\frac{dp}{dx} + \nu\frac{\partial^2 u}{\partial y^2} + \frac{\partial \tau}{\partial y} \tag{5.7}$$

then split, in the limit $\Lambda \to \infty$, to an outer inviscid but rotational flow

$$u\frac{\partial u}{\partial x} + v\frac{\partial u}{\partial y} = -\frac{dp}{dx}, \tag{5.8a}$$

and an inner viscous flow governed by

$$u\frac{\partial u}{\partial x} + v\frac{\partial u}{\partial y} = -\frac{dp}{dx} + \nu\frac{\partial^2 u}{\partial y^2}, \tag{5.8b}$$

i.e., there is a laminar subboundary-layer underneath a sheared inviscid flow. The boundary conditions for the two equations have to be obtained by the method of matched asymptotic expansions. Solutions are quite easily worked out for any given initial flow (Narasimha and Sreenivasan, 1973).

These solutions turn out to be remarkably effective in describing the flow parameters, but before showing this, let us note two very simple consequences of (5.8a), which implies the conservation of total head and vorticity along each streamline in the outer flow. From the former, it follows that the velocity at the edge of the inner layer, say $U_s(x)$ [the inner limit of the solution of (5.8a)], increases downstream sufficiently rapidly that the difference $U(x) - U_s(x)$ decreases. To conserve vorticity, therefore, the boundary layer must thin down. Correspondingly, also the outer edge of the (whole) boundary layer must be a streamline, and the entrainment must vanish (to the lowest order in Λ^{-1}, of course). Thus the total mass flux in the boundary layer, proportional to $U(\delta - \delta^*)$ where δ^* is the displacement thickness, must also remain constant; as δ^* is quite small compared to δ in flows of this kind,

it follows that the boundary layer Reynolds number $U\delta/\nu$ should not show large streamwise variations. Thus we have a flow in which different Reynolds numbers behave in different ways: Ux/ν increases, $U\theta/\nu$ (θ = momentum thickness) decreases, $U\delta/\nu$ varies little, and Δ_p^{-1} first decreases and then increases!

All of these deductions are largely verified by experiment: Fig. 18a,b show representative comparisons for various boundary layer mean flow parameters. The good agreement seen here demonstrates the value of looking at

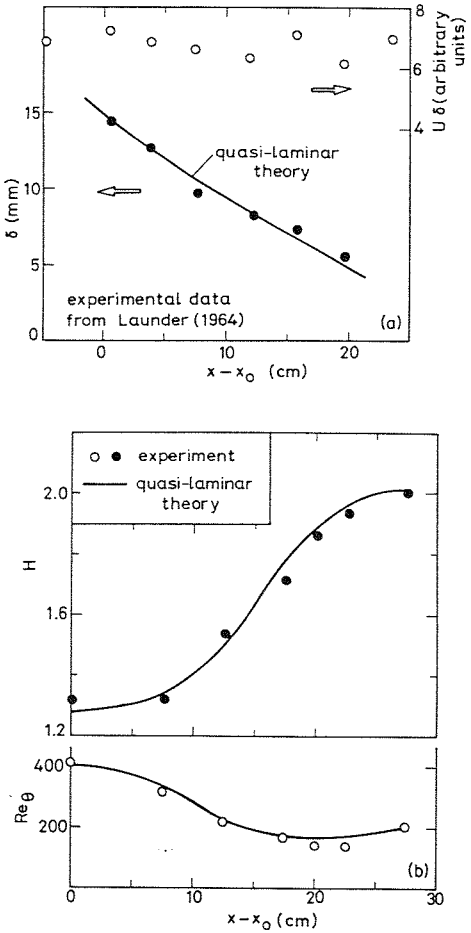

FIG. 18. (a) Streamwise variation of boundary layer thickness and the Reynolds number $U\delta/\nu$ (arbitrary units) in reverting accelerated boundary layer. (b) Streamwise variation of boundary layer Reynolds number and shape factor: comparison between experiment (Badri Narayanan and Ramjee, 1968, run 3) and theory. (From Narasimha and Sreenivasan, 1973.)

reversion as the generation of a new laminar boundary layer, rather as in the extreme case depicted in Fig. 14.

The position regarding wall variables, like the skin friction and heat flux, is slightly different. Figure 19 shows how the skin friction coefficient rises at first as the free stream accelerates, exactly as any reasonable turbulence model suggests [in the present case, the method of Spence (1956) has been used to provide estimates]. However, it is observed that thereafter c_f reaches a maximum and plunges steeply down, in accordance with the quasi-laminar theory, whose predictions are in excellent agreement with measurement especially beyond the point where $\Lambda \simeq 50$. Still further downstream, as the pressure gradient falls, c_f rises once more as the flow goes back to turbulence—note the last experimental point in the diagram! A detailed stability analysis (Narasimha and Sreenivasan, 1973) shows that this retransition occurs very near the point where instability might be expected to set in in the inner laminar boundary layer. Clearly, the maintenance of an effectively laminar inner layer in spite of the highly disturbed state of the flow above it must be attributed to the strong stabilizing influence of the favorable pressure gradient. Corresponding, the slightest sign of instability in the inner layer is all that is required to trigger sufficient energy production to cause quick retransition.

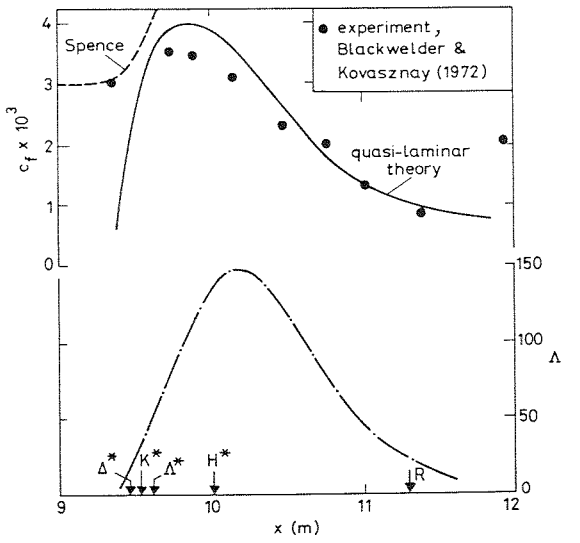

FIG. 19. Variation of skin friction coefficient in a relaminarizing boundary layer: comparison with quasi-laminar theory. Markers on the abscissa denote location of following events. $\Delta^*:\Delta_p = -0.025$; $K^*:K = 3 \times 10^{-6}$; $\Lambda^*:\Lambda = 50$; H^*: minimum in H; R: retransition to turbulence. (From Sreenivasan, 1974.)

3. *The Turbulence Quantities*

An interesting part of this quasi-laminar theory is the ability to predict the turbulence quantities during decay. Consider first the inner layer. Very close to the surface, there is a spanwise structure in the turbulent flow; the length scale of this structure is of order $250\nu/U_*$ during reversion, according to the measurements of Schraub and Kline (1965). Although this length could be small compared to the boundary layer thickness, it is about 10 times larger than the height where the intensity $\hat{u}$ is a maximum. It is therefore conceivable that the fluctuating motion in the inner layer is approximately two-dimensional.

We assume further that it is quasi-steady, which is again plausible as the high-frequency components of the motion are known to decay fast (Launder, 1964). Now the development of *steady* perturbations on a laminar boundary layer has been studied by Chen and Libby (1968); by solving the appropriate eigenvalue problem, they find that, if the basic flow belongs to the Falkner–Skan family $U_s \sim (x - x_0)^m$, the maximum value of the perturbation velocity decays like

$$U_s(x - x_0)^{-\frac{1}{2}(1+m)\lambda_1}, \tag{5.9}$$

where $\lambda_1 = \lambda_1(m)$ is the lowest eigenvalue for the flow. Higher modes decay faster. We may now expand the velocity fluctuation $u'(x_0, t; y)$ at some initial x_0 in a series of the Chen–Libby eigenfunctions. The first term in this expansion, corresponding to the lowest mode, will eventually dominate the higher modes decaying faster, so that the fluctuation intensity $\hat{u}$ finally obeys the inverse power law suggested by (5.9). In those experiments where the above Falkner–Skan assumption is a reasonable approximation for the inner layer, the decay of $\hat{u}$ is indeed found to follow (5.9); Figure 20 shows a comparison.*

In other words, the fluctuating motion in the inner layer appears to be a random low frequency oscillation excited by the ambient turbulence.

Although the basic assumptions of this section cannot all be rigorously justified, experimental data show that it contains a large measure of truth.

In the outer layer, conditions are closer to what is known as rapid distortion theory (e.g., Batchelor and Proudman, 1954), in which both inertial and viscous forces are ignored. Sreenivasan (1974) has estimated that the time of flight of a particle through the region of pressure gradient in reverting flows (e.g., those reported by Badri Narayanan and Ramjee, 1969; Blackwelder and Kovasznay, 1972) is a fifth to a tenth of a characteristic time scale

* The same theory also predicts that the location of the maximum $\hat{u}$ scales on the thickness of the inner laminar layer; this is also borne out roughly by experiment (see Narasimha and Sreenivasan, 1973).

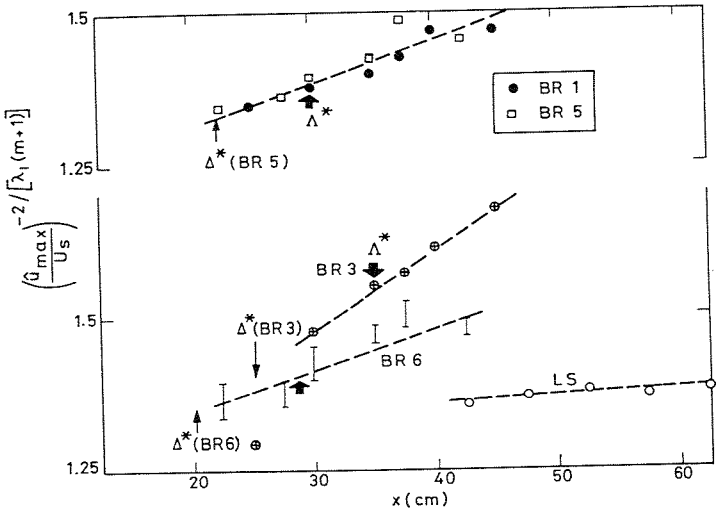

FIG. 20. Decay of velocity fluctuations in inner layer during relaminarization. Points are data from various experiments; theory suggests the points should lie on straight lines. (From Narasimha and Sreenivasan, 1973.) BRn indicates the nth run of Badri Narayanan and Ramjee (1969).

TABLE II

RELATIVE RAPIDITY OF DISTORTION IN VARIOUS FLOWS

Source	Type	Rapidity parameter[a]
MacPhail (1944)	Grid turbulence	0.29–0.83
Dryden-Schubauer (1947)	Grid turbulence	0.67
Hall (1938)	Grid turbulence	0.83
Townsend (1954)	Grid turbulence	1.0
Uberoi (1956)	Grid turbulence	3.3
Ramjee *et al.* (1972)	Channel flow	5.9
Badri Narayanan and Ramjee (1969)	Boundary layer flow	5.5
Blackwelder and Kovasznay (1972)	Boundary layer flow	10.0
Crow (1969)	Sonic boom propagating in the atmosphere	10^2 or more

[a] Defined as $l/\hat{u}t_f$, where l is a characteristic size of energy-bearing eddies, t_f is the time of flight of a fluid particle through distortion. Estimates of parameter from Sreenivasan (1974).

for the energy containing eddies; the distortion is therefore relatively rapid, certainly more so than in many grid turbulence experiments set up to study rapid distortion, as the accompanying Table II shows. Figure 21 shows a comparison of the observed variation of $\hat{u}$ in a rapidly accelerated flow with that predicted by a straight application of the rapid distortion theory of Batchelor and Proudman (1954) for initially isotropic turbulence. The assumption of isotropy in calculating the effect of rapid distortion on each component of the energy yields reasonable results even when the turbulence is not strictly isotropic, as Sreenivasan and Narasimha (1978) have shown.

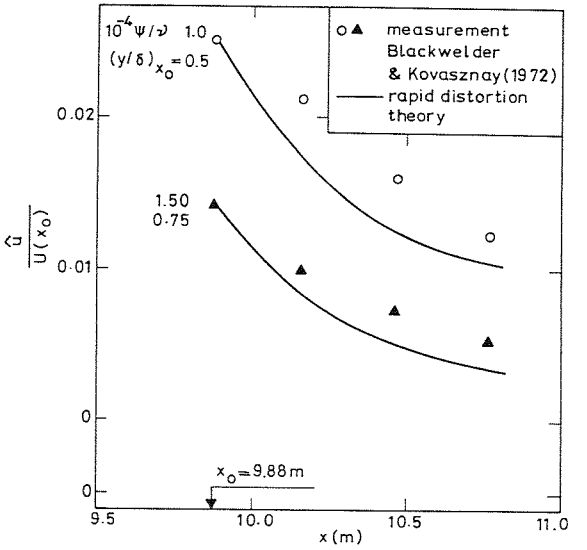

FIG. 21. Variation of turbulence intensity in outer layer. Measurements of Blackwelder and Kovasznay (1972) compared with rapid distortion theory; ψ = stream function.

A simple approximation to the dynamics of such rapid distortion of a *sheared* flow is obtained by ignoring all viscous and nonlinear terms (including in the latter the pressure diffusion term also) in the stress transport equation (2.3), and considering the limit when the strain ratio $(U - U_s)/U'\delta$ is small. (This implies that in the outer flow $\partial u/\partial x \gg \partial u/\partial y$.) We then obtain (Sreenivasan and Narasimha, 1974)

$$\frac{d}{dt}\hat{u}^2 = -2\hat{u}^2\frac{\partial u}{\partial x} + \left[2\tau\frac{\partial u}{\partial y}\right], \tag{5.10a}$$

$$\frac{d}{dt}\hat{v}^2 = 2\hat{v}^2\frac{\partial u}{\partial x}, \tag{5.10b}$$

$$\frac{d}{dt}\hat{w}^2 = 0, \tag{5.10c}$$

$$\frac{d}{dt}q = 0, \tag{5.10d}$$

$$-\frac{d}{dt}\langle u'v'\rangle = \left[\hat{v}^2\frac{\partial u}{\partial y}\right], \tag{5.10e}$$

where the terms in square brackets are one order higher in the strain ratio. To the lowest order, therefore, $\hat{u}$ goes down by the working of the pressure gradient against the normal Reynolds stress, $\hat{v}$ goes up for the same reason; and $\hat{w}, q$, and the shear stress are frozen along each streamline. To the next order, there is a small production of both $\hat{u}$ and τ. Experiment shows reasonable agreement with these predictions. In fact, recent measurements in such a reverting flow (Badri Narayanan *et al.*, 1974) show, consistently, a small drop in $\hat{u}$, a small increase in $\hat{v}$ and hardly any change in either the stress $-\langle u'v'\rangle$ (Fig. 22) or (as we have already noted) the correlation coefficient C_τ.

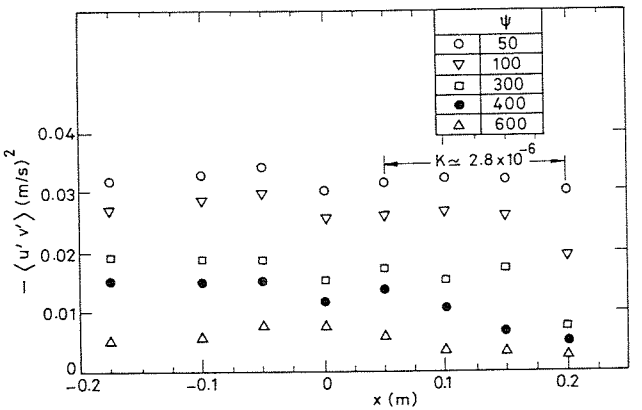

FIG. 22. Variation of Reynolds shear stress in accelerated boundary layer (measurements by Badri Narayanan *et al.*, 1974). Stream function ψ in arbitrary units, in which the edge of the boundary layer is at approximately $\psi = 700$. (Note that in these accelerated flows the edge of the boundary layer is itself a stream line to a good approximation.)

A combination of such a rapid distortion theory in the outer layer, with an eigenfunction theory in the inner layer, produces turbulence intensity predictions in good agreement with observation for the longitudinal intensity (Fig. 23). The theory is not quite as successful for the normal component, in this as in other rapidly distorted flows.

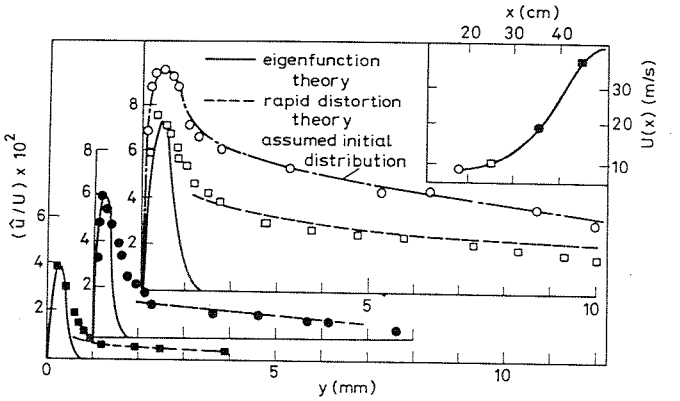

FIG. 23. Comparison of measured $\hat{u}$ distribution (Badri Narayanan and Ramjee (1969), run 3), with calculations using rapid distortion theory in the outer layer and eigenfunction theory in the inner layer (From Narasimha and Sreenivasan, 1973.)

We may in summary divide the flow in highly accelerated boundary layers into different regions as shown in Fig. 24. Region I is fully turbulent; region III is quasi-laminar—in the outer layer it is valid almost from the beginning of the pressure gradient at x_0. Thus, in a narrow but justifiable sense reversion in the outer flow can be said to occur almost immediately after the acceleration at x_0. (It is this kind of behavior that makes the proposals listed in Table

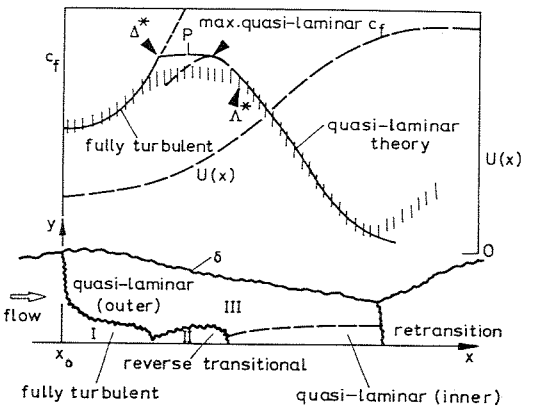

FIG. 24. Flow regimes in reverting boundary layer subjected to acceleration. The variation of true c_f (shown hatched) is predicted closely by fully turbulent theory up to the point Δ^* (corresponding to $\Delta p = -0.025$), and by quasi-laminar theory after the point Λ^*, corresponding to $\Lambda = 50$. The gap between the two theories is patched by a region P of constant c_f. (From Narasimha and Sreenivasan, 1973.)

I seem like an excessive preoccupation with the Reynolds number.) There is only a small bubble-shaped region (numbered II) near the wall where neither the fully turbulent nor the quasi-laminar solution is valid. It is only this region that needs to be modeled more elaborately; but it does not strongly affect many important mean flow characteristics (e.g., the various thicknesses), which can be determined without invoking specific models for turbulence. The reason for such success is chiefly that the turbulence, especially in the outer region, is distorted rather than destroyed by the acceleration, and the Reynolds shear stress is nearly frozen. The reversion observed is thus essentially due to the domination of pressure forces over the slowly responding Reynolds stresses in an originally turbulent flow, accompanied by the generation of a new laminar boundary layer stabilized by the favorable pressure gradient.

4. *Burst Parameters*

Kline *et al.* (1967) have suggested that relaminarization in accelerated flows is associated with the cessation of turbulent bursting. They have correlated the rate of occurrence of bursts per unit span, F [measured by Schraub and Kline (1965) in a boundary layer subjected to a "strongly favorable pressure gradient"], with the acceleration parameter K, and deduced by extrapolation a critical value $K_{cr} \simeq 3.5 \times 10^{-6}$ at which bursting ceases. In coming to such conclusions, the burst parameter has to be assessed against an appropriate scale; Kline *et al.* (1967) suggest a wall scaling

$$F_+ = F\nu^2 U_*^{-3},$$

but Narasimha and Sreenivasan (1973) have shown that an equally appropriate scaling is

$$\tilde{F} = F\nu\delta^*/UU_*,$$

based on the argument that while the lateral spacing of bursts scales on wall variables, the temporal rate scales on outer variables (as shown by Rao *et al.*, 1971). Further, Narasimha and Sreenivasan (1973) found that, whatever scaling is used, the burst parameter falls exponentially in Λ over the whole range covered by the available data (Fig. 25); no critical station in the flow can be identified, nor can an obvious extrapolation to $F = 0$ made. This, of course, is consistent with our earlier description of relaminarization in accelerated flows as an asymptotic process. In particular, in the experiment reported by Schraub and Kline (1965), the skin friction coefficient was still rising at the last measurement station in the flow, and the parameter Λ had not exceeded 30, suggesting that reversion was not complete in the sense of Section V,B,2. It would therefore appear that there is an exponential decrease in the bursting rate in an accelerated turbulent boundary layer before the wall variables begin to assume quasi-laminar values.

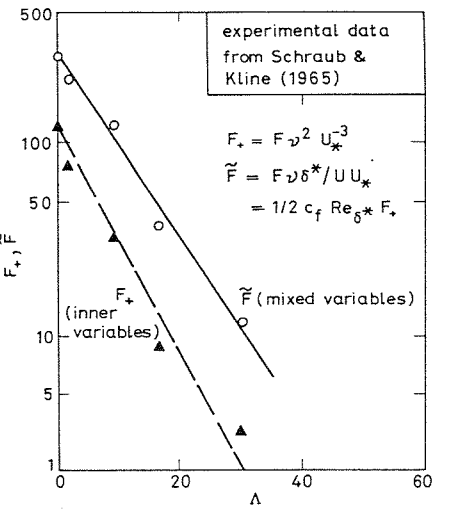

FIG. 25. Burst parameters in accelerated flow: F = number of bursts per unit time, unit span. (From Narasimha and Sreenivasan, 1973.)

There is unfortunately no direct evidence on the effect of a favorable pressure gradient on the time rate of occurrence N_b of bursts at a given point in the flow. Badri Narayanan *et al.* (1974, 1977) report an average frequency (say N_p) for the occurrence of high frequency pulses in filtered u' signals, obtained according to a technique developed by Rao *et al.* (1971). These measurements show that the parameter $N_p\delta/U$ decreases with downstream distance in the region of strong acceleration. This is consistent with the conclusions of Kline *et al.* if $N_p \simeq N_b$, as Rao *et al.* found in the constant-pressure boundary layer. However, as no estimate of the spacing of the wall-layer streaks was obtained by Badri Narayanan *et al.*, F^+ cannot be estimated and hence no direct comparisons can be made.

A rapid (although not catastrophic) drop in the bursting rate is also significant from another point of view. With the cessation of eruptions from the inner layer, and also of the sweeps from the outer layer, there is little or no interaction between the two layers. It thus appears quite justified to ignore the usual transfer processes between the two layers, as is implicitly assumed in the quasi-laminar theory of Narasimha and Sreenivasan (1973).

Simpson and Wallace (1975) and Simpson and Shackleton (1977) have recently reported certain measurements that must be mentioned here. These authors evaluated the frequency (say N_s) corresponding to the peak in the first moment $nF_u(n)$ of the spectral density $F_u(n)$ of the streamwise velocity fluctuation u', and assume that $N_s \simeq N_b$. This assumption was based on the work of Strickland and Simpson (1975) in a constant pressure boundary

layer, where N_b itself had in turn been inferred from an assumed correspondence with the second peak in the short-time autocorrelation function of the wall shear stress. Simpson and Wallace and Simpson and Shackleton also obtained an estimate of the average spacing of the wall-layer streaks. Based on these assumptions it is possible to estimate a parameter equivalent to F mentioned above. In the accelerated flow, it was found that this quantity actually *increases* downstream, contrary to the trend that one expects from the other measurements.

Perhaps these measurements are too indirect to provide a convincing indication of the behavior of the burst rate in accelerated flows; there is need for further work before any firm conclusion can be drawn.

C. Supersonic Flows

These ideas that have proved so successful at low speeds appear to work well at high speeds too, although here detailed turbulent structure measurements are rarely available: the one exception is Morkovin's (1955) work on the interaction between an expansion fan and a turbulent boundary layer on a flat plate. In the Prandtl–Meyer flow past a corner, Sternberg (1954) found a significant drop in the recovery factor downstream; others have found marked changes in boundary layer velocity profiles (Vivekanandan, 1963), in base pressure in sharply boat-tailed bases (Viswanath and Narasimha, 1972), and in heat transfer rates (Zakkay *et al.*, 1964).

The basic idea in Section V,B,1, namely, that during high acceleration the Reynolds stresses over a large part of the boundary layer have little influence on mean flow development, should be valid with even greater force in supersonic flow past an expansion corner, where the pressure gradients are extremely large. Indeed the parameter suggested there as relevant, namely $\Lambda = -p_x \delta/\tau_0$, takes on a simpler form in supersonic corner flow. For, the interaction of the expansion fan with the boundary layer spreads the pressure drop Δp (here considered positive in an expansion, for convenience) over a few boundary layer thicknesses. The extent of this region appears to be relatively insensitive to the total corner flow deflection, from the work of Ananda Murthy and Hammitt (1958). Thus, p_x is of order $\Delta p/\delta$, and Λ is of order $\Delta p/\tau_0$. This reasoning suggests that reversion will occur if $\Delta p/\tau_0$ is sufficiently large. (An alternative approach is to realize that in Prandtl–Meyer flow p_x is nearly a Dirac delta function, and a mean value of Λ would be proportional to $\Delta p/\tau_0$.)

To test this argument, all available experimental data were examined by Viswanath and Narasimha (1975), taking reversion to have occurred if there is evidence either of the growth of a thin new shear layer from the corner, or of an appreciable change in the associated flow characteristic downstream

(e.g., turbulence intensity in boundary layer or base pressure). This definition is not as precise as one may desire, but nothing better is possible at present, and it certainly seems appropriate for engineering calculations.

Using estimates of τ_0 from Tetervin (1967), Narasimha and Viswanath (1975) have plotted these data as shown in Fig. 26 (which is their Fig. 1 with some additional data). Here points are shown (i) as filled symbols where authors reported indication of reversion, (ii) as filled, flagged symbols when reversion is inferred by us, and (ii) as open symbols when no evidence of reversion can be found. It is seen that all points above the line $\Delta p/\tau_0 = 75$ show reversion, those below $\Delta p/\tau_0 = 60$ show no evidence of it, and in-between there are both types. It thus appears that reversion occurs if Δp is more than about $70\tau_0$. Once again, this is clearly a case of reversion by domination of pressure forces over the Reynolds shear stress.

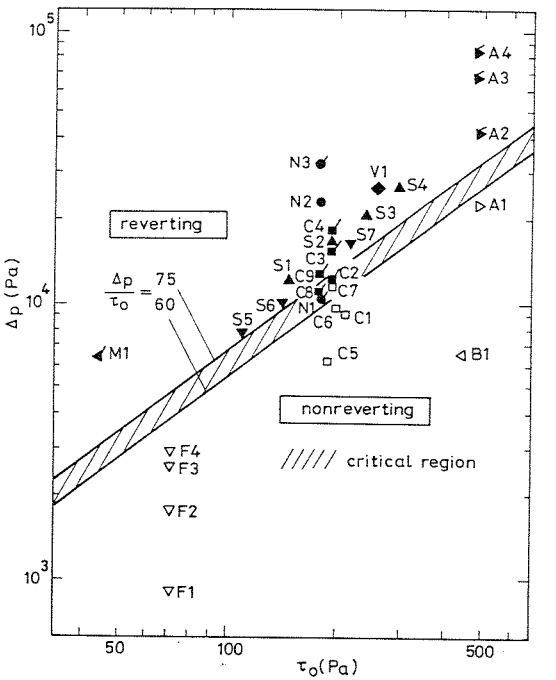

FIG. 26. Pressure drop and wall stress just upstream of corner in supersonic flow past an expansion corner. Filled symbols indicate reversion reported by authors; filled, flagged symbols reversion inferred by us; open symbols no evidence of reversion. Code for experimental points: A, Ananda Murthy and Hammitt (1958); B, Bloy (1975); C, Chapman *et al.* (1952); F, Fuller and Reid (1958); M, Morkovin (1955); N, Viswanath and Narasimha (1972); S, Sternberg (1954); V, Vivekanandan (1963). (After Narasimha and Viswanath, 1975.) The numerical suffix in each case indicates the experimental run.

As pointed out by Sternberg (1954), we may expect that turbulence passing through the expansion fan will be rapidly distorted. Interestingly, as the streamlines spread *apart* during acceleration in supersonic flow, the turbulence is stretched along as well as normal to the flow, leading to a reduction in the turbulent intensity. Such reductions have recently been measured by Gaviglio *et al.* (1977) in their study of a supersonic near-wake; their observations are consistent with the criterion proposed by Narasimha and Viswanath (1975).

D. Concluding Remarks

One striking feature of reversion in highly accelerated flows is that it is not catastrophic, but rather gradual and asymptotic. No unique "point of reversion" can be identified, as it can in direct transition (Narasimha, 1957; Dhawan and Narasimha, 1958). Nevertheless, the process is more rapid than dissipative reversion; typically, in many flows, the shape factor H may reach a minimum in a streamwise distance of the order of 10–20 initial boundary layer thicknesses from the commencement of acceleration, and a maximum in an additional distance of a similar order. There can, of course, be considerable variation in these distances.

We also note that the two pressure gradient parameters K, Λ introduced above are related to each other through the Reynolds number $\mathrm{Re}_\delta \equiv U\,\delta/\nu$:

$$\Lambda = 2K\,\mathrm{Re}_\delta/c_f. \tag{5.11}$$

Most laboratory experiments are carried out at about the same Re_δ (of order 10^4); it is thus difficult to discriminate between the various criteria that have been listed in Table I. If Λ governs the completion of reversion, as argued by Narasimha and Sreenivasan (1973), then according to (5.11) the value of K required for reversion should decrease as Re_δ increases. Although there is as yet no convincing evidence for this prediction, some support is available from certain experiments reported by Nash-Webber and Oates (1972) on nozzle boundary layers. They found that an increase in blowing pressure from 5 to 20 in. Hg abs. (which roughly doubled the Reynolds numbers) brought down the K at the beginning of reversion (identified as the point of minimum H) from about 5.7×10^{-6} to about 2.3×10^{-6} (see Fig. 7 of their paper). This is the trend predicted by the "domination" theory.*

* The final diagram presented by Nash-Webber and Oates appears to contradict this, as the boundary of the laminarizing region in the K–Re plane shows K increasing with Re. However, this region is inclusive, in the sense that reversion does not necessarily occur at the boundary, but somewhere *within* it; hence a relation between K and Re *at* reversion cannot be inferred from the diagram.

This seems to imply that relaminarization should be easier to achieve at higher Reynolds numbers, but note that it would be harder to maintain it, because the Reynolds number of the laminar subboundary-layer would be correspondingly higher and so retransition would also be quicker!

VI. Curved Flows

A. Radial Poiseuille Flow

Consider the flow between two parallel disks, with fluid coming in at the center and moving radially out, as shown in the inset to Fig. 27. If $\bar{U}$ is the mean velocity at radius r, $2a$ is the separation between the disks and $Q = 4\pi r a \bar{U}$ the total volume flow of the fluid, the local Reynolds number of the flow varies inversely with the radius:

$$\mathrm{Re}(r) \equiv a\bar{U}(r)/\nu = Q^* a/r, \qquad Q^* = Q/4\pi\nu a, \tag{6.1}$$

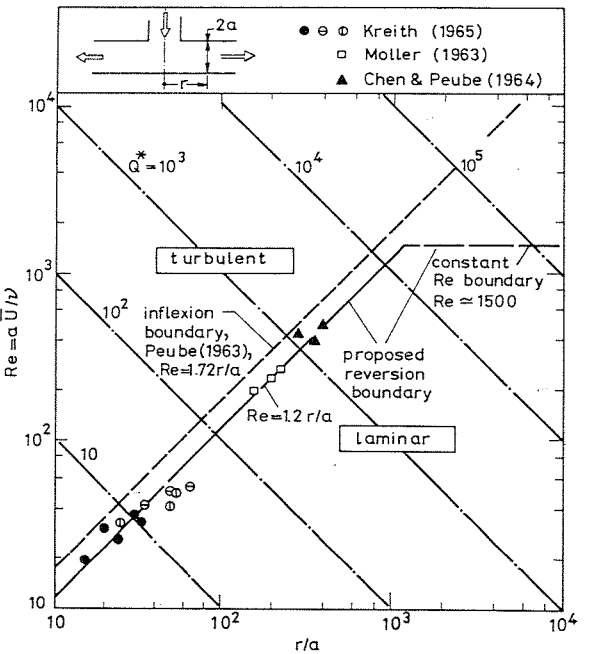

FIG. 27. Transition/reversion boundaries in radial Poiseuille flow. – · – indicates the Re – r/a relation for a given Q^*.

where Q^* is a dimensionless flow-rate number. It may thus be expected that an incoming turbulent flow will relaminarize as its Reynolds number drops downstream.

Reversion has indeed been observed in such flows, but the phenomenon does not appear to occur at a fixed value of the Reynolds number, and so is rather more complex than may be imagined at first sight. The observed critical Reynolds numbers can in fact be very low: they vary from around 400 in the experiments of Moller (1963) to as low as around 15 in those of Kreith (1965). (Kreith does not quote this value, which is inferred by us from the data presented by him.)

Moller judged reversion by the agreement of measured pressure loss with laminar theory; when this is obtained reversion is complete, and so must have been initiated at a location far upstream where the Reynolds number would have been higher. This argument is plausible because of the slowness of dissipative reversion noted in Section III. Moller in fact concluded that the observed critical Reynolds numbers were not far different from those in channel or pipe flows. However this is contradicted by the very low values observed by Kreith (1965).

An alternative explanation is suggested by Chen and Peube (1964). They note that in laminar flow, according to the calculation of Peube (1963), an inflexion point is present in the velocity profile up to a critical radius r_i given by

$$r_i/a = 0.762Q^{*1/2} \qquad \text{or} \qquad \mathrm{Re}_i = 1.72r_i/a. \tag{6.2}$$

Flow at $r < r_i$ is therefore highly unstable, and could become turbulent even at very low values of the Reynolds number. Correspondingly, the value of Re at reversion may also be expected to be relatively low. Chen and Peube therefore suggested a criterion for reversion in terms of r_i/a.

To test the Chen–Peube hypothesis, Kreith (1965) made experiments under different flow conditions in the following way. He placed a hot wire at various radial distances halfway between the disks and slowly varied the volume flow rate until, at a given location of the hot wire, the flow underwent transition from *laminar* to a *turbulent* state. A good fit to his measurements shows that the radius r_{cr} at which this transition occurs is related (to within experimental error) to the corresponding mass flow rate Q by the equation

$$r_{cr}/a = 0.26Q^{*1/2}. \tag{6.3}$$

This relation, although obtained by examining the laminar to turbulent transition at a given radius, holds also for reversion; if the hot wire is moved radially *outward*, (6.3) gives the critical radius at which turbulent fluctuations just cease to exist (or, in some sense, reversion is complete). Kreith's criterion

(6.3) implies that $r_{cr} \sim Q^{1/2}$, whereas a simple constant-Reynolds number criterion implies [from (6.1)] that $r_{cr} \sim Q$.

To see more clearly how the criteria differ we note that, putting (6.1) in (6.3), we get

$$r_{cr}/a \simeq 0.26(4\pi)^{1/2}\bar{U}a/\nu \simeq 0.91\,\mathrm{Re} \qquad \text{or} \qquad \mathrm{Re}_{cr} = 1.2r_{cr}/a. \tag{6.4}$$

In the $\mathrm{Re} - (r/a)$ plane shown in Fig. 27, this plots as a straight line; the same diagram also shows how Re varies with r for given Q^*. According to Kreith's criterion, reversion should occur when the curve for given Q^* intersects the line (6.4); furthermore, as Q^* increases the corresponding critical Reynolds number increases without limit.

However, there should be a critical Reynolds number above which the flow will be turbulent even in the absence of an inflexion point, as in plane Poiseuille flow. The value of this critical Reynolds number for radial Poiseuille flow is not known, but it is reasonable to take it to be of order 1500, as in plane flow (Section III), as the velocity distribution assumes the parabolic form asymptotically.

Based on this argument, we suggest that the region in which the flow will revert is bounded by (6.4) on one side, and by a constant critical Reynolds number above, as shown in Fig. 27.

Experimental data from Moller (1963), Kreith (1965), and Chen and Peube (1964) are also plotted in Fig. 27. Unfortunately none of these points corresponds to sufficiently high Q^*, which is therefore an area that needs further investigation.

To summarize, the radial geometry could produce an unstable mean flow whose critical Reynolds number is lower than in plane Poiseuille flow. For sufficiently large dimensionless flow rate Q^*, however, the critical Reynolds number should reach a constant value independent of Q^*. Reversion in this flow is therefore essentially dissipative, with a Reynolds number criterion that is a function of the flow rate parameter.

B. Convex Boundary Layers

In the last 10 years many detailed studies have been made of boundary layer flow on surfaces with streamwise curvature. One measure of the curvature is the parameter $\kappa\delta$, where κ^{-1} is the radius of curvature (considered positive when convex) and δ is the boundary layer thickness. When $\kappa\delta$ is small, the mean flow may be represented by writing Eqs. (2.1) and (2.2) in a locally Cartesian coordinate system with x along the (curved) surface and y normal to it; the major effects of curvature then appear in these equations as additional terms, comprising a source of strength $-\partial(\kappa v y)/\partial y$ and body

force $(-\kappa uv, \kappa u^2)$ along the streamwise and normal directions respectively (So and Mellor, 1972). As a consequence of the centrifugal component κu^2, there is a normal pressure gradient, the pressure being higher toward the edge in a convex boundary layer. This gradient affects the stability of the flow significantly. For example, a slow lump of turbulence thrown outward from a convex surface possesses a lower centrifugal acceleration than the faster ambient fluid, and so is driven back by the normal pressure gradient that balances the mean flow. Similarly, a faster lump moving toward the surface is thrown out. Consequently, there is a tendency to suppression of turbulence, very much as in an inversion. Indeed, as long ago as 1884, Reynolds had listed "curvature with the velocity greatest on the outside" as one of the factors "conducive to direct or steady (= laminar) motion," and had noted how a small curvature may have a large effect. An analogy between buoyancy and curvature effects in the convection/cylindrical Couette flow stability problems was demonstrated by Jeffreys (1928); Prandtl (1929) drew a similar analogy for turbulent flows.

Although we will speak here only of convex boundary layers, the same effects will be encountered on *concave* surfaces if the flow velocity *decreases* away from the surface. The important thing is that the sense of flow curvature and flow vorticity must be the same; the effects we discuss below for convex boundary layers must be present in other instances of what we may call "co-curving" flows.

Another way of appreciating the effect of curvature is to examine the Reynolds stress transport equations for curved boundary layers. When (2.3) is written in the appropriate coordinate system, the following production terms appear in the respective transport equations (Rotta, 1967; So and Mellor, 1972):

$$\frac{1}{2}u^2 : -\langle u'v'\rangle \frac{\partial}{\kappa\,\partial y}(\kappa u) - 2\kappa u\langle u'v'\rangle$$

$$= -\langle u'v'\rangle \frac{\partial u}{\partial y} - \kappa u\langle u'v'\rangle, \tag{6.5a}$$

$$\frac{1}{2}\hat{v}^2 : 2\kappa u\langle u'v'\rangle, \tag{6.5b}$$

$$q : -\langle u'v'\rangle \frac{\partial u}{\partial y} + \kappa u\langle u'v'\rangle, \tag{6.5c}$$

$$-\langle u'v'\rangle : \hat{v}^2 \frac{\partial u}{\partial y} - \kappa u(2\hat{u}^2 - \hat{v}^2). \tag{6.5d}$$

[These are the leading terms in the limit of small $\kappa\delta$ for a two-dimensional boundary layer, and have been extracted from the complete equations given by So and Mellor (1972), Appendix E.] The tendency of these terms, for *given* $\langle u'v'\rangle < 0$, is to enhance $\hat{u}$ but diminish $\hat{v}$ and the total energy q in a convex boundary layer. However (6.5d) shows that $-\langle u'v'\rangle$ tends to go down as well if $\hat{u} > \hat{v}/2^{1/2}$. The experiments of So and Mellor (1973), at $\kappa\delta \simeq 0.074$, show in fact that all three components of the energy, $\hat{u}^2$, $\hat{v}^2$, $\hat{w}^2$, as well as the stress $-\langle u'v'\rangle$, are lower in a convex boundary layer than on a flat one. Figure 28 shows some of these results; note the spectacular drop in the correlation coefficient C_τ [defined in (3.3)], and the implied disappearance of the shear stress at $y/\delta \simeq 0.4$! The curvature terms in these experiments are comparable to the others; for example, the curvature "absorption" term in (6.5c) is about half the other production term.

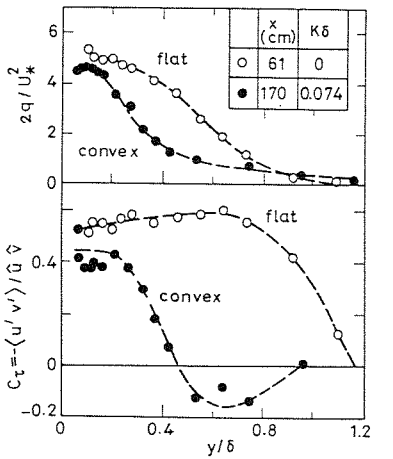

FIG. 28. Effect of convex curvature in turbulence energy and the shear stress correlation coefficient in a boundary layer: experimental data of So and Mellor (1973).

Bradshaw (1969b) has recently made extensive use of the analogy with buoyancy effects to calculate curved turbulent flows; in particular he defines a flux Richardson number for curvature,

$$\mathrm{Rf_c} = \frac{2u}{\partial(u\kappa^{-1})/\partial y} \tag{6.6}$$

which is approximately equal to $\kappa u/(\partial u/\partial y)$ for very small curvatures, and provides a measure of the ratio of the absorption term to the production term in, say, (6.5c). This Richardson number tends to be very small near the wall, where the flow is therefore hardly ever affected.

As in buoyant flows, however, even a relatively small value of the curvature Richardson number (6.6), i.e., even mild surface curvature, can cause significant changes in the turbulence structure. The experiments of Thomann (1968) in supersonic flow, which were so arranged that the external Mach number remained constant as the flow curved, revealed changes in wall heat flux

that would be 10 times more than in laminar flow at the same value of $\kappa\delta$ (Bradshaw, 1973). Furthermore, Bradshaw finds a 10% change in the mixing length when the boundary layer thickness is still only a three-hundredth part of the radius of curvature! Thus, even when the magnitude of the terms *explicitly* involving curvature in the stress transport equations is very small, the effects of curvature are not negligible, and clearly spread to the other terms as well. We now examine the effects more closely.

As Fig. 28 shows, there is not only a reduction in turbulence intensity q on a convex surface, but a significant decorrelation of the velocity components contributing to $\langle u'v' \rangle$: the correlation coefficient C_τ drops from about 0.6 in the flat boundary layer to zero in the convex one at $y/\delta = 0.4$. Clearly, curvature is not only affecting the amplitudes of the fluctuating motion but their relative phases as well.

That these effects reflect basic changes in turbulence structure are shown by the detailed measurements recently reported by Ramaprian and Shivaprasad (1978) at $\kappa\delta \simeq 0.013$. They find that, compared to a flat boundary layer, the production and dissipation in a convex boundary layer are not significantly different (the wall stress drops only slightly), but the diffusion [represented by the terms (va) and (vb) in Eq. (2.5)] is: There is a small gain by diffusion over a large part of the boundary layer ($y/\delta \gtrsim 0.1$), from a supply apparently very close to the wall. (In these measurements, the diffusion term does not show the expected change in sign across the boundary layer; there must therefore be a peak on the loss side for the convex flow, but this apparently occurs too close to the surface to be detected by the probe used.)

Equally interesting are the spectacular changes found in the large scale motions even with $\kappa\delta$ as low as 0.01. Fig. 29 shows the integral time scale

$$T_u \equiv \int_0^{T_0} \frac{\langle u'(t)u'(t+\tau)\rangle}{\hat{u}^2}\, d\tau,$$

where T_0 is the time delay up to the first zero of the autocorrelation function $\langle u'(t)u'(t+\tau)\rangle$. Figure 30 shows the spectrum E_{22} of the v' fluctuations, normalized so that

$$\int_0^\infty E_{22}(k_1\delta)\, d(k_1\delta) = 1,$$

k_1 being the longitudinal wave number. Both diagrams show the large changes caused by convex curvature, especially at low wave numbers (integral scale is given by this end of the spectrum). Clearly the stabilizing influence of curvature is first destroying the organization of the motion in the large-scale structures in the boundary layer: the effects must later spread to the high wave number end and presumably also to the bursting process through

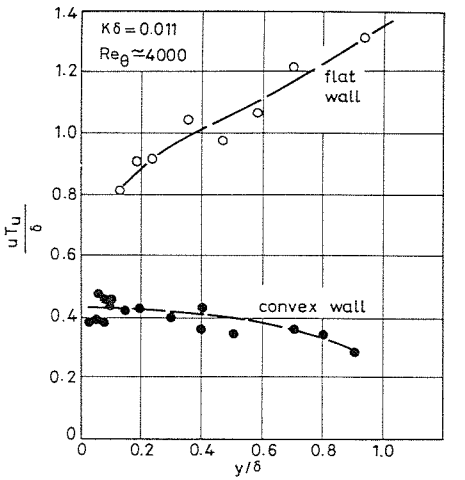

FIG. 29. Integral time scale T_u in convex boundary layer; measurements of Ramaprian and Shivaprasad (1978).

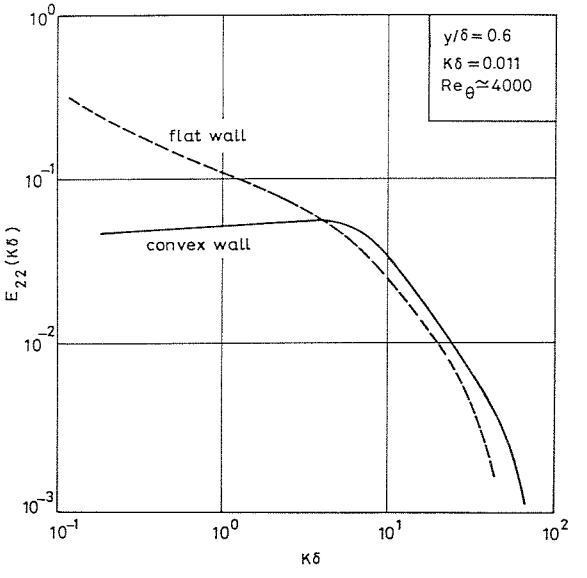

FIG. 30. Power spectral density of normal velocity component v' in curved flow; measurements of Ramaprian and Shivaprasad (1978).

the couplings that have recently been revealed by experimental studies (Rao *et al.*, 1971; Badri Narayanan *et al.*, 1977; Brown and Thomas, 1977).

With the Reynolds shear stresses suppressed, and the viscous stresses anyway negligible, it follows that the flow in the outer layer must be effectively inviscid and rotational, as in the rapidly accelerating flows of Section V. This is indeed found to be the case; Fig. 31 shows how the measured velocity profile in one of Ramaprian and Shivaprasad's experiments compares very well with an inviscid calculation, in which the vorticity was assumed conserved along each stream line from a station about 14δ upstream.

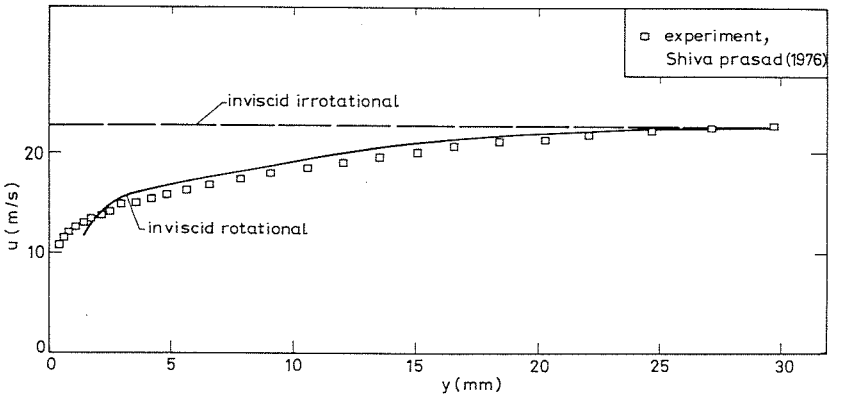

FIG. 31. Velocity profile in convex boundary layer; comparison between measurement at station 35 (Shivaprasad, 1976) and inviscid calculations.

In the inner layer, on the other hand, the effective curvature Richardson number usually remains small (because $\partial u/\partial y$ is very large), and a turbulent wall flow of the classical type remains, although even this corresponds to a slightly reduced skin friction. In analogy again with the discussion of Section V, we may expect to observe departures in the wall flow from the standard law of the wall when the curvature scaled on wall variables,

$$\kappa_+ = \kappa\nu/U_*,$$

is sufficiently large. In So and Mellor's experiments, with $\kappa\delta \simeq 0.074$, κ_+ is only of order 5×10^{-6}—still far too small to be significant.

To summarize, therefore, the outer flow in a convex boundary layer reverts to a quasi-laminar state, as the turbulence energy is "absorbed" by curvature forces, the organization of the motion is destroyed and the Reynolds shear stresses are suppressed.

VII. Relaminarization by Rotation

A. Dynamics of Mean and Fluctuating Velocity

Like curvature, rotation can also produce reversion from turbulence to a laminar state. Experiments in an effectively two-dimensional channel rotating about a spanwise axis (Halleen and Johnston, 1967; Lezius and Johnston, 1971; Johnston *et al.*, 1972) have shown that reversion occurs on what these authors call the trailing side; as this is the side on which the imposed rotation and the basic flow vorticity have the same sense, it is convenient to call it the corotating side. For small rotation rates, the flow remains essentially turbulent although it is slightly modified, but for rotation rates higher than a certain value, flow visualization studies have shown that the following changes occur progressively on the corotating side:

(a) appearance of intermittency in the streaky wall-layer;
(b) basic laminar flow interspersed with turbulent spotlike characteristics;
(c) quiet, purely laminar layer close to the wall.

Furthermore, turbulent bursting ceases, intensities decrease, the velocity profile departs from the standard log-law form, and the skin-friction goes down considerably.

Rotation introduces two additional forces in the rotating frame of reference. The centrifugal force, which is $\frac{1}{2}\Omega^2 r^2$ per unit mass (where Ω is the angular velocity of rotation and r is the radial distance of the field point from the axis of rotation), can be combined with the static pressure and does not then explicitly enter the equations of motion. The Coriolis force, on the other hand, will have to be considered explicitly. For a rotating channel with no flow variation in the streamwise coordinate x, we have the momentum equations (y being parallel to the smallest dimension of the channel)

$$dp/dx = \partial\tau/\partial y \tag{7.1}$$

$$2\Omega u = -\frac{\partial P}{\partial y} - \frac{\partial \hat{v}^2}{\partial y}, \tag{7.2}$$

where $P \equiv p - \frac{1}{2}\Omega^2 r^2$. Usual order of magnitude estimates in (7.2) show that

$$\partial\hat{v}^2/\partial y = o(2\Omega u)$$

everywhere in the flow, so that to a first approximation

$$2\Omega u = -\partial P/\partial y. \tag{7.3}$$

Thus, an important effect of the Corolis force is to produce a normal pressure gradient proportional to Ω. As in co-curving flows (Section VI,B), this pressure gradient has a stabilizing effect: if a fluid particle from layer (1) moves accidentally outwards to layer (2) and preserves its momentum and (thus) its Coriolis force, the inward-acting pressure gradient in position (2), being larger than the Coriolis force acting on this fluid particle, will push it back to its original position. Similarly, a fluid particle moving from position (2) to position (1) is pushed back to position (2). The same argument shows that on the opposite (antirotating) side, the Coriolis force is destabilizing.

Consider now the transport equation for the components of the Reynolds stress. The relevant generation terms are:

$$\tfrac{1}{2}\hat{u}^2 : 2\Omega\langle u'v'\rangle - \langle u'v'\rangle(\partial u/\partial y), \tag{7.4}$$

$$\tfrac{1}{2}\hat{v}^2 : -2\Omega\langle u'v'\rangle, \tag{7.5}$$

$$\tfrac{1}{2}\hat{w}^2 : 0, \tag{7.6}$$

$$q : -\langle u'v'\rangle\,\partial u/\partial y, \tag{7.7}$$

$$-\langle u'v'\rangle : 2\Omega(\hat{u}^2 - \hat{v}^2) + \hat{v}^2\,\partial u/\partial y, \tag{7.8}$$

where the sign convention is such that on the co-rotating side $\Omega < 0$. The tendency of these terms in co-rotating flows is to enhance $\hat{u}$, diminish $\hat{v}$, and leave $\hat{w}$, q unaffected, for *given* $\langle u'v'\rangle$, $\partial u/\partial y$, etc. However, as in curved flows, $-\langle u'v'\rangle$ is itself reduced, and hence also $\partial u/\partial y$, so that we may expect all the Reynolds stress components to be altered.

B. Criterion for Reversion

The ratio of the additional 'absorption' term [in Eq. (7.4), for example] to the conventional production again defines an appropriate Richardson number for rotating flows,

$$\mathrm{Rf}_r = -\frac{2\Omega}{\partial u/\partial y}, \tag{7.9}$$

which we may expect to play a role similar to that in curved flows*: thus, the flow should be more stable for $\mathrm{Rf}_r > 0$.

* From an analogy with curved and stratified flows, Bradshaw (1969b) concluded that the appropriate Richardson number governing the stability of the flow is the parameter

$$-2\Omega\left(\frac{\partial u}{\partial y} - 2\Omega\right)\Big/\left(\frac{\partial u}{\partial y}\right)^2,$$

but as noted by Johnston *et al.* this parameter is nearly equal in magnitude to (7.9) in most boundary layer situations where $\Omega \ll \partial u/\partial y$.

Johnston *et al.* (1972) used an inverse Rossby number $\mathrm{Ro}^{-1} = 4\Omega a/u$ as a convenient measure of the rotation, and identified, in a Re–Ro plot, regions of the fully turbulent, reverse-transitional and laminar states (as schematically indicated in Fig. 32). This classification is based on the flow visualization studies in the wall region: the laminar state is defined by the absence of spotlike individual turbulent structures in hydrogen bubble and dye visualizations, and fully developed turbulent flow by the absence of isolated laminar-like regions. Figure 32 shows that, with increasing Reynolds number, reversion occurs at an increasingly higher value of rotation, and that no unique value of Ro describes the boundaries between the different flow regimes.

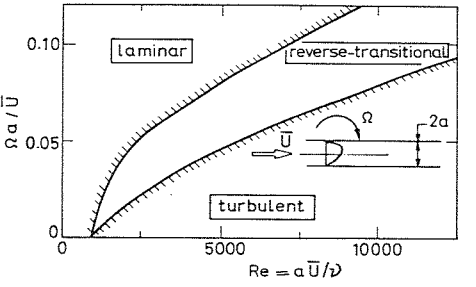

FIG. 32. Boundaries between different flow regimes in corotating channel layer; classification based on flow visualization using hydrogen bubble and dye techniques. (Data of Johnston *et al.*, 1972.)

However, close to the wall, an appropriate measure of $\partial u/\partial y$ in (7.9) is not U/a but U_*^2/ν, so that we expect the "wall flow" Richardson number $\Omega_+ \equiv \Omega\nu/U_*^2$ to be a logical parameter with which to attempt a correlation of the *onset* of reversion. (Note the analogy here to the parameters Δ_p, Δ_τ of Section V,A.) We have therefore plotted the data of Johnston *et al.* as Ω_+ vs. Re in Fig. 33.* From our analysis of Section III, we know that reversion occurs even in the zero-rotation case when the Reynolds number $\mathrm{Re} < 1500$. From Fig. 33, the rotation required to cause reversion sharply increases with Re for $1500 < \mathrm{Re} < 3000$, and thereafter attains a nearly constant value of $\Omega_{+\mathrm{cr}} \simeq 2.5 \times 10^{-3}$. No unique value of Ω_+ can be identified along the boundary between the laminar and reverse-transitional regimes; this again

* Here, we have used U_{*0}, the friction velocity corresponding to the nonrotating case at any given Reynolds number, because of its greater predictive convenience. Rotation modifies the friction velocity, as we shall discuss shortly, and so a more logical choice may appear to be the friction velocity U_* in the rotating case. However, it turns out that U_*/U_{*0} depends chiefly on Ω_+, so that the critical value of $\Omega\nu/U_*^2 = (U_{*0}/U_*)^2\Omega_+$ is proportional to $\Omega_{+\mathrm{cr}}$ $[(\Omega\nu/U_*^2)_{\mathrm{cr}} \simeq 4.3 \times 10^{-3}]$.

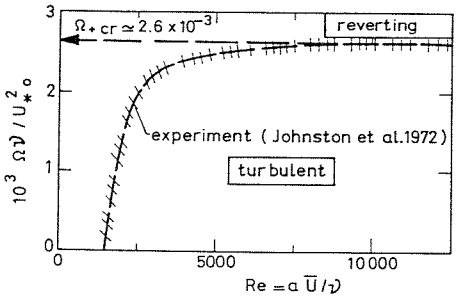

FIG. 33. A replot of the turbulent/reverse transitional boundary of Fig. 32, in terms of a wall-scaled rotation Richardson number Ω_+.

is consistent with the discussion in Section V of how wall-scaled parameters do not govern the completion of reversion.

It is useful to ascertain independently the validity of this argument by considering some other more easily measurable parameter. Figure 34, which is essentially a replot of the data of Johnston *et al.* converted to the present coordinate Ω_+ using estimated values of c_f, shows the ratio of the friction velocity U_* in the rotating flow to that in the nonrotating flow (U_{*0}) at the same Reynolds number, as a function of Ω_+. For $\Omega_+ \lesssim 2.5 \times 10^{-3}$, there is only a small and gradual reduction in the wall friction as a result of rotation; presumably, this line represents a turbulent state. Beyond $\Omega_+ \simeq 2.5 \times 10^{-3}$ a sharper change in U_*/U_{*0} seems to occur, thus possibly marking the onset of reversion.

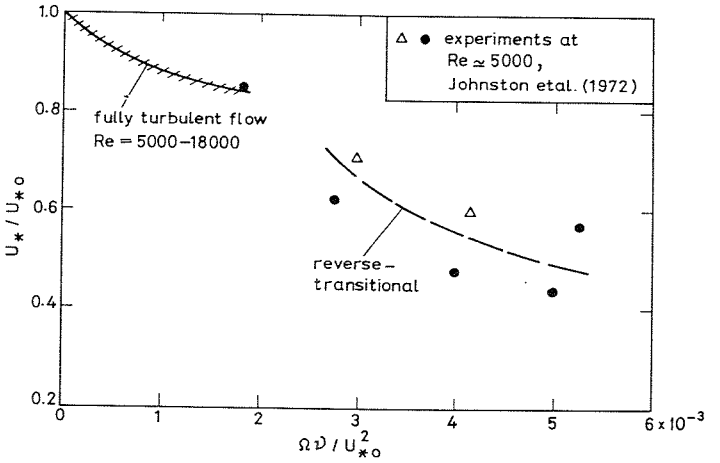

FIG. 34. Friction velocity in corotating channel layer.

VIII. Thermal Effects

A. Heated Horizontal Gas Flows

There is considerable evidence that an initially turbulent internal gas flow reverts to a laminar state when the pipe carrying the gas is heated sufficiently (Perkins and Worsoe-Schmidt, 1965; Magee and McEligot, 1968; and especially Coon and Perkins, 1970; Bankston, 1970; Perkins *et al.*, 1973). An important effect of laminarization in this case is a sharp reduction in energy transfer to the gas, with a consequent large rise in the wall temperature (which can be high enough to be of practical concern in gas-cooled nuclear reactors).

The most usual experimental configuration used in these studies is a tube heated either resistively or by an external heat exchanger. The gas entering the tube is often pre-cooled to achieve higher values of wall-to-bulk gas temperature ratio without operating at excessively high tube temperatures; in this manner, the experiments of Perkins and Worsoe-Schmidt achieved a ratio as high as 7.

In principle, it appears possible that an internal gas flow at any entry Reynolds number can be made to revert to a laminar state by heating it enough so that, due to the increase in kinematic viscosity, the local Reynolds number falls below the critical value (as in the flows discussed in Section III). Flows with entry bulk Reynolds numbers of the order of 10^4 are known to have reverted to an effectively laminar state on heating (the Reynolds number being based on pipe radius a, average flow velocity $\bar{U}$ and kinematic viscosity $\bar{\nu}$ corresponding to the average flow temperature at a given section). However, reversion has been observed to be *complete* (i.e., the heat transfer characteristics, for example, have reached the appropriate laminar values) at bulk Reynolds numbers of about 2500, and is possibly initiated at Reynolds numbers of about 4000–5000 (see, for example, Coon and Perkins, 1970; Bankston, 1970). These Reynolds numbers are substantially higher than the critical value of 1500 determined in Section III for reversion in adiabatic pipe or channel flows.

The reason could well be fluid acceleration: with heating, the gas density goes down and velocity increases (to conserve mass flow) with distance downstream. The (bulk) acceleration parameter $\bar{K} = \bar{\nu}(d\bar{U}/dx)/\bar{U}^2$ attains values of the order of 2×10^{-6} in the experiments of Bankston (1970), Coon and Perkins (1970), and Perkins *et al.* (1973). Accelerations of this magnitude are not far from values thought sufficient to cause reversion in external (initially turbulent) boundary layers (see Section V). Although the induced acceleration in these internal flows is not an independent parameter, being

controlled by the retarding effects of the wall friction, its magnitude is sufficient to warrant a further investigation to demarcate the acceleration and Reynolds number effects.

If the primary mechanism causing reversion is the viscous dissipation, we expect a Reynolds number criterion to hold. In the heated flow we may expect the critical Reynolds number to depend on a parameter like $\bar{K}$ characterizing the acceleration (which itself is related to the amount of heating). Unfortunately, obtaining such a functional relation is not easy in the experiments cited above. The reasons are that reconstruction of various details of the experimental data is rarely possible from the published information, and that no consistent definition of reversion has been used in the various experiments; also no quantitative data on turbulent fluctuations are available. The data collected by McEligot *et al.* (1970) suggest that the departure of a measured-wall parameter (such as the Stanton number) from the empirically established "wall-laws" occurs at a bulk inlet Reynolds number

$$\mathrm{Re}_i \simeq 6.1 \times 10^4 (q_i^*)^{1/2}, \tag{8.1}$$

where the surface heat flux is

$$q_w = q_i^* \bar{\rho} \bar{U} \bar{C}_p \bar{T};$$

the suffix i indicates the inlet conditions, and overbars denote sectional averages. Further, if one defines reversion to be complete when the local Stanton number approaches the laminar value corresponding to the local Reynolds number, the data collected by McEligot *et al.* show that the corresponding bulk inlet Reynolds number is

$$\mathrm{Re}_i = 1.72 \times 10^4 (q_i^*)^{1/2}. \tag{8.2}$$

Both (8.1) and (8.2) hold for $q_i^* > 6 \times 10^{-4}$. For square ducts, Perkins *et al.* (1973) propose, instead of (8.2), the relation

$$\mathrm{Re}_i = 2.5 \times 10^3 (q_i^*)^{3/4},$$

but we shall not consider this further because of the uncertain effects of duct geometry.

From energy balance across a short section of pipe of radius a,

$$2\pi a q_w = \frac{\pi a^2}{4} \frac{d}{dx} (\bar{\rho} \bar{C}_p \bar{T} \bar{U});$$

if $\bar{\rho}$, $\bar{C}_p$, $\bar{T}$ and p do not vary much, and taking $\bar{\mu}/\bar{\mu}_i$ as approximately $\bar{T}/\bar{T}_i$, we get $\bar{K} = 2q^*/\mathrm{Re}$. From (8.1) and (8.2), therefore

$$\mathrm{Re}_i = 1.85 \times 10^9 \, \bar{K} \, (\bar{T}_i/\bar{T})$$

for "initiation of reversion," and

$$\mathrm{Re}_i = 1.48 \times 10^8 \, \bar{K} \, (\bar{T}_i/\bar{T})$$

for "completion of reversion." Both of these equations express the *local* critical Reynolds numbers in terms of the *local* acceleration parameter and the inlet-to-local temperature ratio. The result is shown in Fig. 35.

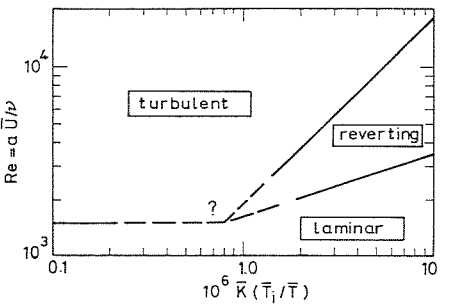

FIG. 35. Proposed variation of critical Reynolds number with acceleration parameter in heated pipe flows, based on McEligot *et al.* (1970).

Finally, we note that the dynamic viscosity of a gas increases with temperature while that of a liquid decreases. So, reversion would perhaps occur also when liquid flows are cooled sufficiently, although the flow in this case would not undergo an acceleration.

B. Heated Vertical Gas Flows

Steiner (1971) has observed reversion in the airflow passing upward through an insulated vertical pipe subjected to a constant heat flux. Measurements were made at initial Reynolds numbers Re ($\equiv \bar{U}a/\nu$) of about 2000, 3000, 4000, and 6000. It was observed that, in the first three cases, the Nusselt number based on the difference between wall and mean temperatures decreased to half the values appropriate to the turbulent flow; reversion to a laminar state may thus be suspected. In the experiment at the highest Reynolds number, on the other hand, no such reduction in the Nusselt number was observed; this and other corroborating mean velocity and mean temperature data showed that reversion had not occurred here.

Steiner attributed the observed reversion to the acceleration associated with the decrease in density due to the heating of the air. But two other mechanisms are also possible in this flow: absorption of turbulence by buoyancy effects, and decrease in Reynolds number below the critical value

because of the increase in kinematic viscosity associated with the heating. Accurate demarcation of these effects cannot be made from the data available, but a rough estimate will be attempted below.

Consider first the acceleration effects. Steiner quotes the maximum value K_{max} of the acceleration parameter K in the pipe to be in the range 0.3×10^{-6} (Re $\simeq$ 6000) to 3×10^{-6} (Re $\simeq$ 2000). However the parameter K_{max} does not have the same significance in internal flows as K does in external flows: a more useful indicator is perhaps the bulk acceleration parameter $\bar{K}$, defined using average values over a cross section (as in Section VIII,A). However, $\bar{K}$ is rather lower than K_{max}; for instance, $\bar{K} \simeq (3/5)K_{max}$ in the flow with Re $\simeq$ 2000. Thus, in Steiner's experiments $\bar{K} \simeq 2 \times 10^{-6}$ in the flow with Re $\simeq$ 2000, and less than 10^{-6} in the other three flows. The acceleration effects thus cannot be very important except in the flow with Re $\simeq$ 2000.

We now use the arguments of the previous section to examine whether because of heating, the Reynolds numbers in these flows could have reached critical values. Although the mean temperature rise in these flows is not known directly, other data seem to suggest that it is of the order of a couple of hundred degrees centigrade. Noting that

$$\bar{K}(\bar{T}_i/\bar{T}) \simeq (3/5)\, K_{max}\, (\bar{T}_i/\bar{T}) \simeq 0.3\, K_{max} \simeq 10^{-6},$$

we find from Fig. 35 that Re_{cr} would not be very different in these flows from the adiabatic value of about 1500 (see Section III). As Reynolds numbers in all the flows are above 1500, it is unlikely that reversion occurred by dissipation.

Consider now possible buoyancy effects. We first note that the flux Richardson number

$$Rf \simeq Gr/(Re^3\, c_f\, Pr),$$

where

$$Gr = gl\Delta T/(\nu^2 T)$$

is the Grashoff number, Pr is the fluid Prandtl number ($\simeq$0.72 for air), l is the vertical distance between two measuring stations along the pipe, and ΔT the mean temperature difference between them. From the values of Gr and Re quoted by Steiner, using estimated values of c_f, it is easy to show that

$$Gr/(Re^3\, c_f\, Pr) \simeq 0.0125$$

for the Re $\simeq$ 6000 experiment, whereas for the other three flows it is about 0.09 (Re $\simeq$ 4000), 0.16 (Re $\simeq$ 3000), and 0.32 (Re $\simeq$ 2000). The last three values are comparable to the critical Richardson number in buoyant flows (see Section IV), thus strongly suggesting that the observed reversion is possibly due to buoyancy effects.

IX. Surface Mass Transfer

A. Injection

Eckert and Rodi (1968) and Pennell *et al.* (1972) showed that a fully developed turbulent pipe flow exhibits some laminar features when a uniform circumferential injection is applied to the flow. Their experimental configuration consisted essentially of a long pipe, a part of whose length was porous (see inset to Fig. 36). The flow at the entrance to the porous section was turbulent and fully developed, and the fluid was injected over a length of 24 diameters uniformly across the porous surface. The injection velocity V_w was 1–5% of the average flow velocity at the entrance of the porous section, and was low enough to cause no flow separation or vortex formation. As a consequence of fluid injection, the velocity in the porous section increases with the streamwise distance x (measured from the beginning of injection):

$$\bar{U}(x) = \bar{U}_0 + 2V_w(x/a), \tag{9.1}$$

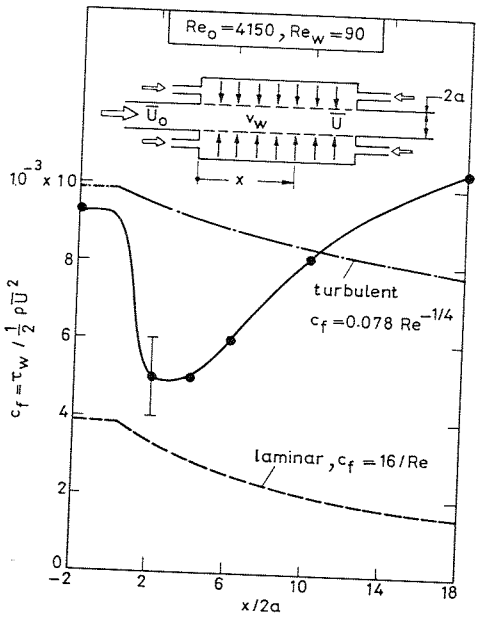

FIG. 36. Skin friction coefficient in pipe flow with injection, based on mean velocity data of Pennell *et al.* (1972): $Re_0 = 2a\bar{U}_0/\nu$, $Re_w = 2aV_w/\nu$.

where $\bar{U}(x)$ is the average flow velocity at the station x, and

$$\bar{U}_0 = \bar{U}\ (x = 0).$$

Several changes occur in the flow as a result of fluid injection, but a large number of these are confined to the downstream vicinity of the beginning of injection (i.e., $x/a \lesssim 6$–10), even though injection continues at the same rate a long way downstream ($0 < x < 48a$). Thus, within the first two diameters, the skin-friction coefficient c_f ($\equiv \tau_w/\frac{1}{2}\rho\bar{U}^2$) drops almost to the local laminar value (Fig. 36); these c_f values have been estimated from the slope of the velocity profiles measured by Pennell *et al.* (1972). Further downstream, however, c_f quickly catches up with the preinjection level, and, beyond $x/a = 24$, even exceeds the standard turbulent values.

There is also a dramatic reduction in the intensity of the streamwise velocity fluctuation $\hat{u}$ near the wall: at $\mathrm{Re}_0 \equiv 2a\bar{U}_0/\nu \simeq 4250$, $x \simeq a$, $y \simeq 0.036a$, $\hat{u}$ is less than a sixth of its initial value! This reduction increases with the injection velocity, and, at $y_+ = 12$, for example, is approximately

$$\Delta\hat{u} \simeq 3.75\ V_w$$

for $V_w/\bar{U}_0 \lesssim 0.04$. This reduction is again confined in streamwise extent to $x/a < 4$, downstream of which turbulent fluctuations increase fairly rapidly. Along the pipe centerline, there is a smaller and more gradual reduction in the turbulent intensity, extending to $x/a \simeq 10$. In the annular region, there may or may not be any reduction; in fact, $\hat{u}$ may sometimes increase continuously. As a consequence of the large reduction of $\hat{u}$ near $y_+ \simeq 12$ and little or no reduction further away from the wall, there is physically an inward movement—toward the axis of the pipe—of the peak in $\hat{u}$, which now occurs around $y/a \simeq 0.3$ or $y_+ \simeq 25$. The new peak in $\hat{u}$ in its new location is lower by about 40% than the preinjection peak at $y_+ \simeq 12$, and is considerably more spread out.

From this brief description, it is clear that the response of the turbulent flow to fluid injection is quite complex. The catastrophic drop in the mean-square intensity in the wall region is probably a result of the strong interference of fluid injection with the bursting process mainly responsible for the turbulent energy production. In a fully developed turbulent boundary layer, the processes of low speed streak formation, lift-up, oscillatory growth, and breakup, followed by a large scale in-rush, are all in statistical equilibrium. One may speculate that injection upsets this equilibrium by affecting the low-speed streak formation, and thus the complete cycle of events. Coles, on several occasions (see, especially, Coles, 1978), and Brown and Thomas (1977) have proposed that streak formation may be the result of an intermittent Taylor–Görtler instability in the wall-layer, possibly driven by the large eddies of the outer flow. The essential idea is that when the high speed

outer fluid moves close to the wall, the sublayer will be thinned, and locally concave (i.e., anticurving) fluid trajectories could be created, thus triggering the Taylor–Görtler instability. For the flow with injection, it is clear that the curvature is strongly convex (cocurving) immediately downstream of $x = 0$; so the instability may be suppressed, streak formation and bursting will be inhibited and turbulent intensities and shear stress will drop. Further downstream, however, the curvature and the turbulence production cycle begin to assume their normal form.

Close to the pipe axis, where injection effects cannot be directly felt, the observed initial reduction in turbulent intensity must be due to the concomitant fluid acceleration. The maximum value of the bulk acceleration parameter $\bar{K}$ (see Section VIII) reached in the different experiments of Pennell *et al.* varies between 4×10^{-6} and 4×10^{-5}; the pressure-gradient parameter Λ (Narasimha and Sreenivasan, 1973; see also Section V) attains values as high as 20. Thus, acceleration effects are significant in the core, especially in the region $x/a \lesssim 2$, where both $\bar{K}$ and Λ reach their maximum values. If the observed reduction in the turbulent intensity is solely due to the effect of sudden acceleration, we should expect rapid distoration theories to be able to predict the observed changes.

Figure 37 shows a comparison of the measured turbulent intensity at several points along the axis of the flow in the region $x/a \lesssim 10$, with results

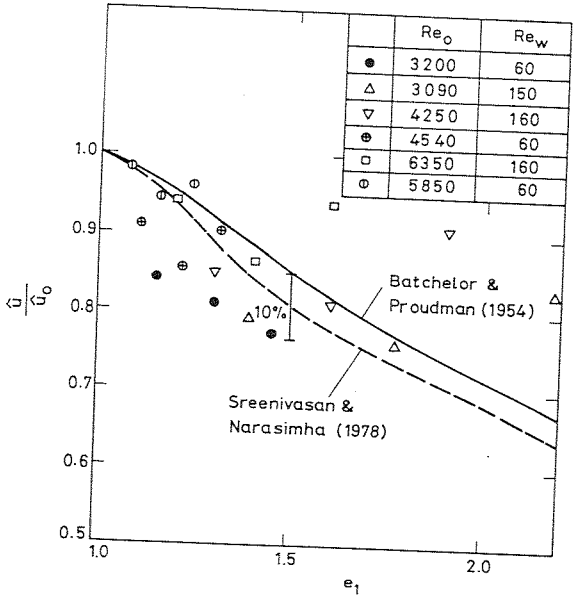

FIG. 37. Turbulence intensity in pipe flow with injection: comparison between measurement (data from Pennell *et al.*, 1972) and rapid distortion theories.

from the rapid-distortion theories of Batchelor and Proudman (1954) for initially isotropic turbulence, and of Sreenivasan and Narasimha (1978) for initially axisymmetric turbulence. (The applicability of these rapid distortion theories in the nonhomogeneous environment has already been discussed in Section V.) It is clear that the rapid-distortion calculations are reasonably successful.

The recovery of the flow downstream may be due partly to turbulent diffusion, and partly to the diminishing importance of fluid injection; when the injection *rate* remains unaltered, and the average flow velocity increases according to (9.1) in the streamwise direction, the ratio $V_w/\bar{U}$ drops. For example, in the experiment of Pennell *et al.* with the highest injection rate, the ratio $V_w/\bar{U}$ at $x/a = 36$ is nearly half of its value at $x = 0$. It would be interesting to observe the flow development in a case where $V_w/\bar{U}$ remains constant.

B. Suction

When a uniformly distributed suction is applied to a flat plate laminar boundary layer, it is known that the distribution of velocity in the boundary layer, and the skin friction coefficient, become asymptotically independent of the streamwise direction x and the fluid viscosity, being determined solely by the suction ratio V_s/U, where V_s is the suction velocity (see, for example, Rosenhead, 1963, p. 141). The boundary layer is then said to have reached the laminar asymptotic state.

In the case of a turbulent boundary layer, on the other hand, Dutton (1960) found an asymptotic layer whose form is independent of x only for a certain critical value of the suction ratio. Further, this asymptotic profile depended on such conditions as the initial boundary layer Reynolds number and the precise manner in which suction was applied.

Of particular interest to us here is an observation of Dutton (1960) that for suction ratios higher than a critical value, the boundary layer thins down, the shape factor of the velocity profile increases, the turbulent energy production decreases and, for suction ratios of about 0.01, the initially turbulent boundary layer approaches the *laminar* asymptotic state appropriate to the particular value of the suction ratio (see Fig. 38).

Details of the process of actual relaminarization in this case have not yet been sufficiently well-documented. We can get some insight into the nature of the process by examining energy balance in the asymptotic turbulent boundary layer (corresponding, for one particular set of experimental conditions, to a suction ratio of about 0.007). The Reynolds shear stress distribution in this layer can be evaluated easily from the mean momentum balance.

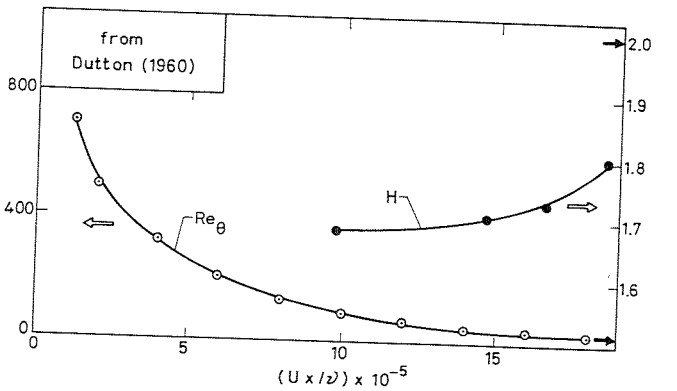

FIG. 38. Variation of the momentum-thickness Reynolds number Re_θ and the shape factor H for an initially turbulent boundary layer undergoing relaminarization. Suction ratio = 0.0125. Arrows on the right ordinate scale are values of Re_θ and H corresponding to the appropriate asymptotic laminar profile having the same suction ratio.

Dutton (1960) showed that the Reynolds stress so calculated is small all across the boundary layer, its maximum value being only about $0.2U_*^2$. These calculations further showed that 75% of the energy lost by the mean flow is dissipated directly by viscosity acting on the mean velocity gradient, only the remaining 25% being converted to turbulent energy. The reduced turbulent energy production comes about because of the reduced Reynolds shear stress, which more than offsets the increased mean velocity gradient near the wall. It is plausible that for higher suction ratios, essentially the same mechanisms operate with only quantitative differences, eventually resulting in the relaminarization of the flow.

Reversion has also been observed when there is concentrated suction. Wallis (1950) has studied the problem with suction through a single two-dimensional slot. When the entire turbulent boundary layer is sucked off, a completely new laminar boundary layer grows downstream of the slot, at the rate given by the laminar theory. This useful limiting case is however not interesting in the present context, because the turbulent boundary layer on which we seek to establish the effects of suction has been completely removed form the scene.

Even in the less extreme case when a sizeable part (but not all) of the turbulent boundary layer is removed by suction, all measures of the boundary layer thickness decrease for a certain distance downstream of the slot; for example, when 3/8 of the mass flux of the approaching turbulent boundary layer is removed, this thinning occurs over a distance of about five times the thickness of the oncoming turbulent boundary layer (Wallis, 1950). Further downstream, however, the boundary layer grows in thickness.

In the region of decreasing thickness, an essentially new laminar subboundary-layer develops downstream of the slot, underneath the remnants of the oncoming turbulent boundary layer. Low frequency u' and v' fluctuations are both present in this inner laminar layer, although the Reynolds shear stress is much lower than in the normal turbulent boundary layer. Clearly, a decorrelation mechanism operates here also. (Incidentally, the effect of suction is very much higher on the normal velocity fluctuation v' than on the streamwise velocity fluctuation u'.) Eventually, this inner layer undergoes transition to turbulence like a normal laminar flow.

On the other hand, the local suction thins down the outer layer, and hence also reduces the total boundary layer thickness, even though the laminar subboundary-layer itself grows. Both u' and v' are reduced in the outer layer.

Under these circumstances, the boundary layer just downstream of the suction slot can be said to have reached a quasi-laminar state (Section V). In fact, the similarity to rapidly accelerated boundary layers is so striking that we suspect that a major part of the quasi-laminar theory of Narasimha and Sreenivasan (1973) (see Section V) would in principle be applicable here, although the extent of the relaminarization region is relatively short. Unfortunately, data are not available in enough detail to test this suggestion.

X. Magnetohydrodynamic Duct Flows

A. Introduction

An electrically conducting fluid flowing in a magnetic field experiences a magnetic body force

$$\rho \mathbf{X} = \mathbf{j} \times \mathbf{B} \tag{10.1}$$

per unit volume, where $\mathbf{j}$ is the current density and $\mathbf{B}$ the magnetic field (more precisely the induction); the fluid also suffers an energy loss of j^2/σ per unit volume by "ohmic" dissipation, σ being the electrical conductivity. It has been known for some time that these effects can often relaminarize an originally turbulent flow; we consider here some simple duct shear flows in which such relaminarization has been studied.*

The precise effect of the field depends on its orientation relative to the mean flow. In a channel, for example, the field could be either longitudinal (i.e., aligned with the mean flow) or normal. It may appear necessary to

* There are also situations where the magnetic force alters the flow so as to make it unstable, e.g., by creating free shear layers that quickly break down to turbulence; an example is given by Lehnert (1955).

consider two possible normal directions, respectively parallel to the shorter and longer sides of the channel when its cross section is not a square; however, it is convenient to discuss instead the equivalent problem of the effect of a given normal field on channels of different aspect ratio.

We restrict ourselves to a consideration of low magnetic Reynolds numbers,

$$\mathrm{Rm} \equiv Ua/\lambda, \qquad \lambda = 1/\mu\sigma, \tag{10.2}$$

where U and a are characteristic velocity and length scales of the flow, μ is the magnetic permeability and λ, the magnetic diffusivity. The value of Rm provides us a measure of the ratio of convective to (magnetic) diffusion times, or of the induced to the imposed field (see, e.g., the discussion in Shercliff, 1965, Chapter 3). For the fluids used in most laboratory experiments $\nu \ll \lambda$; thus (see, e.g., Kirko, 1965) $\nu/\lambda \simeq 1.5 \times 10^{-7}$ for mercury at 20°C, and 2.3×10^{-6} for sodium at 300°C. This means that even when the flow Reynolds number is quite high, the magnetic Reynolds number tends to be low. Whereas at high Rm the field is convected with (or "frozen" into) the fluid, at low Rm the field varies chiefly by diffusion, and is hardly affected by the flow.

The current density is taken here to be given by a simple Ohm's law,

$$\mathbf{j} = \sigma(\mathbf{E} + \mathbf{u} \times \mathbf{B}), \tag{10.3}$$

where $\mathbf{E}$ is the electric field. The field puts energy into the fluid at the rate $\mathbf{E} \cdot \mathbf{j}$ per unit volume and unit time; a part of this, given by j^2/σ, is dissipated irreversibility into heat.

Taking the curl of (2.2) with $\mathbf{X} = \mathbf{j} \times \mathbf{B}/\rho$ we obtain the vorticity equation (with $B^2 = |\mathbf{B}|^2$)

$$\frac{d\boldsymbol{\omega}}{dt} - (\boldsymbol{\omega} \cdot \nabla)\mathbf{u} - \mathbf{F} = \frac{\sigma}{\rho}\left[-\operatorname{curl} B^2\mathbf{u} + (\mathbf{u} \cdot \mathbf{B})\operatorname{curl} \mathbf{B} + (\mathbf{u} \cdot \mathbf{B}) \times \mathbf{B} + \operatorname{curl}(\mathbf{E} \times \mathbf{B})\right], \tag{10.4}$$

where $\mathbf{F}$ is a term involving the viscous and Reynolds stresses. The effect of the field on the vorticity is thus quite complex; but if the field is normal to the flow and (as at low Rm) hardly affected by it, and the last term in (10.4) involving $\mathbf{E}$ is negligible, it is clear that the first term on the right of (10.4) acts to suppress the vorticity with a characteristic decay time $\tau = \rho/\sigma B^2$.

B. Aligned Fields

If $\mathbf{B}$ is in the direction of the mean flow and $\mathbf{E}$ is negligible, the magnetic force is zero, and the mean momentum balance can be affected only indirectly, through the action of the field on the Reynolds stresses. Many

experiments have shown a tendency toward suppression of turbulence (e.g., Globe, 1961, and Fraim and Heiser, 1968, in pipes; Sajben and Fay, 1967, in a jet). It may be shown by a detailed examination of the vorticity equation (Moreau, 1969) that, as above, the field tends to suppress (turbulent) vorticity normal to it in times of the order $\rho/\sigma B^2$. The turbulence should thus tend to become axisymmetric about **B**, and eventually even two-dimensional with vorticity only along **B**.

The experiments of Fraim and Heiser (1968) suggest that reversion occurs for sufficiently small values ($\lesssim 30$) of the ratio of the Reynolds to the Hartmann number

$$\frac{\mathrm{Re}}{\mathrm{Ha}} = \frac{U}{B}\left(\frac{\rho}{\nu\sigma}\right)^{1/2} \tag{10.5}$$

where the Hartmann number

$$\mathrm{Ha} = \mathrm{B}a(\sigma/\rho\nu)^{1/2},$$

when squared, provides a measure of the ratio of the magnetic to the viscous forces. Note that the parameter (10.5) does not involve any length scale characteristic of the reverting flow. Earlier explanations of the role of this parameter (interpreting it as "the square root of the product of the viscous and magnetic forces divided by the inertial forces," as Fraim and Heiser do, for example) are unnecessarily obscure and do not give us an insight into the physical phenomena involved. We offer a simpler interpretation below.

A measure of the ratio of the magnetic to the inertial forces is the Stuart number or interaction parameter, which is given by $\mathrm{S} = \mathrm{Ha}^2/\mathrm{Re}, = \sigma B^2 l/\rho u$ for eddies of size l and velocity u. This parameter is large for the larger eddies, which therefore tend to be damped out by *ohmic* dissipation (Moffatt, 1967; Moreau, 1969). The largest eddy that escapes ohmic dissipation is of size $U\tau \sim \rho U/\sigma B^2$, which can be much smaller than the characteristic flow length scale when B is high. Reversion must occur if eddies of this size or smaller are dissipated by viscosity, i.e., if the Reynolds number based on $U\tau$, namely,

$$\frac{U}{\nu}\frac{U\rho}{\sigma B^2} = [\mathrm{Re/Ha}]^2$$

is sufficiently small. It is thus no surprise to find a critical value for the ratio Re/Ha.

This explanation suggests then that when the field is aligned with the flow, reversion occurs by dissipation—ohmic for the large eddies, viscous for those not so large.

C. Normal Fields

The same two sources of dissipation must affect the turbulence even when the field is normal to the flow, but the $\mathbf{j} \times \mathbf{B}$ force may now act in addition to suppress the *mean* vorticity of the flow normal to **B**. Using the previous estimate of the decay time, the characteristic streamwise distance should be of order

$$U\rho/\sigma B^2 \sim a/\mathrm{S},$$

where S is now the Stuart number based on U and a. Further downstream the velocity therefore tends to become uniform across the duct, except in thin "Hartmann" layers at the surface that ensure that the no-slip condition is satisfied. At large values of the Hartmann number the thickness δ of this layer is proportional to $a/\mathrm{Ha} = (\rho\nu/B^2\sigma)^{1/2}$.

The first experiments on the effects of a magnetic field on laminar flow were conducted in a channel by Hartmann and Lazarus (1937); since then there have been many other studies in turbulent flow as well (an interesting survey of earlier Western and Russian work is Branover *et al.*, 1967). Such experiments present many difficulties: measurement techniques are not easy (see, e.g., Branover and Gershon, 1976; Branover *et al.*, 1977), and the flow situations are bedeviled by such effects as the absence of a fully developed state due to insufficient length of duct or field, the fringing of the magnetic field lines near the ends of the magnet, and the finite aspect ratio of the cross section of the duct when it is a channel. Thus, while many interesting experiments have been made (Murgatroyd, 1953; Branover *et al.*, 1977; Gardner and Lykoudis, 1971; Hua and Lykoudis, 1974; Reed and Lykoudis, 1978), and much insight obtained, one can hardly say that the picture is yet complete.

All experiments show that with a sufficiently strong field, the skin friction changes from the initial turbulent value to one characteristic of laminar m.h.d. flow. As an example, we show in Fig. 39 the measurements of Gardner and Lykoudis (1971) in a pipe. Note that the final m.h.d. laminar value of c_f is generally much higher than the non-m.h.d. turbulent value at the same Reynolds number! At the higher Re, the skin friction shows a dip before rising again as the field increases. At lower Re, the recent measurements of Reed and Lykoudis (1978) show an even more involved behavior of c_f than the data of Fig. 39: there is a small but noticeable initial dip, then a hump followed by another dip before c_f rises to the laminar value. The first dip manifests itself because of the damping of turbulence by the magnetic field while the Hartmann flattening has not yet become dominant. The flow is presumably still fully turbulent at this stage. With increasing field strength, the Hartmann effect wins over, accounting for the rise in c_f. The presence

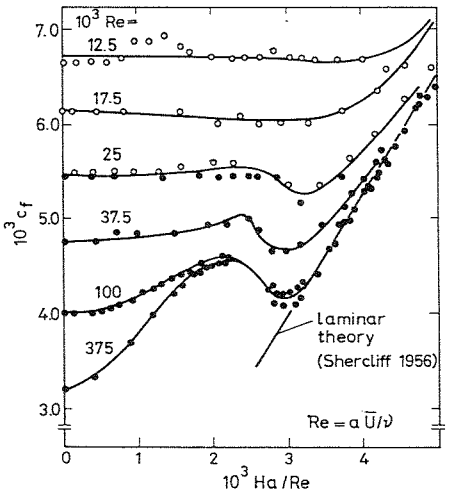

FIG. 39. Typical skin friction coefficient data for a pipe flow in a normal magnetic field (Gardner and Lykoudis, 1971).

of the following hump and the (second) dip is not surprising and are easily explained if we allow that during transition (or reversion) there is a regime in which the flow alternates between the laminar and turbulent states. If at the point of change in flow character the turbulent skin friction is higher than the laminar, a dip must appear (as in a flat plate boundary layer; see Dhawan and Narasimha, 1958); otherwise it will not. The crucial fact is that at low Re, the laminar c_f is comparable to the turbulent c_f near reversion, but at high Re it is much lower. Of course a convincing theory for the variation of turbulent c_f with magnetic field is required before this argument can be considered complete.

It is generally thought that relaminarization—as judged by the agreement between measured c_f (or pressure loss) and laminar theory—occurs when Ha/Re exceeds a critical value. This can by no means be considered to have been established firmly yet; indeed Fig. 39 suggests that the value of Re/Ha at which laminar skin friction is attained decreases with increasing Re, and we shall return to this point shortly. A related point is that the values quoted for $(\mathrm{Re/Ha})_{cr}$ by different workers do not agree. Murgatroyd (1953) suggested $(\mathrm{Re/Ha})_{cr} \simeq 225$ for a channel; the more recent measurements of Hua and Lykoudis (1974) indicate the higher value of nearly 330. Hua and Lykoudis show that it is important to take into account the effect of the aspect ratio on the laminar solution in attempting to judge when reversion is complete. They also observe a departure from the laminar solution at high Ha/Re, and attribute it to magnetic entrance effects that prevent the establishment of the fully developed flow.

Branover and Gershon (1976) suggest the empirical formula

$$(\mathrm{Re/Ha})_{cr} = 215 - 85\exp(-0.35\beta),$$

where

$$\beta = \frac{\text{side perpendicular to field}}{\text{side parallel to field}}$$

is the aspect ratio of the channel.

Note that all these values for $(\mathrm{Re/Ha})_{cr}$ are appreciably higher than those with aligned fields, presumably reflecting the additional effect on the mean flow due to the magnetic force. The relatively lower value of $(\mathrm{Re/Ha})_{cr}$ at lower β is again consistent with this idea, because the Hartmann effect now operates on the shorter sides of the channel and is therefore weaker.

To examine this effect more closely, we note that when Ha is large the Hartmann number based on δ,

$$\mathrm{Ha}_\delta = B\,\delta(\sigma/\rho\nu)^{1/2},$$

is $O(1)$; it follows that

$$\frac{\mathrm{Re}}{\mathrm{Ha}} \sim \frac{U}{B}\left(\frac{\rho}{\nu\sigma}\right)^{1/2} \sim \frac{\mathrm{Re}_\delta}{\mathrm{Ha}_\delta} \sim \mathrm{Re}_\delta.$$

At high Ha, the velocity profile in the Hartmann layer takes the simple form (see, e.g., Shercliff, 1965, Sect. 6.5)

$$u = U\left[1 - \exp\left(-\frac{y}{a\mathrm{Ha}}\right)\right],$$

where y is distance measured from the surface; this velocity distribution is the same as in the asymptotic suction profile (Rosenhead, 1963, p. 241). The critical Reynolds number for this profile is about 45,000 (see Rosenhead, 1963, p. 543) based on the displacement thickness; the Reynolds number at turbulence suppression in m.h.d. channel flow, corresponding to Re_δ of a few hundreds, is thus some orders of magnitude lower than this critical value. The "Hartmann effect" of the normal field therefore produces a highly stable mean velocity distribution. Indeed, the detailed linear stability analysis of *laminar* flow by Lock (1955) finds that the chief reason for the greater stability of channel flow subjected to high normal magnetic fields is the significant alteration of the mean flow.

As the time required for suppression of either the mean or the fluctuating vorticities is apparently of order $\rho/\sigma B^2$, it seems *a priori* possible that the two effects reinforce each other. Interesting experiments on the turbulent quantities in these flows have been conducted by Gardner and Lykoudis (1971) in pipes, and by Branover *et al.* (1977) and Branover and Gershon (1976) in channels. These measurements depict the decay of turbulence at a

fixed point in the channel as the field is increased, and do not unfortunately trace the streamwise variation at a fixed field. Nevertheless, the experiments do show that at a station where the surface friction has reached laminar values, turbulent fluctuations have not vanished, although they evidently do not contribute to momentum transport. In fact, Reed and Lykoudis (1978) find that the Reynolds shear stress was completely suppressed even though u' and v' were not; clearly a decorrelating mechanism is again at work here. The flow is therefore quasi-laminar, in the sense of Section V. There has been some discussion whether these fluctuations are a residue of the original turbulent flow, or arise from the creation of unstable velocity profiles in the channel where the (originally turbulent) flow enters the magnetic field: gradients in the field due to the "fringe effect" at the poles used in the experiment can *create* vorticity (see Shercliff, 1965, pp. 94–95), and so lead to the so-called M-shaped profiles possessing inflexion points. Branover and Gershon argue that the occurrence of such profiles depends on the Stuart number, and offer evidence that in those experiments where S was lower (and hence the M-profile effect weaker), the residual turbulence was also weaker.

At the same time, Branover and Gershon also find evidence that the residual turbulence approaches two-dimensionality; as may be seen from Fig. 40, the correlation coefficient of the longitudinal velocity fluctuations at

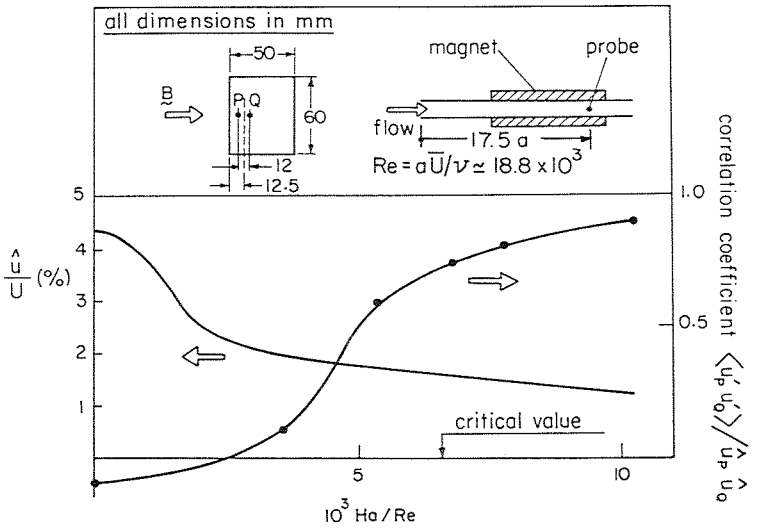

FIG. 40. Longitudinal velocity fluctuations and field-wise correlation coefficient in channel flow subjected to a normal field. (Data from Fig. 3.3, Branover *et al.*, 1977). Note that at the critical value of $Ha/Re \simeq 6.6 \times 10^{-3}$, when the skin friction has attained the laminar value, the turbulence intensity is still appreciable but the correlation coefficient very large.

two fixed points along the field shows, in one case, an increase from near zero at $Re/Ha \simeq 10^3$ to about 0.9 at $Re/Ha \simeq 10^2$.

On the other hand, Gardner and Lykoudis (1971) found that the magnetic entrance effect extends only a few diameters in their pipe experiments. However, in other respects the situation in a pipe is rather complex, as the current flows in two loops in the cross-sectional plane—across the field in a central core, then around the circumference. This introduces a dependence on the azimuthal angle in the flow parameters; e.g., the turbulence is suppressed first along the field. The Hartmann flattening of the velocity profile is also most pronounced in the same direction. This azimuthal dependence makes interpretation of pipe data difficult. Gardner and Lykoudis point out that there is some evidence, nevertheless, that on the application of the magnetic field the large eddies are damped out first, presumably by ohmic dissipation (Fig. 41). This indicates that the changes in mean velocity profile occur faster, and that these changes, through the creation of stabler profiles, bring viscous dissipation into play. At a later stage of relaminarization, there is however *relatively* greater energy at the lower frequencies (the *total* energy is of course much less).

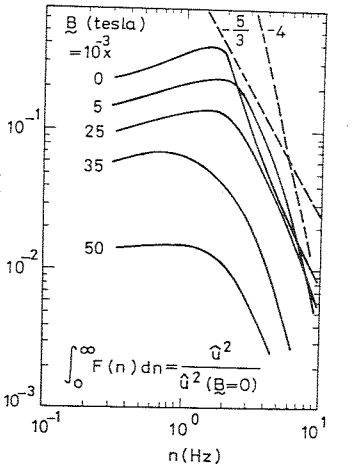

FIG. 41. Spectra of axial velocity fluctuations at center-line in m.h.d. pipe flow: $Re = 5150$. (From Gardner and Lykoudis, 1971.)

It must be noted that the variation of turbulence intensity in these experiments correlates better with $Ha^2/Re^{0.75}$ than with Ha/Re, especially at low fields.

To summarize, a normal field should directly suppress turbulent vorticity not aligned with it, but the associated Hartmann effect, altering the mean velocity profile in a stabilizing way, must also play a strong role in relaminarizing the flow, if indeed it is not the rate-controlling mechanism. An

indication of this is the much higher value of $(\mathrm{Re}/\mathrm{Ha})_{cr}$ in normal fields as compared to aligned fields (around 300 vs. about 30). Further support is lent by the lower value of $(\mathrm{Re}/\mathrm{Ha})_{cr}$ when the field is along the longer side of the channel; the Hartmann effect, confined now to the shorter sides, is obviously weaker in this case. The presence of significant turbulence even when the skin friction has attained laminar values bears a strong resemblance to several other cases discussed earlier (Sections III and IV) and is of course not peculiar to m.h.d. flows, in spite of the impression sometimes given in the literature of the subject.*

If the primary (or rate-controlling) mechanism of reversion should be the domination of the magnetic force over the Reynolds stress gradient in the originally turbulent flow, we may expect the correlating parameter (following the arguments on accelerating flow in Section V) to be

$$\text{at low fields:}\ \frac{\sigma UB^2}{\tau_0/D} \sim \frac{\mathrm{Ha}^2}{c_f\,\mathrm{Re}}, \tag{10.6a}$$

$$\text{at high fields:}\ \frac{\sigma UB^2}{\tau_0/\delta} \sim \frac{\mathrm{Ha}^2}{c_f\,\mathrm{Re}} \cdot \frac{\delta}{D} \sim \frac{\mathrm{Ha}}{c_f\,\mathrm{Re}}. \tag{10.6b}$$

The experiments of Hua and Lykoudis (1974) in a channel show that the decrease in turbulence intensity with increase in field correlates with $\mathrm{Ha}^2/\mathrm{Re}$ at low field strengths; Gardner and Lykoudis (1971) similarly find the correlating parameter in pipes to be $\mathrm{Ha}^2/\mathrm{Re}^{0.75}$, which is the same as (10.6a) if c_f is taken to obey the well-known Blasius law in turbulent flow, $c_f \sim \mathrm{Re}^{-1/4}$. The Blasius law should be a reasonable approximation at low fields and relatively low Re, but as the field and Re increase it appears from Gardner and Lykoudis's experiments that the c_f varies less with Re than the Blasius law suggests. The correlation of $(\mathrm{Ha}/\mathrm{Re})_{cr}$ with Re provided in Fig. 27 of their paper shows two distinct regions, which we may describe by

$$(\mathrm{Ha}/\mathrm{Re})_{cr} \sim \mathrm{Re}^{-0.05}, \qquad 10^4 < \mathrm{Re} < 8 \times 10^4$$

$$\sim \mathrm{Re}^{-0.3}, \qquad 10^5 < \mathrm{Re} < 5 \times 10^5.$$

The high Re correlation is rather like (10.6b).

Considering the difficulties in these experiments (e.g., the c_f in the relaminarized region shows a systematic departure from the laminar solution of Shercliff (1956), which according to the authors could have been due to roughness, insufficient entry length or the residual turbulence), all we can say is that the criterion for reversion appears to be a parameter of the form $\mathrm{Ha}/\mathrm{Re}^n$, where n is definitely less than 1, and probably around $\frac{1}{2}$ for relatively

* Branover and Gershon (1976) say that "the problem of remaining disturbances constitutes one of the most paradoxical phenomena of fluid mechanics."

low fields. Recalling that reversion in the non-m.h.d. flow in a channel occurs at $\mathrm{Re} \simeq 1500$ (see Section III,B,2), we may sketch the likely boundary between laminar and turbulent flow as in Fig. 42.

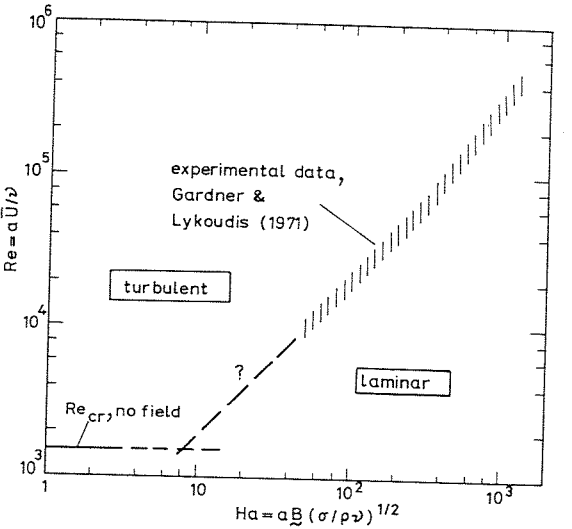

FIG. 42. Sketch of proposed reversion boundaries in m.h.d. pipe flow.

XI. Other Instances of Relaminarization

It was pointed out by Landau and Lifshitz (1959, p. 137) that an axisymmetric turbulent wake should eventually revert to a laminar state. The wake behind any body of nonzero, finite drag is characterized by a momentum thickness θ which remains constant along the wake. Sufficiently far downstream, the momentum deficit in the wake $U^2\theta^2$ is proportional to $\delta^2 U\,\Delta U$, where ΔU is the maximum velocity defect, U is the free stream velocity, and δ is the wake thickness. It follows that the wake Reynolds number $\mathrm{Re}_\delta = \delta\,\Delta U/\nu \sim (U\theta/\nu)(\theta/\delta)$, so that if the wake keeps growing its Reynolds number must keep decreasing. A detailed calculation of the wake, assuming that it is "self-preserving" (Townsend, 1956, Section 7.15), shows that $\delta \sim x^{1/3}, \Delta U \sim x^{-2/3}$, $\mathrm{Re}_\delta \sim x^{-1/3}$. Sufficiently far downstream, therefore, the Reynolds number becomes so small that the wake must relaminarize, by dissipation; standard turbulent behavior cannot therefore be expected. It is probably for similar reasons that Freymuth's (1975) search for the final period of decay in the wake behind a sphere proved fruitless. However, the

Reynolds number variation with x is very weak, and we have already seen in Section III that dissipative reversion is very slow; it is therefore no great surprise that explicit observations of such relaminarization have not been made.

The argument for relaminarization is valid for the wake behind any finite drag-producing body. However, there is no tendency to reversion in the wake behind a *two-dimensional* body, as the corresponding wake Reynolds number remains constant in this case.

The tip vortex produced behind a finite wing also appears to exhibit reversion, presumably as a result of the curvature of the flow. Poppleton (1971) shows very interesting photographs of flow visualization using smoke in the wing-tip vortex generated by a Hercules aircraft in flight. There is a delicate relationship between axial and transverse velocities in such vortices: the axial velocity relative to the wing changes sign across the vortex, with the result that there is co-curving flow in the core; the photographs show that the vortex core is laminar, although the outer part is turbulent.

Laboratory experiments reported by Singh and Uberoi (1976) also suggest a reversion in the wing-tip vortex; they find that, while at a distance of one chord behind the tip the flow is turbulent, at 30 chords the vortex appears laminar, with a periodic instability (see their Fig. 4). At 60 chords, however, no periodicity was evident, but turbulent patches appeared in the velocity signals.

We believe that the relaminarization observed in swirling flames (e.g., Beer *et al.*, 1971) is a related phenomenon.

We have discussed at great length in Section V how spatially accelerated shear flows may relaminarize. It may be expected that when the acceleration is temporal similar effects should be observed. Some preliminary experiments during transient flow in a pipe by Leutheusser and Lam (1977) show that such acceleration certainly delays transition, i.e., the critical Reynolds number increases. In analogy with spatial acceleration, we may also anticipate that the relevant parameters governing departure from the law of the wall and completion of reversion respectively would be (with superscript t standing for the temporal problem)

$$\Delta^{(t)} = \nu\dot{U}/U_*^2, \; \Lambda^{(t)} = \dot{U}\,\delta/U_{*0}^2$$

where $\dot{U} \equiv dU/dt$ is the time derivative of a characteristic flow velocity. When variations in c_f may not be appreciable, we may also expect the free stream parameter

$$K^{(t)} = \nu\dot{U}/U_*^3$$

to play a role similar to that of K in Section V. However, there is not enough experimental data yet to make a detailed analysis.

When the temporal variations are not monotonic, a complex series of transitions and reversions may be expected, depending on ratios of the time scales characterizing the acceleration to those characterizing transition and reversion.

We may briefly return to the reversion observed in coiled pipes, which was mentioned in Section I. There is probably a combination of several mechanisms at work here. There is first of all the suppression of turbulence on a convex wall—in the present instance on the inside of the bend—that was discussed at some length in Section VI. On the outside of the bend, the concave flow curvature should if anything enhance the turbulence, but this effect may be counteracted by the secondary flow that is known to be generated. Lighthill (1970) has pointed out that one effect of the secondary flow is to shift the velocity maximum outward, with the formation on the outside of the bend of a thin layer with an effectively lower Reynolds number. For example, measurements by Rowe (1970, Fig. 1) in a pipe bent to a radius of 12 diameters show that, after a 60° bend, the maximum total pressure has moved out from the centre by about two-thirds of the radius. Such a reduction in the Reynolds number may well dissipate turbulence on the outside of the bend, and allow the development of a laminar subboundary layer there. More detailed experimental investigations are necessary to elucidate the mechanisms operating in this flow.

There is also the possibility of reversion on swept wings in an aircraft—the turbulent boundary layer on the fuselage is first swept down the leading edge of the wing before rolling over to chordwise flow; in the process, it is subjected to a large favorable pressure gradient near the leading edge. Thompson (1973) has shown how it might be possible to exploit the possibilities of reversion in such flows to save a few percent on the drag of the wings of large transport aircraft. It remains to be seen whether, and if so to what extent, the beneficial effect of the favorable pressure gradient is counteracted in this case by the curvature that the boundary layer experiences along the flow.

XII. Conclusion

In the preceding sections we have examined and described a variety of flows in which relaminarization has been observed or may be expected to occur. It is certain that many other reverting flows exist, and more will be discovered in future.

It is instructive however to compare the different types of reversion that we have already described. In both dissipative and absorptive types of

reversion, there is a net decrease in turbulence energy: in the first instance, this energy is lost essentially by the action of a molecular transport parameter like the viscosity or the electrical resistivity; in the second, it is destroyed by the work done against a body force like gravity. In the enlarged pipes discussed in Section III, even when the final Reynolds number drops to as low as half of the critical value, the distance required to complete reversion is of the order of a hundred diameters: thus the reversion is very slow. In contrast, in the Richardson type reversions, the destruction of turbulence energy appears to proceed rapidly once the critical value of the parameter is exceeded: turbulence is suppressed in a few jet widths in Fig. 2. In both cases, there is evidence that what happens goes beyond a mere decrease in turbulence energy; in fact some mechanism seems to be at work to decorrelate the velocity components that generate the crucial Reynolds stresses.* In particular, the effects of even mild curvature on a turbulent shear flow seem astonishingly strong. Clearly one is not merely wearing the mechinery of turbulence down in these cases—it is more as if one were throwing a spanner into the works! In other words, these external influences imposed on the flow must be interfering with its organization—with the coherent structures and the bursting cycle that sustain turbulence.

In making this statement, we have come full circle from the thermodynamic objection against the possibility of reversion, mentioned in Section I. For reversion can also be viewed in many cases as the destruction of the large scale quasi-order of turbulent flows into the molecular-scale disorder of laminar flows! A naive order–disorder approach to relaminarization can therefore be misleading for more reasons than one.

The third type of reversion, viz., that which occurs during acceleration, shares some characteristics with the other two types, but has some obviously distinctive features also. For example, the generation of a new laminar layer (inevitably involving dissipation of turbulent energy) is common to reverting flows of different types; and the pressure gradient parameter Λ resembles a "bulk" Richardson number. On the other hand, the shear stresses during acceleration are not really destroyed; rather they are frozen, and everything is over, so to speak, before the machinery of turbulence has time to adjust itself to the external agency (i.e., the imposed pressure gradient). In low speed flows, this agency therefore continues to dominate the dynamics of the flow—not because the turbulence is dissipated or destroyed in absolute magnitude, but rather because the agency is so much larger. One is reminded of the story about Emperor Akbar and Birbal; one way of shortening a stick without wearing it out or breaking it is to place a bigger stick next to it.

* In general, all forms of reversion seem particularly sensitive to interference with the relatively small normal velocity.

We recall our pragmatic definition of reversion (Section I) according to which a flow has laminarized if its development does not demand understanding of the dynamics of turbulence. Thus, it is not necessary for the characteristically random velocity fluctuations of turbulence to be entirely absent in a relaminarized flow, but only that such fluctuations, even if present, should not lead to appreciable momentum or energy transport. We have specifically demonstrated that this is true (although for different reasons) in reverting pipe or channel flows (Section III) and in accelerated reverting boundary layers (Section V), but it is likely to be true at least in a somewhat restricted sense in all the other flows discussed here: perhaps the most restrictive case is that with injection, where the dynamics of turbulence becomes unimportant only fairly locally, close to the beginning of injection. By the same token, it is not clear at present whether our definition of reversion encompasses the technologically important case of drag reduction by dilute polymer addition, even though a phenomenal reduction of turbulent intensities and Reynolds stress has been observed here.

It is sometimes suggested that one ought to decide whether a flow has reverted to the laminar state by examining whether it becomes turbulent again as in direct transition. This seems an attractive idea; in some reverting boundary layers it has been possible to recognize the generation of new turbulent spots leading to a second transition to turbulence. However, as an invariable criterion the idea bristles with difficulties. The chief reason is that unlike direct transition, which is often catastrophic, reversion is often asymptotic. Thus, the birth of a spot in a boundary layer is a dramatic event that heralds turbulence; but during reversion, there is no such event whose occurrence guarantees that the flow is going to become laminar downstream, although, as we have seen in Section V, many flow parameters do vary *rapidly* during reversion. A reverting flow is often in a rather noisy quasi-laminar state, in which even the occurrence of what might otherwise have been a dramatic event (e.g., birth of a spot indicating retransition) tends to get masked.

In any case, it is neither practical nor fruitful to try and decide whether a flow has reverted at any given point by having to investigate whether it could go turbulent again in some standard way. In fact, the concept would be meaningful only if *points* of reversion (as of transition) could be uniquely determined.

In many situations where reversion does occur, a combination of the different basic mechanisms can be at work. For example, in a highly heated duct flow, it is still not certain how much of the resulting changes are due to:

(i) the increase in viscosity, and hence in dissipation, that follows the higher temperatures;

(ii) the acceleration consequent on the reduction in gas density;
(iii) the stratification introduced into the flow by heating;
(iv) the possible domination of the conduction heat flux over the other forms of heat transfer.

It is possible that in any given situation, more than one of these mechanisms contribute; thorough studies are still required to determine which of the different mechanisms are the more significant in any given situation.

A key to understanding these complex situations will surely be an appreciation for the *rate* at which different mechanisms operate. We have seen evidence for the slowness with which dissipative reversion takes place. On the other hand, an external agency can quickly alter the mean flow significantly, and hence either suppress or overwhelm the turbulence; it is also possible that the turbulent energy is either quickly absorbed, or the phase relations promoting momentum exchange destroyed, with *consequent* changes in the mean flow. The possible pathways are schematically illustrated in Fig. 43. Further studies should perhaps concentrate on helping us to decide what the rate-controlling mechanism is in any given flow situation.

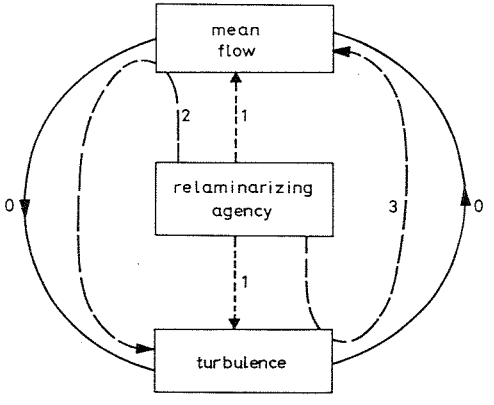

FIG. 43. Pathways to relaminarization. 0, the coupling between mean flow and turbulence in fully developed turbulent flow; 1, relaminarizing agency, working on both mean flow and turbulence at comparable rates; 2, mean flow affected more rapidly than turbulence; 3, turbulence affected more rapidly than mean flow.

We may conclude by remarking on how often reversion apparently occurs, and how easy it appears to be to suppress turbulence—it looks almost as if whether you suck or blow, squeeze or bend, heat or cool, or do any of a vast number of other things to it, turbulence can be destroyed, or at least disabled; *provided* of course the operation is done properly. There are just

now beginning to be a few technological examples where turbulence might be controlled by promoting reversion. Thus, we have already noted Thompson's (1973) suggestion that it might be possible to engineer reversion near the leading edge of swept wings on the larger transport aircraft, and so save a few percent on the drag. In many rocket nozzles, wind tunnel contractions, and other such devices, reversion has undoubtedly been occurring without having been explicitly designed in. It would be very useful if high-speed wind tunnel test sections, which tend to be noisy because of sound radiated from the turbulent boundary layers on the wall, could be made "quiet" by the device of relaminarization. Nevertheless, "turbulence control" is still something that remains a bit of a dream. Perhaps when there is greater understanding of the nature of coherent structures and of their role in turbulence, it will be possible to aim spanners better at the machinery of turbulence and so win the ability to control it when necessary.

ACKNOWLEDGMENTS

This paper is an extended version of an invited lecture given by R.N. at the Sixth Canadian Congress of Applied Mechanics, Vancouver 1977. The work described here has been the result of collaboration with several colleagues; we particularly wish to acknowledge out debt to Dr. P. R. Viswanath, Dr. M. A. Badri Narayanan, Dr. A. Prabhu, and Dr. B. G. Shivaprasad.

The preparation of the paper has been supported in part by a grant from the Indian National Science Academy. K.R.S. acknowledges his indebtedness to Professor S. Corrsin for making available financial support from NASA Grant NSG 2303 during the later stages of this work at the Department of Mechanics and Materials Science of The Johns Hopkins University.

REFERENCES

ABRAMOWITZ, M., and STEGUN, I. A., (eds.) (1965). "Handbook of Mathematical Functions." Dover, New York.

ALVI, S. H. (1975). Flow characteristics of sharp-edged orifices, quadrant-edged orifices and nozzles. Ph. D. Thesis, Dept. Civ. Eng., Ind. Inst. Sci., Bangalore.

ANANDA MURTHY, K. R., and HAMMITT, A. G. (1958). "Investigation of the Interaction of a Turbulent Boundary Layer with Prandtl-Meyer Expansion Fan at M = 1.88," Rep. No. 434. Dept. Aero. Eng., Princeton University, Princeton, New Jersey.

ANTONIA, R. A., CHAMBERS, A. J., PHONG-ANANT, D., RAJAGOPALAN, S., and SREENIVASAN, K. R. (1979). Response of atmospheric surface layer turbulence to a partial solar eclipse. *J. Geophys. Res.* **84**, 1689.

BACK, L. H., and SEBAN, R. A. (1967). Flow and heat transfer in a turbulent boundary layer with large acceleration parameter. *Proc. Heat Transfer Fluid Mech. Inst.* **20**, 410.

BACK, L. H., MASSIER, P. F., and GIER, H. L. (1964). Convective heat transfer in a convergent-divergent nozzle. *Int. J. Heat Mass Transfer* 7, 549.

BADRI NARAYANAN, M. A. (1968). An experimental study of reverse transition in two-dimensional channel flow. *J. Fluid Mech.* **31**, 609.

BADRI NARAYANAN, M. A., and RAMJEE, V. (1969). On the criteria for reverse transition in a two-dimensional boundary layer flow. *J. Fluid Mech.* **35**, 225.

BADRI NARAYANAN, M. A., RAJAGOPALAN, S., and NARASIMHA, R. (1974). "Some Experimental Investigations on the Fine Structure of Turbulence," Rep. No. 74 FM 15. Dept. Aero. Eng., Ind. Inst. Sci., Bangalore.

BADRI NARAYANAN, M. A., RAJAGOPALAN, S., and NARASIMHA, R. (1977). Experiments on the fine structure of turbulence. *J. Fluid Mech.* **80**, 237.

BANKSTON, C. A. (1970). The transition from turbulent to laminar gas flow in a heated pipe. *J. Heat Transfer* **92**, 569.

BATCHELOR, G. K. (1953). "The Theory of Homogeneous Turbulence." Cambridge Univ. Press, London and New York.

BATCHELOR, G. K., and PROUDMAN, I. (1954). The effect of rapid distortion of a fluid in turbulent motion. *Quart. J. Mech. Appl. Math.* **7**, 83.

BATCHELOR, G. K., and TOWNSEND, A. A. (1948). Decay of turbulence in the final period. *Proc. R. Soc. London, Ser. A* **194**, 527.

BEER, J. M., CHIGIER, N. A., DAVIES, T. W., and BASSINDALE, K. (1971). Laminarisation of turbulent flames in rotating environments. *Combust. Flame* **16**, 39.

BLACKWELDER, R. F., and KOVASZNAY, L. S. G. (1972). Large scale motion of a turbulent boundary layer during relaminarisation. *J. Fluid Mech.* **53**, 61.

BLOY, A. W. (1975). The expansion of a hypersonic turbulent boundary layer at a sharp corner. *J. Fluid Mech.* **67**, 647.

BRADSHAW, P. (1969a). A note on reverse transition. *J. Fluid Mech.* **35**, 387.

BRADSHAW, P. (1969b). The analogy between streamline curvature and buoyancy in turbulent shear flow. *J. Fluid Mech.* **36**, 177.

BRADSHAW, P. (1973). Effects of streamline curvature on turbulent flow. *AGARDograph* **169**.

BRANOVER, G. G., GELFGAT, YU. M., and TSINOBER, A. B. (1967). Turbulent mhd flows in prismatic and cylindrical pipes. *NASA Tech. Transl.* **F-482**.

BRANOVER, H., and GERSHON, P. (1976). "MHD Turbulence Study, Part 2," Rep. ME 6-76. Dept. Mech. Eng., Ben-Gurion University.

BRANOVER, H., GERSHON, P., and YAKHOT, A. (1977). "MHD Turbulence and Two-phase Flow," Rep. ME 5-77. Dept. Mech. Eng., Ben-Gurion University.

BROWN, G. L., and THOMAS, A. S. W. (1977). Large structure in a turbulent boundary layer. *Phys. Fluids* **20**, S243.

BUSINGER, J. A., and ARYA, S. P. S. (1974). Height of the mixed layer in the stably stratified planetary boundary layer. *Adv. Geophys.* **18A**, 73.

CHAPMAN, D. R., WIMBROW, W. R., and KESTER, R. H. (1952). Experimental investigation of base pressure on blunt trailing edge wings at supersonic velocities. *Natl. Advis. Comm. Aeronaut., Rep.* **1109**.

CHEN, C. P., and PUEBE, J. L. (1964). Sur l'écoulement radial divergent d'un fluide visqueux incompressible enter deux plans paralleles. *C. R. Hebd. Seances Acad. Sci.* **258**, 5353.

CHEN, K. K., and LIBBY, P. A. (1968). Boundary layers with small departures from the Falkner-Skan profiles. *J. Fluid Mech.* **33**, 273.

COLES, D. (1962). Interfaces and intermittency in turbulent shear flow. *In* "Mécanique de la turbulence," pp. 229–248. CNRS, Paris.

COLES, D. (1978). A model for flow in the viscous sublayer. *In* "Workshop on Coherent Structure of Turbulent Boundary Layers" (C. R. Smith and D. E. Abbott, eds.), p. 462. Lehigh University, Bethlehem, Pennsylvania.

COON, C. W., and PERKINS, H. C. (1970). Transition from the turbulent to the laminar regime for internal convective flow with large property variations. *J. Heat Transfer* **92**, 506.

CROW, S. C. (1969). Distortion of sonic bangs by atmospheric turbulence. *J. Fluid Mech.* **37**, 529.

DHAWAN, S., and NARASIMHA, R. (1958). Some properties of boundary layer flow during transition from laminar to turbulent motion. *J. Fluid Mech.* **3**, 418.

DRYDEN, H. L., and SCHUBAUER, G. B. (1947). The use of damping screens for the reduction of wind tunnel turbulence. *J. Aeron. Sci.* **14**, 221.

DUTTON, R. A. (1960). "The Effect of Distributed Suction on the Development of Turbulent Boundary Layers." ARC R & M No. 3155.

ECKERT, E. R. G., and RODI, W. (1968). Reverse transition turbulent-laminar for flow through a tube with fluid injection. *J. Appl. Mech.* **35**, 817.

ELLISON, T. H. (1957). Turbulent transport of heat and momentum from an infinite rough plane. *J. Fluid Mech.* **2**, 456.

ELLISON, T. H., and TURNER, J. S. (1960). Mixing of dense fluid in a turbulent pipe flow. *J. Fluid Mech.* **8**, 514.

FIEDLER, H., and HEAD, M. R. (1966). Intermittency measurements in the turbulent boundary layer. *J. Fluid Mech.* **25**, 719.

FRAIM, F. W., and HEISER, W. H. (1968). The effect of strong longitudinal magnetic field on the flow of mercury in a circular tube. *J. Fluid Mech.* **33**, 397.

FREYMUTH, P. (1975). Search for the final period of decay of the axisymmetric turbulent wake. *J. Fluid Mech.* **68**, 813.

FULLER, L., and REID, J. (1958). "Experiment in Two-dimensional Base Flow at M = 2.4." ARC R & M No. 3064.

GARDNER, R. A., and LYKOUDIS, P. S. (1971). Magneto-fluid-mechanic pipe flow in a transverse magnetic field. Part 1. Isothermal flow. *J. Fluid Mech.* **47**, 737.

GAVIGLIO, J., DUSSAUGE, J.-P., DEBIEVE, J. F., and FAVRE, A. (1977). Behavior of a turbulent flow, strongly out of equilibrium, at supersonic speeds. *Phys. Fluids* **20**, S179.

GLOBE, S. (1961). The effect of a longitudinal magnetic field on pipe flow of mercury. *Trans. ASME* **83**, 445.

HALL, A. A. (1938). "Measurements of the Intensity and Scale of Turbulence." ARC R & M No. 1852.

HALLEEN, R. M., and JOHNSTON, J. P. (1967). "The Influence of Ratation on Flow in a Long Rectangular Channel—An Experimental Study," Rep. MD 18. Thermosci. Div., Dept. Mech. Eng., Stanford University, Stanford, California.

HARTMANN, J., and LAZARUS, F. (1937). Hg-dynamics. II. *K. Dan. Vidensk. Selsk., Mat.-fys. Medd.* **15**, 7.

HUA, H. M., and LYKOUDIS, P. S. (1974). Turbulence measurements in a magnetofluid-mechanic channel. *Nucl. Sci. Eng.* **54**, 445.

JEFFREYS, H. (1928). Some cases of instability in fluid motion. *Proc. R. Soc. London. Ser. A* **118**, 195.

JOHNSTON, J. P., HALLEEN, R. M., and LEZIUS, D. K. (1972). Effects of spanwise rotation on the structure of two-dimensional fully developed turbulent channel flow. *J. Fluid Mech.* **56**, 533.

KIRKO, I. M. (1965). "Magnetohydrodynamics of Liquid Metals." Consultants Bureau, New York.

KLINE, S. J., REYNOLDS, W. C., SCHRAUB, F. A., and RUNSTADLER, P. W. (1967). The structure of turbulent boundary layers. *J. Fluid Mech.* **30**, 741.

KREITH, F. (1965). Reverse transition in radial source flow between two parallel planes. *Phys. Fluids* **8**, 1189.

LANDAU, L. D., and LIFSHITZ, E. M. (1959). "Fluid Mechanics." Pergamon, Oxford.

LAUFER, J. (1962). Decay of non-isotropic turbulent field. *In* "Miszellaneen de angewandte Mechanik, Festschrift Walter Tollmien," Akademie-Verlag, Berlin.

LAUFER, J. (1975). New trends in experimental turbulence research. *Ann. Rev. Fluid Mech.* **7**, 307.

LAUNDER, B. E. (1963). "The Turbulent Boundary Layer in a Strongly Negative Pressure Gradient," Rep. No. 71. Gas Turbine Lab., Massachusetts Institute of Technology, Cambridge.

LAUNDER, B. E. (1964). "Laminarisation of the Turbulent Boundary Layer by Acceleration," Rep. No. 77. Gas Turbine Lab., Massachusetts Institute of Technology, Cambridge.

LAUNDER, B. E., and STINCHCOMBE, H. S. (1967). "Non-normal Similar Turbulent Boundary Layers," Imp. Coll. Note TWF/TN 21. Dept. Mech. Eng.

LEHNERT, B. (1955). An instability of laminar flow of mercury caused by an external magnetic field. *Proc. R. Soc. London, Ser. A* **233**, 299.

LEUTHEUSSER, H. H., and LAM, K.-W. (1977). Laminar-to-turbulent transition in accelerated fluid motion. *Proc. Congr. IAHR, 17th*, 1977 p. 124.

LEZIUS, D. K., and JOHNSTON, J. P. (1971). "The Structure and Stability of Turbulent Wall Layers in Rotating Channel Flow," Rep. No. MD-29. Thermosci. Div., Dept. Mech. Eng., Stanford University, Stanford, California.

LIEPMANN, H. W. (1943). Investigations on laminar boundary layer stability and transition on curved boundaries. *Natl. Advis. Comm. Aeronaut., Wartime Rep.* **W107** (ACR 3H 30).

LIEPMANN, H. W. (1945). Investigations of boundary layer transition on concave walls. *Natl. Advis. Comm. Aeronaut., Wartime Rep.* **W87** (ACR 4J 28).

LIGHTHILL, M. J. (1970). Turbulence. *In* "Osborne Reynolds and Engineering Science Today" (D. M. McDowell and J. D. Jackson, eds.), pp. 83–146. Manchester Univ. Press.

LOCK, R. C. (1955). The stability of the flow of an electrically conducting fluid between parallel planes under a transverse magnetic field. *Proc. R. Soc. London, Ser. A* **233**, 105.

LYONS, R., PANOFSKY, H. A., and WOLLASTON, S. (1964). The critical Richardson number and its implications for forecast problems. *J. Appl. Meteorol.* **3**, 136.

MCELIGOT, D. M., COON, C. W., and PERKINS, H. C. (1970). Relaminarization in tubes. *Int. J. Heat Mass Transfer* **13**, 431.

MACPHAIL, D. C. (1944). "Turbulence Changes in Contracting and Distorted Passages," RAE Rep. No. 1928.

MAGEE, P. M., and MCELIGOT, D. M. (1968). Effect of property variation on the turbulent flow of gases in tubes: The thermal entry. *Nucl. Sci. Eng.* **31**, 337.

MILES, J. W. (1961). On the stability of heterogeneous shear flows. *J. Fluid Mech.* **10**, 496.

MOFFATT, H. K. (1967). On the suppression of turbulence by a uniform magnetic field. *J. Fluid Mech.* **28**, 571.

MOLLER, P. S. (1963). Radial flow without swirl between parallel plates. *Aeron. Quart.* **14**, 163.

MONIN, A. S., and YAGLOM, A. M. (1971). "Statistical Fluid Mechanics." MIT Press, Cambridge, Massachusetts.

MOREAU, R. (1969). On mhd turbulence. *In* "Turbulence of Fluids and Plasmas" (J. Fox. ed.), pp. 359–372. Polytechnic Press, Brooklyn.

MORETTI, P. H., and KAYS, W. M. (1965). Heat transfer in turbulent boundary layer with varying free stream velocity and varying surface temperature—an experimenting study. *Int. J. Heat Mass Transfer* **8**, 1187.

MORKOVIN, M. V. (1955). Effects of high acceleration on a turbulent supersonic shear layer. *Proc. Heat Transfer Fluid Mech. Inst.*

MURGATROYD, W. (1953). Experiments on mhd channel flow. *Philos Mag.* [7] **44**, 138–1354.

NARASIMHA, R. (1957). On the distribution of intermittency in the transition region of a boundary layer. *J. Aeron. Sci.* **24**, 711.

NARASIMHA, R. (1977). "The Three Archtypes of Relaminarisation," Rep. No. 77 FM 7. Dept. Aero. Eng., Ind. Inst. Sci., Bangalore.

NARASIMHA, R., and SREENIVASAN, K. R. (1973). Relaminarization in highly accelerated turbulent boundary layers, *J. Fluid Mech.* **61**, 417.

NARASIMHA, R., and VISWANATH, P. R. (1975). Reverse transition at an expansion corner in supersonic flow. *AIAA J.* **13**, 693.

NASH-WEBBER, J. L., and OATES, G. C. (1972). An engineering approach to the design of laminarizing nozzle flows. *Am. Soc. Mech. Eng.* [*Pap.*] **72-FE-19**.

NICHOLL, C. I. H. (1970). Some dynamical effects of heat on a boundary layer. *J. Fluid Mech.* **40**, 361.

OKAMOTO, T., and MISU, I. (1977). Reverse transition of turbulent boundary layer on plane wall of two-dimensional contraction. *Trans. Jpn. Soc. Aerosp. Sci.* **20**, 1.

OWEN, P. R. (1969). Turbulent flow and particle deposition in the trachea. *In* "Circulatory and Respiratory Mass Transport" (G. E. W. Wolstenholme and J. Knight, eds.), p. 236. Churchill, London.

PAO, Y. H. (1969). Undulance and turbulence in stably stratified media. *In* "Clear Air Turbulence and Its Detection," p. 73. Plenum, New York.

PATEL, V. C. (1965). Calibration of the Preston tube and limitations on its use in pressure gradients. *J. Fluid Mech.* **23**, 185.

PATEL, V. C., and HEAD, M. R. (1968). Reversion of turbulent to laminar flow. *J. Fluid Mech.* **34**, 371.

PENNELL, W. T., ECKERT, E. R. G., and SPARROW, E. M. (1972). Laminarization of turbulent pipe flow by fluid injection. *J. Fluid Mech.* **52**, 451.

PERKINS, H. C., and WORSOE-SCHMIDT, P. M. (1965). Turbulent heat and momentum transfer for gases in a circular tube at wall to bulk temperature ratios to seven. *Int. J. Heat Mass Transfer* **8**, 1011.

PERKINS, H. C., SCHADE, K. W., and MCELIGOT, D. M. (1973). Heated laminarising gas flow in a square duct. *Int. J. Heat Mass Transfer* **16**, 897.

POPPLETON, E. D. (1971). "Exploratory Measurements of the Flow in the Wing-tip Vortices of a Lockheed Hercules," Aero. Tech. Note 7104. University of Sydney, Sydney, Australia.

PRANDTL, L. (1929). Einfluss stabilisierender Krafte auf die Turbulenz. *Gesammelte Abh.* **2**, 778.

PRANDTL, L., and REICHARDT, H. (1934). Einflusse von Warmeschichtung auf die Eigenschaften einer turbulenten Strömung. *Dtsch. Forschungsges.* No. 21.

RAMAPRIAN, B. R., and SHIVAPRASAD, B. G. (1978). The structure of turbulent boundary layers along mildly curved surfaces. *J. Fluid Mech.* **85**, 273.

RAMJEE, V. (1968). Reverse transition in a two-dimensional boundary layer flow. Ph.D. Thesis, Dept. Aero. Eng., Ind. Inst. Sci., Bangalore.

RAMJEE, V., BADRI NARAYANAN, M. A., and NARASIMHA, R. (1972). Effect of contraction on turbulent channel flow. *Z. Angew. Math. Phys.* **23**, 105.

RAO, K. N., NARASIMHA, R., and BADRI NARAYANAN, M. A. (1971). The "bursting" phenomenon in a turbulent boundary layer. *J. Fluid Mech.* **48**, 339.

REYNOLDS, O. (1884). The two manners of motion of water. *Proc. R. Inst. G. B.* **11**, 44.

RICHARDSON, L. F. (1920). The supply of energy to and from atmospheric eddies. *Proc. R. Soc. London, Ser. A* **97**, 354.

ROSENHEAD, L., ed. (1963). "Laminar Boundary Layers." Oxford Univ. Press, London and New York.

ROTTA, J. C. (1967). Effect of streamwise wall curvature on compressible turbulent boundary layers. *Phys. Fluids* **10**, S174.

ROWE, M. (1970). Measurements and computations of flow in bends. *J. Fluid Mech.* **43**, 771.

SAJBEN, M., and FAY, J. A. (1967). Measurement of the growth of a turbulent mercury jet in a coaxial magnetic field. *J. Fluid Mech.* **27**, 81.

SCHRAUB, F. A., and KLINE, S. J. (1965). "A Study of the Structures of the Turbulent Boundary Layer with and without Longitudinal Pressure Gradients, "Rep. No. MD-12. Thermosci. Div., Stanford University, Stanford, California.

SCHUBAUER, G. B., and SKRAMSTAD, H. K. (1947). Laminar boundary layer oscillations and stability of laminar flow. *J. Aeron. Sci.* **14**, 69.

SCORER, R. S. (1958). "Natural Aerodynamics." Pergamon, Oxford.

SENOO, Y. (1957). The boundary layer on the end wall of a turbine nozzle cascade. *Am. Soc. Mech. Eng.* [*Pap.*] **A-172.**

SERGIENKO, A. A., and GRETSOV, K. V. (1959). Transition from turbulent to laminar boundary layer. *Dokl. Akad. Nauk SSSR* **125** (RAE Translation No. 827).

SHERCLIFF, J. A. (1956). The flow of conducting fluids in circular pipes under transverse magnetic fields. *J. Fluid Mech.* **1**, 644.

SHERCLIFF, J. A. (1965). "A Textbook of Magnetohydrodynamics." Pergamon, Oxford.

SHIVAPRASAD, B. G. (1976). An experimental study of the effect of "mild" longitudinal curvature on the turbulent boundary layer. Ph.D. Thesis, Dept. Aero. Eng., Ind. Inst. Sci., Bangalore.

SIBULKIN, M. (1962). Transition from turbulent to laminar flow. *Phys. Fluids* **5**, 280.

SIMPSON, R. L., and SHACKLETON, C. R. (1977). "Laminariscent Turbulent Boundary Layers: Experiments on Nozzle Flows," Proj. SQUID Tech. Rep. No. SMU-2-PU.

SIMPSON, R. L., and WALLACE, D. B. (1975). "Laminariscent Turbulent Boundary Layers: Experiments on Sink Flows," Proj. SQUID Tech. Rep. No. SMU-1-PU.

SINGH, P. I., and UBEROI, M. S. (1976). Experiments on vortex stability. *Phys. Fluids* **19**, 1858.

SO, R. M. G., and MELLOR, G. L. (1972). An experimental investigation of turbulent boundary layers along curved surfaces. *NASA Contract. Rep. NASA* **CR-1940**.

SO, R. M. G., and MELLOR, G. L. (1973). Experiment on convex curvature effects in turbulent boundary layer. *J. Fluid Mech.* **60**, 43.

SPENCE, D. (1956). The development of turbulent boundary layer. *J. Aeron. Sci.* **23**, 3.

SREENIVASAN, K. R. (1972). "Notes on the Experimental Data on Reverting Boundary Layers," Rep. No. 72 FM2. Dept. Aero. Eng., Ind. Inst. Sci., Bangalore.

SREENIVASAN, K. R. (1974). Mechanism of reversion in highly accelerated turbulent boundary layers. Ph.D. Thesis, Dept. Aero. Eng., Ind. Inst. Sci., Bangalore.

SREENIVASAN, K. R., and NARASIMHA, R. (1974). Rapid distortion of shear flows. *Aero. Soc. Indian Silver Jubilee Tech. Conf., 1974* Paper 2.3.

SREENIVASAN, K. R., and NARASIMHA, R. (1978). Rapid distortion of axisymmetric turbulence. *J. Fluid Mech.* **84**, 497.

STEINER, A. (1971). Reverse transition of a turbulent flow under the action of buoyancy forces. *J. Fluid Mech.* **47**, 503.

STERNBERG, J. (1954). "The Transition from a Turbulent to a Laminar Boundary Layer," Rep. No. 906. Ballistic Res. Lab, Aberdeen.

STEWART, R. W. (1959). The problem of diffusion in a stratified fluid. *Adv. Geophys.* **6**, 303.

STRICKLAND, J. H., and SIMPSON, R. L. (1975). Bursting frequencies obtained from wall shear stress fluctuations in a turbulent boundary layer. *Phys. Fluids* **18**, 306.

TAYLOR, G. I. (1929). The criterion for turbulence in curved pipes. *Proc. R. Soc. London, Ser. A* **124**, 243.

TETERVIN, N. (1967). "An analytical Investigation of the Flat Plate Turbulent Boundary Layer in Compressible Flow," NOL TR 67-39, Aerodyn. Res. Rep. No. 286. Nav. Ord. Lab., Silver Spring, Maryland.

THOMANN, H. (1968). Effect of streamwise wall curvature on heat transfer in a turbulent boundary layer. *J. Fluid Mech.* **33**, 283.

THOMPSON, B. G. J. (1973). "The Production of Boundary-Layer Behaviour and Profile Drag for Infinite Yawed Wings," RAE Tech. Rep. No. 73091.

TOWNSEND, A. A. (1954). The uniform distortion of homogeneous turbulence. *J. Mech. Appl. Math.* **7**, 104.

TOWNSEND, A. A. (1956). "The Structure of Turbulent Shear Flow." Cambridge Univ. Press, London and New York.

TOWNSEND, A. A. (1958). Turbulent flow in a stably stratified atmosphere. *J. Fluid Mech.* **3**, 361.

UBEROI, M. S. (1956). Effect of wind tunnel contraction on free stream turbulence. *J. Aerosp. Sci.* **23**, 754.

VISWANATH, P. R., and NARASIMHA, R. (1972). "Base Pressure on Sharply Boat-tailed Aft Bodies," Rep. No. 72 FMI. Dept. Aero. Eng. Ind. Inst. Sci., Bangalore.

VISWANATH, P. R., and NARASIMHA, R. (1975). "Supersonic Flow Past a Sharply Boat-tailed Step." Rep. No. 75 FM13. Dept. Aero. Eng. Ind. Inst. Sci., Bangalore.

VISWANATH, P. R., NARASIMHA, R., and PRABHU, A. (1978). Visualization of relaminarizing flows. *J. Indian Inst. Sci.* **60**, 159.

VIVEKANANDAN, R. (1963). A study of boundary layer expansion fan interactions near a sharp corner in supersonic flow. M.Sc. Thesis, Dept. Aero Eng., Ind. Inst. Sci., Bangalore.

WALLIS, R. A. (1950). "Some Characteristics of a Turbulent Boundary Layer in the Vicinity of a Suction Slot," Aerodyn. Note 87. Aero. Res. Lab., Dept. Supply, Melbourne, Australia.

WEBSTER, C. A. G. (1964). An experimental study of turbulence in a density-stratified shear flow. *J. Fluid Mech.* **19**, 221.

WILSON, D. G., and POPE, J. A. (1954). Convective heat transfer to gas turbine blades. *Proc., Inst. Mech. Eng., London* **168**, 861.

ZAKKAY, V., TOBA, K., and DUO, T.-J. (1964). Laminar, transitional and turbulent heat transfer after a sharp corner. *AIAA J.* **2**, 1389.